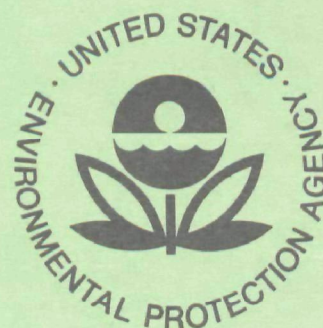


EPA-660/3-75-005  
MARCH 1975

Ecological Research Series

# Mathematical Modeling of Phytoplankton in Lake Ontario

## 1. Model Development and Verification



National Environmental Research Center  
Office of Research and Development  
U.S. Environmental Protection Agency  
Corvallis, Oregon 97330



## RESEARCH REPORTING SERIES

Research reports of the Office of Research and Development, U.S. Environmental Protection Agency, have been grouped into five series. These five broad categories were established to facilitate further development and application of environmental technology. Elimination of traditional grouping was consciously planned to foster technology transfer and a maximum interface in related fields. The five series are:

1. Environmental Health Effects Research
2. Environmental Protection Technology
3. Ecological Research
4. Environmental Monitoring
5. Socioeconomic Environmental Studies

This report has been assigned to the ECOLOGICAL RESEARCH STUDIES series. This series describes research on the effects of pollution on humans, plant and animal species, and materials. Problems are assessed for their long- and short-term influences. Investigations include formation, transport, and pathway studies to determine the fate of pollutants and their effects. This work provides the technical basis for setting standards to minimize undesirable changes in living organisms in the aquatic, terrestrial and atmospheric environments.

This report has been reviewed by the Office of Research and Development, EPA, and approved for publication. Approval does not signify that the contents necessarily reflect the views and policies of the Environmental Protection Agency, nor does mention of trade names or commercial products constitute endorsement or recommendation for use.



# ERRATA

Please note the following corrections in EPA-660/3-75-005, MATHEMATICAL MODELING OF PHYTOPLANKTON IN LAKE ONTARIO:

<u>Page</u>		<u>Change to</u>
31	Equation (18)	$S_{N_{1,j}} = \frac{a_1}{a_c} \Sigma D_z Z + a_1 P_j \left(1 - \frac{a_{zp} K_g}{K_g + P_j}\right) C_{gzp} Z^1$ $+ a_1 D_p P - K_1 N_1 + \frac{a_1}{a_c} Z^1 (1 - a_z) C_{g21} Z^2$
33	Equation (22)	$S_{p_{1,j}} = \frac{a_p}{a_c} \Sigma D_z Z + a_p P_j \left(1 - \frac{a_{zp} K_g}{K_g + P_j}\right) C_g Z^1$ $- K_1 P_1 + \frac{a_p}{a_c} Z^1 (1 - a_z) C_{g21} Z^2 + a_p D_p P$

<u>Page</u>		<u>Change</u>	<u>To</u>
60	Table 8	0 - 90 cm <sup>2</sup> /sec	0 - 6.86 cm <sup>2</sup> /sec
60	Table 8	0 - 778 m <sup>2</sup> /day	0 - 59.3 m <sup>2</sup> /day
64	Paragraph 2	90 cm <sup>2</sup> /sec	6.86 cm <sup>2</sup> /sec
65	Figure 10 (b)	100	7.63
		50	3.81
		3.0	0.229
		1.0	0.0763
		Delete remaining values on ordinates	
160	Table A-1	see Fig A-4	see Fig A-3
161	Paragraph	.0003 mi <sup>2</sup> /day	.229 10 <sup>-4</sup> mi <sup>2</sup> /day
164	Fig A-3	3.0	.229
		1.0	.0763
		100	7.63
		50	3.81
		Delete remaining values on ordinates	



MATHEMATICAL MODELING OF PHYTOPLANKTON  
IN LAKE ONTARIO

1. MODEL DEVELOPMENT AND VERIFICATION

By

Robert V. Thomann  
Dominick M. DiToro  
Richard P. Winfield  
Donald J. O'Connor  
Manhattan College, Bronx, NY

Grant No. R800610  
Program Element 1BA026  
ROAP/Task No. 21AKP/15

Project Officer

William Richardson  
Grosse Ile Laboratory  
National Environmental Research Center  
Grosse Ile, Michigan 48138

NATIONAL ENVIRONMENTAL RESEARCH CENTER  
OFFICE OF RESEARCH AND DEVELOPMENT  
U.S. ENVIRONMENTAL PROTECTION AGENCY  
CORVALLIS, OREGON 97330



## ABSTRACT

The basic mathematical structure for describing the dynamics of phytoplankton in Lake Ontario is presented in this report. Data on chlorophyll and principle nutrients are reviewed and summarized and the mathematical modeling strategy is detailed.

The modeling strategy begins with the construction of a horizontally completely mixed lake with vertical layers, LAKE 1. This spatially simplified model is used to develop the interactions and kinetic behavior of the various components of each subsystem. A more detailed 3-dimensional model is then used to describe open lake and near shore variations in phytoplankton biomass. Ten biological and chemical variables are used in both models and include four trophic levels above the phytoplankton, chlorophyll a as a measure of phytoplankton biomass, two phosphorus components and three nitrogen components. For LAKE 1, using three vertical segments, a total of 30 simultaneous non-linear differential equations must be solved while for the 3-dimensional model, using 67 segments a total of 670 equations are solved. In both cases, the models are run for a period of one year or longer.

Under reasonable sets of model parameters as reported in the literature, the Lake 1 model output compared favorably with observed data on the dependent variables. Spring growth and peak chlorophyll concentrations are related primarily to increasing light and temperature. The model indicates that growth ceases due to phosphorus



limitation. Zooplankton grazing and subsequent recycling of nutrients due to excretion and plankton endogenous respiration result in a late summer increase in phytoplankton biomass. Both nitrogen and phosphorus are then limiting resulting in a broad fall peak in phytoplankton biomass. A decline then results from low temperatures due to fall overturn.

The results to date indicate that the mathematical model of phytoplankton in Lake Ontario as developed herein is a reasonable first approximation to observed data. As such, the model can form a basis for preliminary estimates of the effects of nutrient reduction programs on Lake Ontario.

This report was submitted in partial fulfillment of Grant Number R800610 by the Environmental Engineering and Science Program, Manhattan College, Bronx, New York, under the sponsorship of the U.S. Environmental Protection Agency. Work was completed as of October 1974.



## CONTENTS

		<u>Page</u>
<u>Sections</u>		
I	Conclusions	1
II	Recommendations	3
III	Introduction	4
IV	Lake Ontario - Background	8
V	Lake Ontario Model Structure	18
VI	Lake 1 Model	58
VII	Lake 2 Analytical Investigations	101
VIII	Preliminary Lake 3 Model	131
IX	Appendix	159



# LIST OF TABLES

	<u>Page</u>
1. Flow budget . . . . .	9
2. Nutrient loadings . . . . .	11
3. Nutrient load split . . . . .	11
4. CCIW limnological data report summary (Number of cruises with adequate spatial defination) . . . . .	14
5. Thermodynamic properties at 25°C . . . . .	44
6. Thermodynamic properties at 25°C . . . . .	44
7. Temperature dependence comparison . . . . .	46
8. Basic physical data of the Lake 1 model . . . . .	60
9. Principal parameter values used in Lake 1 model output shown in figures 21-23 . . . . .	88
10. Log <sub>10</sub> (G/d+μ) for exponentially decreasing growth rate . . . . .	115
11. Monthly heat flux values . . . . .	142
12. Regional to Lake 3 segmentation equivalence . . . . .	144
A-1 Lake 1 physical parameters . . . . .	160
A-2 Lake 1 Mass loadings and initial conditions . . . . .	170
A-3 System parameters . . . . .	171



# LIST OF FIGURES

	<u>Page</u>
1. General basin map of Lake Ontario . . . . .	5
2. Typical CCIW cruise track, April 1969 . . . . .	13
3. Typical output from data reduction - main lake average @ 1 meter . . . . .	16
4. Eutrophication modeling strategy . . . . .	21
5. System diagram - Lake 1 model . . . . .	23
6. Relationship of pH and the ratio, $\text{Alk}/\text{C}_\text{T}$ . . . . .	38
7. Per cent error in assuming $(\text{CO}_2 - \text{Acy}) \approx (\text{CO}_2)$ . . . . .	41
8. Computations for $\text{CO}_2 - \text{H}_2\text{O}$ system . . . . .	49
9. Major physical features included in Lake 1 model . . . . .	59
10. Effect of vertical mixing . . . . .	65
11. Effect of phytoplankton settling velocity, $K_\text{mp} = 10\mu\text{g}/\ell$ . . . . .	67
12. Effect of phytoplankton settling velocity $K_\text{mp} = 1\mu\text{g}/\ell$ . . . . .	69
13. Effect of phytoplankton settling velocity on nutrients and nutrient limitation $K_\text{mp} = 10\mu\text{g}/\ell$ . . . . .	70
14. Effect of Michaelis constant for phosphorus on primary variables . . . . .	73
15. Effect of Michaelis constant for phosphorus on nutrient limitation of nitrogen and phosphorus . . . . .	74
16. Responses due to two photoplankton growth formulations . . . . .	76
17. Sixteen year computed output of phytoplankton chlorophyll . . . . .	78
18. Long term behavior of model components under two phosphorus Michaelis constants . . . . .	80
19. Preliminary comparison of model output and observed data . . . . .	82
20. Preliminary comparison of model output and observed data, continued . . . . .	83



21.	Lake 1 model verification, 0 - 17 meters . . . . .	85
22.	Lake 1 model verification (cont.), 0 - 17 meters . . . . .	86
23.	Lake 1 model verification, 50 - 150 meters . . . . .	87
24.	Dynamics of the phytoplankton growth rate . . . . .	90
25.	Dynamics of the phytoplankton death rate . . . . .	92
26.	Dynamics of the phytoplankton net production . . . . .	93
27.	Dynamics of nitrogen and phosphorus limitations . . . . .	95
28.	Biological and hypolimnetic recycling of phosphorus . . . . .	97
29.	Lake Ontario Phytoplankton Biomass, horizontal averages 1973. IFYGL . . . . .	106
30.	Central Lake Erie Phytoplankton Biomass, four station log averages, 1970. Project Hypo . . . . .	107
31.	Onondaga Lake Phytoplankton Biomass, two stations, 1969 . . . . .	109
32.	St. Margaret's Bay Phytoplankton Biomass, station A, 1969 . . . . .	110
33.	Eigenvalue equation solutions for constant growth layer and exponentially decreasing growth rate cases . . . . .	114
34.	Settling velocity-growth rate interaction. The effect of dispersion. Exponentially decreasing growth rate case . . . . .	117
35.	Population growth rate versus maximum growth rate. The effect of Euphotic zone. The exponentially decreasing growth rate case . . . . .	119
36.	Population growth rate versus settling velocity - the effect of Euphotic zone depth. The exponentially decreasing growth rate case . . . . .	121
37.	Population growth rate versus dispersion coefficient and the effect of Euphotic zone depth. The exponentially decreasing growth rate case . . . . .	122
38.	The effect of negative sinking velocity. The exponentially decreasing growth rate case . . . . .	123
39.	Application to Lakes and Oceans - the range of biologically relevant dimensionless numbers . . . . .	125
40.	Lake 3 segmentation . . . . .	132



41.	Assumed summer circulation for Lake 3 model . . . . .	136
42.	Assumed winter circulation for Lake 3 model . . . . .	138
43.	Assumed horizontal and vertical dispersion coefficients for Lake 3 model . . . . .	139
44.	Regional division of Lake Ontario by Lee <sup>8</sup> . . . . .	145
45.	Comparison of computed temperatures from Lake 3 model with data from Lee <sup>8</sup> , winter, fall . . .	146
46.	Comparison of computed temperatures from Lake 3 model with data from Lee <sup>8</sup> , summer, spring . .	147
47.	Principal IFYGL stations and the Lake 3 grid . . . . .	150
48.	Preliminary results of Lake 3, 0 - 4 meters . . . . .	151
49.	Preliminary comparison of Lake 3 output to observed data at two segments for June . . . . .	153
50.	Data output flow diagram used fro verification and display purposes . . . . .	154
51.	Three dimensional plot of phytoplankton chlorophyll calculated from Lake 3 model-June, 0 - 4 meters . . . . .	156
A-1	Variation of volume with depth . . . . .	162
A-2	Variation of area with depth . . . . .	162
A-3	Temporal variation of vertical dispersion coefficient - interface 1-2 . . . . .	164
A-4	Temporal variation of water temperature . . . . .	164
A-5	Temporal variation of solar radiation . . . . .	165
A-6	Temporal variation of photoperiod . . . . .	166
A-7	Determination of background water clarity - Ke . . .	168



## ACKNOWLEDGMENTS

The cooperation of many IFYGL investigators who generously supplied their data for use in this report is acknowledged. Special thanks are due to EPA personnel at the Grosse Ile Laboratory including Messrs. William Richardson, Nelson Thomas, and Dr. Tudor Davies. Finally, the excellent cooperation and assistance of the Canada Centre for Inland Waters is also gratefully acknowledged.



## SECTION I

### CONCLUSIONS

The dynamic behavior of lake-wide phytoplankton and associated nutrients can be adequately modeled with a simplified model. Such a model is horizontally well-mixed, but is vertically stratified and therefore represents an average open lake condition for Lake Ontario.

The phytoplankton modeling structure used in previous estuarine and delta applications is therefore also appropriate for describing phytoplankton biomass in lakes.

Analytical studies of the one dimensional vertical phytoplankton biomass equation indicate that when the biomass is increasing, then asymptotically the log growth rate of the population will approach a value independent of depths. Data for four bodies of water including Lake Ontario support this theoretical prediction.

Detailed verification analyses using four years of data on Lake Ontario indicate that the spring growth phase and peak phytoplankton biomass are primarily controlled by increasing light and temperature and phosphorus limitation. The mid-summer minimum in phytoplankton is estimated to be due primarily to zooplankton grazing and nitrogen limitation. The broad fall peak in phytoplankton is a complex interaction of nutrient regeneration (up to five times the external nutrient inputs), subsequent nutrient limitation and then the fall overturn. Both nitrogen and phosphorus are important nutrients in this dynamic succession.



It is estimated that a period of 10-20 years may be necessary for the whole of Lake Ontario to reach a new level of dynamic equilibrium in phytoplankton biomass after a nutrient reduction program is instituted.

It is also concluded that a sufficient verification base for the lake wide model has been established to permit the use of the model for preliminary simulations of the effects of various levels of nutrient reduction.



## SECTION II

### RECOMMENDATIONS

Primary emphasis in this report is on the scientific foundation and validity of the model, principally the LAKE 1 model. It is recommended that simulations and projections of the effects of nutrient reductions be carried out, first, in the Lake 1 model and then explored at a greater level of detail in the 3-dimensional Lake 3 model. These projections should be long term and attempt to delineate the time required to reach a new dynamic equilibrium in Lake Ontario.

A detailed examination of the behavior of the Lake 3 model is warranted especially in view of the importance of near shore versus open lake problems. The three dimensional nature of this model requires a significantly greater effort for verification purposes and for understanding the response of the Lake 3 model under different environmental conditions of flow and near shore temperature and waste discharges.

Following the analysis of Lake 3 model responses, it is recommended that simulations be made of nutrient reduction programs. Such simulations should be carried out to determine the expected phytoplankton biomass and the time to reach that level for the different regions of Lake Ontario.

It is also recommended that the modeling structure of Lake 1 be expanded to include phytoplankton species dependence and a more flexible food web arrangement for the higher trophic levels. The primary data source would be the data collected as part of the IFYGL effort.



### SECTION III

#### INTRODUCTION

##### PURPOSE OF RESEARCH

The overall purpose of this research is to structure a mathematical modeling framework of the major features of eutrophication in large lakes. Lake Ontario, the subject of intensive field work as part of the International Field Year for the Great Lakes (IFYGL) is used as the problem setting (Fig.1). The overall objectives of the research include:

- a. determination of important interactions in lake eutrophication;
- b. analysis of lake water quality and biological responses to natural and man-made inputs;
- c. formation of a basis for estimating the direction of change to be expected under remedial environmental control actions.

The problems of impairment of the quality of lake systems are magnified for "large lakes" such as the Great Lakes. The size of these lakes is such as to preclude any immediate improvement in quality after control actions are taken. Further, it is much more difficult to obtain reliable data on water quality, biological structure and hydrodynamic circulation, again because of the difficulty of sampling large lake systems. The general circulation itself may not be adequately known in relation to climatological and hydrological factors. In the biological area, measures of phytoplankton populations are temporally and spatially dependent



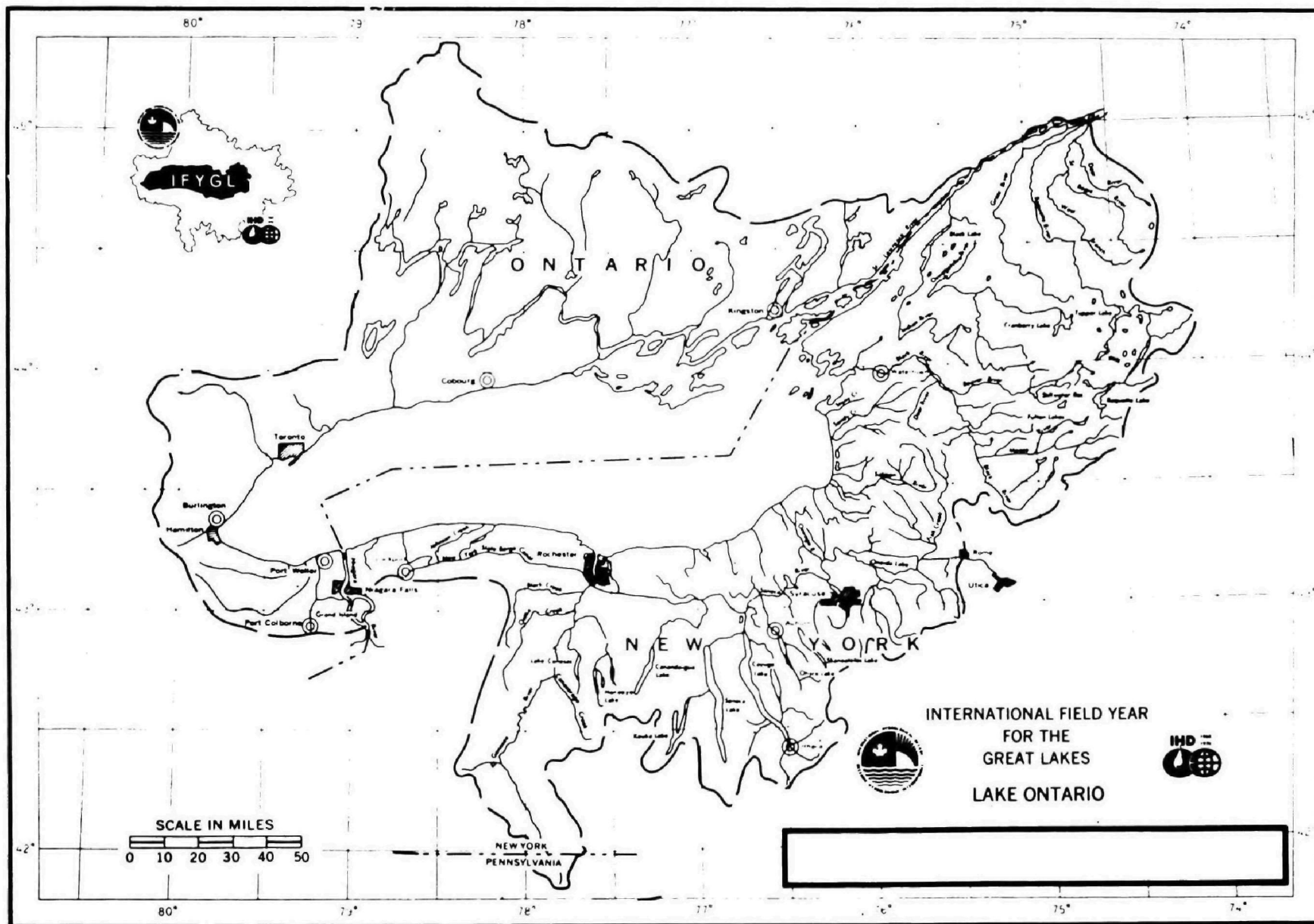


Figure 1. General basin map of Lake Ontario



and reflect complex interactions with nutrients, such as nitrogen and phosphorus, and upper trophic level predation. This report reviews work accomplished to date on development of a mathematical model of phytoplankton in Lake Ontario that hopefully will form a reasonable basis for estimating the effects of nutrient removal programs.

#### SCOPE OF RESEARCH

The scope of this research is therefore lake wide and attention is directed primarily to the behavior of the phytoplankton for the lake as a whole. The smallest scale considered in the more advanced model (Lake 3) is on the order of 10-40 km. Detailed near-shore behavior on a scale less than this is not a part of this research. Furthermore, this research is concerned with phytoplankton dynamics as described on a time scale of weeks to months. Therefore the seasonal progression of the phytoplankton throughout a year and from year to year is the time scale of interest. Short term fluctuations, in the order of hours or days are not described herein.

Finally, the modeling structure developed as part of this research is aimed at the phytoplankton biomass as a measure of eutrophication and associated water quality. Attached algae, such as cladophora, are not modeled. Particular emphasis is placed on the interaction of the passive phytoplankton biomass (as characterized by the concentration of chlorophyll) with the nutrients, principally nitrogen and phosphorus and the grazing by herbivorous zooplankton and higher order trophic levels.



The primary thrust of the research is to provide a more rational and scientifically defensible structure for environmental decision making on the efficacy of nutrient control and removal programs. As such, there are various levels of detail that could be explored. The goal is to include the "right" level of detail that explains the observed data, provides a basis for prediction but is not too inordinately complex.

This report summarizes work performed to date on model development and strategy, data reduction and compilation, sensitivity analyses and verification analyses. Simulations of conditions under varying levels of nutrient reduction are not included in this report and will be part of a separate document.



## SECTION IV

### LAKE ONTARIO - BACKGROUND

With the Niagara River, the outflow of Lake Erie and hence the cumulator of all the upper Great Lakes outflow, as its principle source of inflow and the St. Lawrence River its outflow, Lake Ontario is the last in the **chain** of Laurentian Great Lakes. Lake Ontario's narrow and deep rock basin was formed by the action of glacial corrasion.<sup>1</sup>

#### MORPHOMETRY

Lake Ontario is the smallest of the Great Lakes in terms of surface area,  $19,477\text{km}^2$  ( $7,520\text{mi}^2$ ), with a drainage area of  $90,132\text{km}^2$  ( $34,880\text{mi}^2$ ).<sup>2</sup> The mean depth of Lake Ontario, 90 meters (296 feet), is second only to Lake Superior for the Great Lakes and can be considered one of its most important physical features.<sup>2,3</sup> Lake Ontario's volume is  $1,669\text{km}^3$  ( $401\text{mi}^3$ ), with a maximum depth of 244 meters (801 feet)<sup>3,4</sup>. The lake's elevation above sea level is 74.01 meters (242.8 feet)<sup>4</sup> which makes its depth of cryptodepression to be 170 meters (558 feet). Lake Ontario's length is 307km (191 miles), with a maximum width of 87km (54 miles)<sup>4</sup>. The lake's shoreline length is 1,380 km (858 miles)<sup>1</sup>. The variation of volume and area with depth is illustrated in Appendix A (Figs. A-1 and A-2).

#### HYDROLOGY

The Niagara River is the major source of inflow for Lake Ontario, being the cumulative outflow of the other Great Lakes. The average flow of the Niagara River is 195,000 cfs<sup>5</sup>, and accounts for 84 percent of the flow discharged via the St. Lawrence River, as can be seen in Table 1. The average annual precipitation on Lake Ontario's water surface is 83.28cm (32.79 inches) and the average annual evaporation is 71cm (28 inches)<sup>6</sup>.



TABLE 1 - FLOW BUDGET

Source	Flow (cfs)	% of Discharge
Major Tributaries		
Niagara River	195,000	84.1
Twelve Mile Creek	6,400	2.8
Oswego River	6,200	2.7
Trent River Region	4,200	1.8
Black River	3,800	1.6
Genesee River	2,700	1.2
Welland Canal	1,200	0.5
Other Tributaries	5,900	2.5
Other Sources (Precipitation - Evaporation and Other)	6,600	2.8
Discharge		
St. Lawrence River	232,000	



The thermal bar development which precedes the development of the full thermocline begins in late April or early May in Lake Ontario<sup>5</sup>. The offshore movement of the thermal bar is such that within 17 to 28 days the nearshore ring of stratified water covers over half the area of the lake. The average depth of the thermocline is 17 meters (55.8 feet), with its dissipation beginning in late September<sup>5</sup>. The hydraulic detention time of Lake Ontario (volume divided by flow) is 8.1 years, and is significant in that it gives some indication of the response time of the lake. (See Section VI)

#### NUTRIENT INPUTS

Nitrogen and phosphorus are the nutrients used in the present configuration of the model, though silica will most likely be incorporated in the future. The only nutrient loading information available at the beginning of this project was for total nitrogen and phosphorus. Loading information for the individual forms of the nutrients (ammonia, orthophosphate, etc.) similar to those used in the model's nutrient systems, would be of great utility.

Nutrient loads for Lake Ontario are shown in Table 2. These reflect the total loads from the various sources (industrial, municipal and tributary) and were obtained by the International Joint Commission (IJC). These loads are broken down to individual waste discharges in the IJC's excellent 1969 three volume publication.<sup>5</sup> Table 2 indicates that the Niagara River accounts for over one-half of Lake Ontario's nutrient load. Table 3 gives the loading information as it was incorporated into the Lake 1 model. It can be noted that the loads are also shown as equivalent boundary concentrations, for an



TABLE 2 - NUTRIENT LOADINGS

SOURCE	N I T R O G E N			P H O S P H O R U S		
	lbs/Day	kg/Day	%	lbs/Day	kg/Day	%
Niagara	522,200	236,900	59	42,200	19,100	56
Tributaries	191,000	86,600	22	15,600	7,100	21
Municipal	72,600	32,900	8	16,200	7,300	22
Industrial	97,300	44,100	11	1,000	500	1
Total	883,100	400,500		75,000	34,000	

TABLE 3 - NUTRIENT LOAD DISTRIBUTION

System	Nutrient Load		As Boundary Concentration
	lbs/Day	kg/Day	mg/l
<u>Nitrogen</u>			
Non-Living organic N	551,400	250,100	0.443
Ammonia N	18,800	8,500	0.015
Nitrate N	312,900	141,900	0.250
<u>Phosphorus</u>			
Non-Living organic P	57,100	25,900	0.0457
Inorganic P	17,900	8,100	0.0143



average inflow of 232,000 cfs. The inorganic forms of the nutrients were set at the lake's winter concentrations with the remaining load inputted in the non-living organic form.

#### AVAILABLE LAKE DATA

The bulk of the data used for this investigation was obtained from three sources:

1. Limnological Data Reports, Lake Ontario, 1966-1969  
Canada Centre for Inland Waters (CCIW)
2. STORET, Environmental Protection Agency (EPA)
3. Report to the International Joint Commission on the  
Pollution of Lake Ontario and the International  
Section of the St. Lawrence River.<sup>5</sup>

These sources were supplemented with other data available in the literature. The Limnological Data Reports (LDR) of CCIW comprise the largest single source of Lake Ontario survey data available. CCIW's cruises not only had adequately dense spatial grids (see Fig. 2 for a typical grid) but also comprised good temporal coverage for the years surveyed (see Table 4).

STORET, the Environmental Protection Agency's water quality storage and retrieval system is the prime residence of all U.S. collected water quality data. The pre-IFYGL STORET data base consisted mainly of data from three 1965 synoptic cruises. The temporal coverage by these cruises was not sufficient to be of direct use for verification analysis. The data were therefore considered only as supplemental to the basic data set. STORET's utility is for storage and analysis of IFYGL data and as a data base for tributary nutrient concentration data. It was therefore decided to use the data contained in the LDR as a verification data base for the preliminary models and the STORET data as a verification data base for the



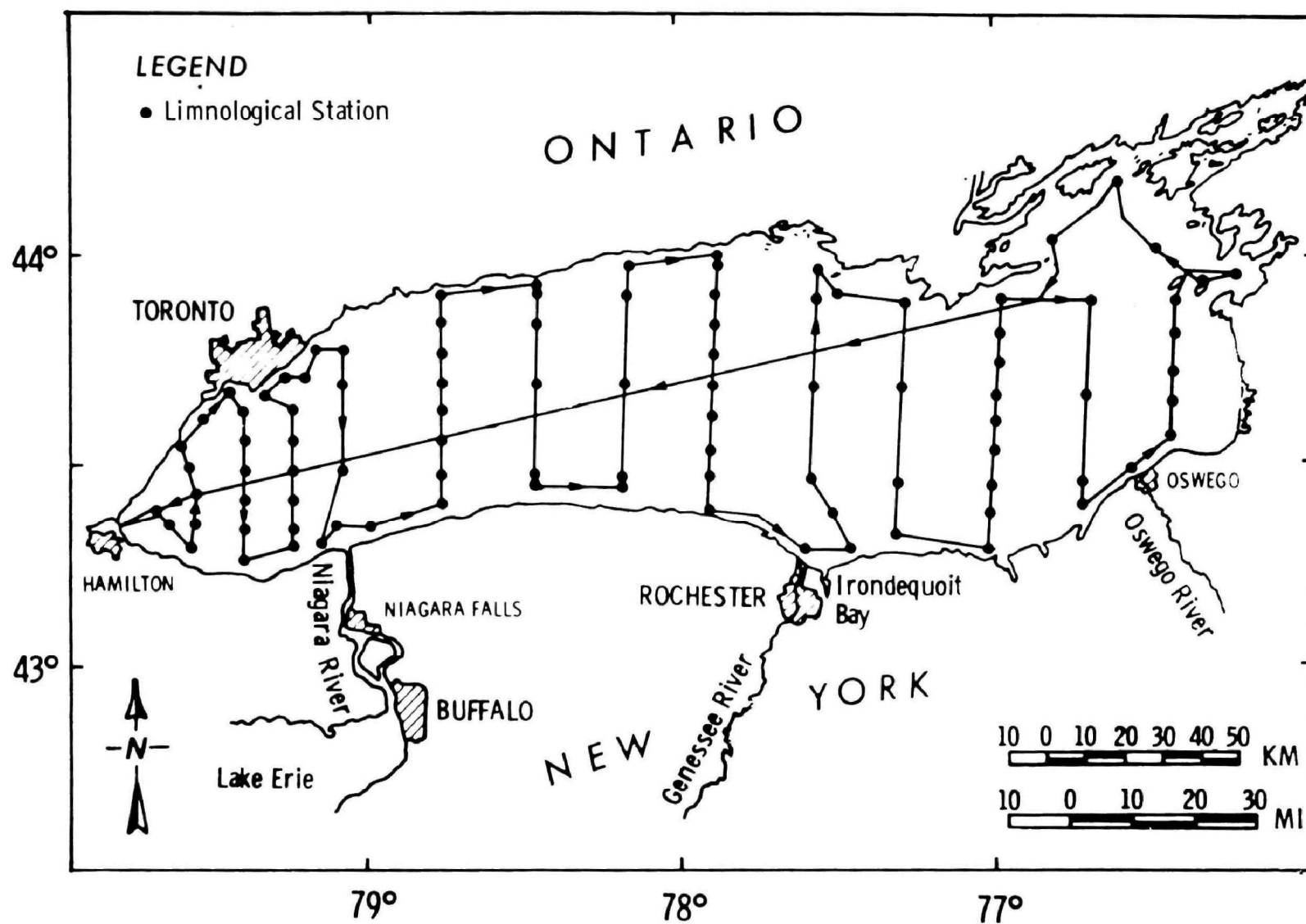


Figure 2. Typical CCIW cruise track, April 1969



TABLE 4 -

CCIW LIMNOLOGICAL DATA REPORT SUMMARY  
(Number of Cruises with adequate spatial definition)

	1966 (June-Sept.)	1967 (June-Nov.)	1968 (April-Nov.)	1969 (April-Dec.)
Nitrogen:				
Organic or Kjeldahl-N	-	11	-	-
Ammonia Nitrogen	-	10	5	9
Nitrate Nitrogen	4	10	6	9
Phosphorus:				
Total Phosphate	-	4	5	8
Reactive Phos- phate	5	10	6	9
Temperature	9	11	9	9
Chlorophyll <sub>a</sub>	-	11	6	9



more advanced models.

Due to the magnitude of data in the LDR, a data reduction mechanism had to be implemented. The main criterion for the data reduction was compatibility with model output so as to facilitate comparison. Considerable effort was expended on this task, with the principal product being main lake means and standard deviation for the relevant variables at individual sample depths. Main lake statistics were obtained, since this is what the Lake 1 and 2 models were designed to represent. Stations which had sounding depths of greater than 50 meters were considered main lake stations. Data were also reduced for depth intervals corresponding to segment depth for some years. Main lake, near shore or entire lake reductions can be computed using the present software. Also latitude-longitude blocks can be specified to give more refined spatial definition to the data retrievals. Therefore Lake 3 comparison data is readily obtained with this option. Figure 3 is a sample output of the data reduction.

The Lake 1 model was designed to aid in the understanding of the principal mechanisms which underlie the process of eutrophication. A key criterion in evaluating the validity of a model is to compare the models output to the data observed in the field. Analysis of the field data of the water quality parameters under consideration revealed temporal patterns that were observed year after year. These patterns can be seen in the summary data plots used for the evaluation of model output - (See Section VI). Therefore it is apparent that data accumulation and reduction are key steps in the modeling framework, for only when these are completed can the validity of the model be determined.



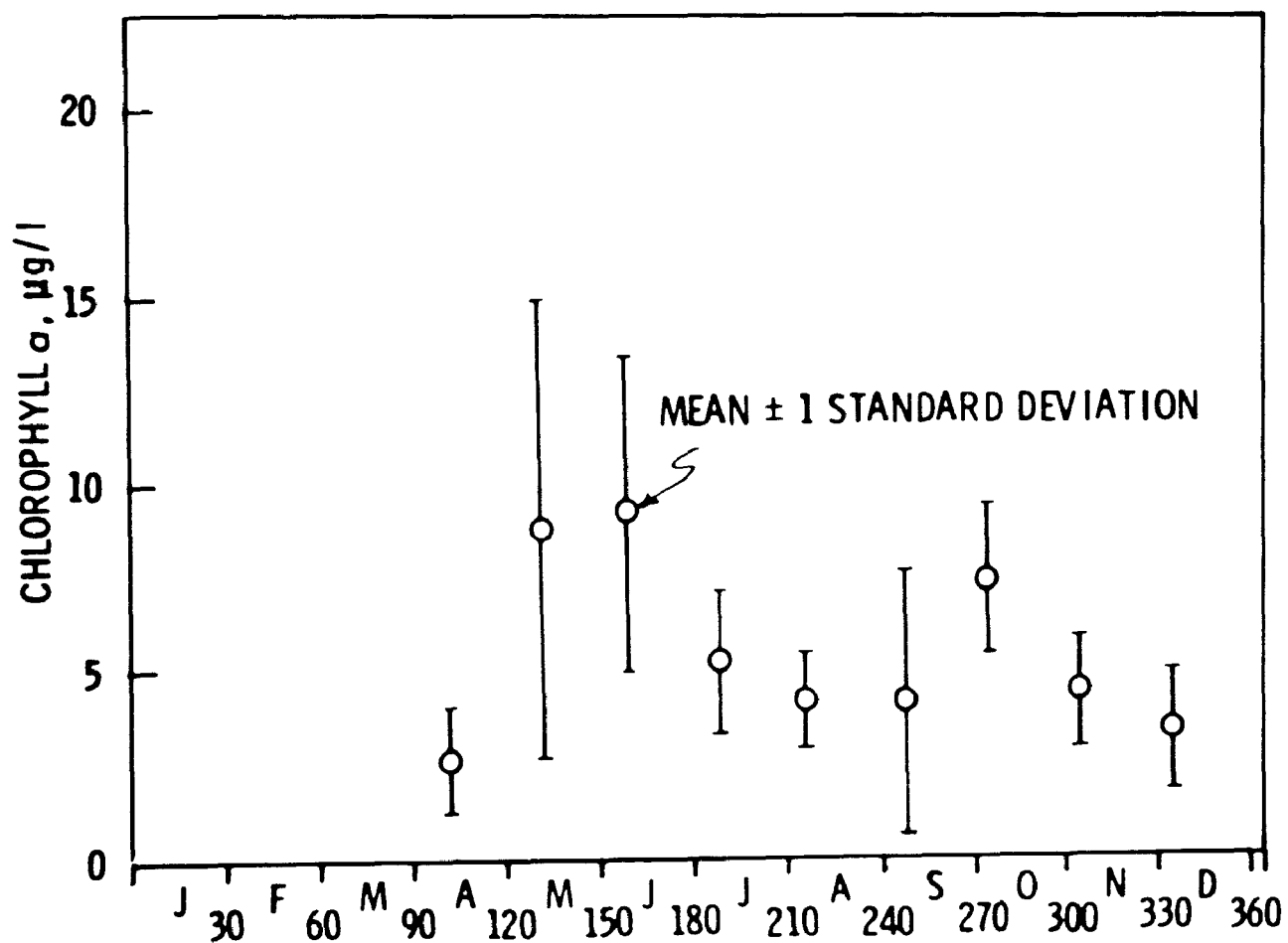


Figure 3. Typical output from data reduction - main lake average @ 1 meter



## REFERENCES

1. Hutchinson, G., A Treatise on Limnology, Vol. 1.  
John Wiley & Sons Inc., N.Y. 1957.
2. Beeton, A.M. and D.C. Chandler, "The St. Lawrence Great Lakes," Limnology in North America (D.C. Frey, ed.).  
University of Wisconsin Press, Milwaukee. 1963.
3. Canada Center for Inland Waters, Descriptive Limnology  
Section. Personal communication (see Appendix A).
4. Canadian Hydrographic Service. Bathymetric Chart (881)  
Lake Ontario. Department of Energy, Mines & Resources,  
Ottawa. 1970.
5. International Lake Erie & International Lake Ontario -  
St. Lawrence River Water Pollution Control Boards.  
Report to the International Joint Commission on the  
Pollution of Lake Ontario and the International Section  
of the St. Lawrence River, Vol. 3. 1969.
6. Great Lakes Basin Commission. "Appendix 11, Levels & Flows,"  
Great Lakes Framework Study, Draft No. 3, Ann Arbor. 1971.
7. Canada Centre for Inland Waters. Limnological Data Reports,  
Lake Ontario, 1966-1969. Canadian Oceanographic Data  
Centre, Burlington, Ontario.



## SECTION V

### LAKE ONTARIO MODEL STRUCTURE

#### THEORETICAL BACKGROUND

The basic theory used for the Lake Ontario model makes use of previous model structures (DiToro, et.al.<sup>1</sup> Hydrosience, Inc.,<sup>2</sup> Thomann, et.al.,<sup>3</sup>) and essentially represents a mass balance around each ecological or nutrient compartment and around physical space.

The basic structure consists of three parts:

1. transport and dispersion sub-system
2. biological sub-system
3. chemical sub-system

The latter two sub-systems represent the kinetic behavior or the extent and complexity of interactions between relevant variables while the first system represents the physical processes of water movement and mixing. The theory of each of the sub-systems is presently developed to a different degree with the transport and dispersion theory developed to a more advanced degree than the biological and chemical systems.

The general equation which results from applying the principle of the conservation of mass is

$$\begin{aligned} \frac{\partial s_k}{\partial t} = & -\frac{\partial}{\partial x} (us_k) - \frac{\partial}{\partial y} (vs_k) - \frac{\partial}{\partial z} (ws_k) + \frac{\partial}{\partial x} (E_x \frac{\partial s_k}{\partial x}) \\ & + \frac{\partial}{\partial y} (E_y \frac{\partial s_k}{\partial y}) + \frac{\partial}{\partial z} (E_z \frac{\partial s_k}{\partial z}) \\ & \pm S_k(x, y, z, t, s_\ell, s_k) \pm W_k(x, y, z, t); \quad \begin{array}{l} k = 1..m \\ \ell = 1..m \\ k \neq \ell \end{array} \end{aligned} \quad (1)$$



where  $s_k$  is the  $k$ th dependent variable (biological or chemical),  $u, v, w$  are the velocity components in the  $x, y$  and  $z$  directions respectively,  $E_x, E_y$  and  $E_z$  are the dispersion coefficients in each respective spatial direction,  $S_k$  represents the kinetic interactions between the  $k$  variables and  $W$  is the direct inputs of the substance,  $s_k$ . It should be noted that Eq. (1) as written, does not include any interaction between the variables  $s_k$  and the transport and dispersion regime. Thus, the physical system is separable, in the sense that it can be externally supplied and once determined, it can be used for all variables. In vector form, Eq. (1) is:

$$\frac{\partial s_k}{\partial t} = (\nabla \cdot [E] (\nabla s_k) - \nabla \cdot \vec{U} s_k) \pm S_k \pm W_k \quad (2)$$

where  $[E]$  is a diagonal matrix of dispersion coefficients,  $(s_k)$  is a column vector,  $U$  is the velocity vector and

$$\nabla \equiv \frac{\partial}{\partial x} \vec{i} + \frac{\partial}{\partial y} \vec{j} + \frac{\partial}{\partial z} \vec{k}$$

In Eq. (2), the first term in parenthesis on the right hand side represents the dispersive and advective field in three dimensions, as given by the general circulation. In this work, it is assumed that the circulation is "known", either through observation or from output from a hydrodynamic model. The inputted circulation can be validated by utilizing Eq. (2) for a tracer such as dye or water temperature to compare computed results to observed data. Water temperature has been used in some of this work and the results of that analysis are given in section VIII. Primary interest therefore



centers about the reaction kinetics, their functional forms and numerical values.

A finite difference approximation to Eq. (2) is necessary in order to apply the equation to an actual water body. Thus, if the lake is divided into a series of finite completely mixed volumes,  $n$  in number and each with volume  $V_j$ , then it can be shown that

$$[V] \frac{d(s)_k}{dt} = [A] (s)_k + (S)_k + (W)_k \quad (3)$$

where  $[V]$  is an  $n \times n$  diagonal matrix of volumes,  $(s)_k$  is an  $n \times 1$  vector of the variable  $s_k$ ,  $[A]$  is an  $n \times n$  matrix of advection and dispersion terms;  $(S)_k$  is an  $n \times 1$  vector of kinetic interactions and  $(W)_k$  is an  $n \times 1$  vector of inputs of variable  $s_k$ . For  $m$  interacting variables and  $n$  physical locations, Eq. (3) indicates that a total of  $m \times n$  equations must be solved. In general, the equations are both linear and non-linear.

When one recognizes that initially up to 10-15 interacting variables can be specified and that 50-100 initial spatial segments may be required, it is obvious that the computer program and data preparation necessary to obtain solutions are of a substantial magnitude. Accordingly, prudent practice would dictate a modeling strategy that allows one to proceed sequentially from simple models to the more complex. Such a strategy is utilized in this work and is illustrated in Fig. 4.



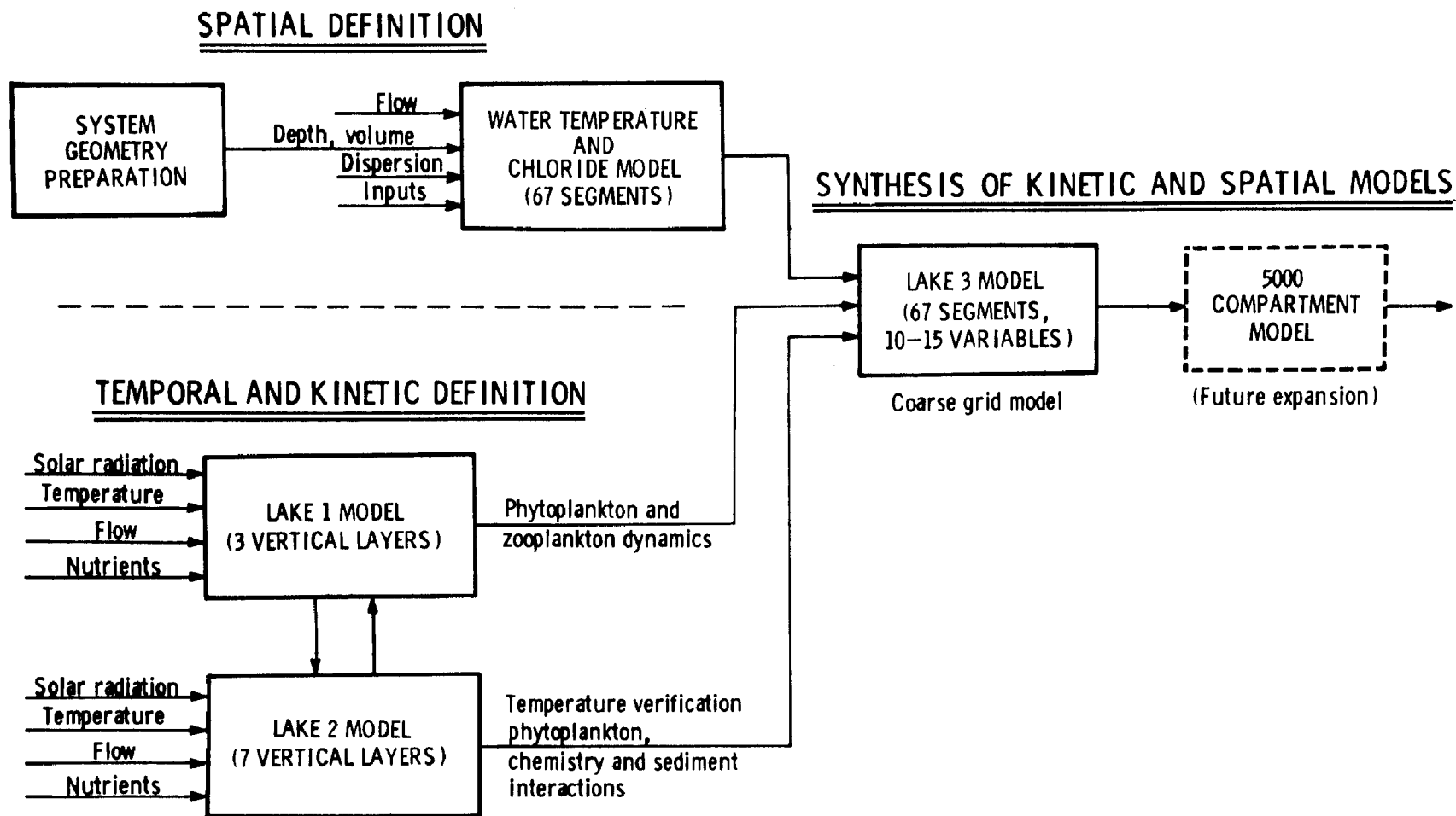


Figure 4. Eutrophication modeling strategy



As indicated, two parallel paths are being followed. The upper path involves the gathering of data on the lake geomorphology and transport and dispersion structure. The model used is a single variable model of water temperature or chlorides both representing tracer variables that can be used to validate various sectors of the inputted circulation. A three dimensional grid of 67 segments is employed.

The emphasis in the lower parallel path is on the sub-system kinetics with spatial detail held to a minimum. The lake is assumed to be horizontally completely mixed and is divided into a series of vertical layers. Attention is specifically directed to the interactions between phytoplankton, zooplankton and water chemistry. Two models, Lake 1 and Lake 2 are explored in this path.

The synthesis of the spatial definition of transport and mixing with the kinetic interactions is accomplished in Lake 3. This model, a coarse grid model, is three-dimensional and incorporates the major kinetic features of the Lake 1 and 2 models. With 67 segments and 10 variables, a total of 670 equations or "compartments" must be solved. Future expansion calls for an approximate order of magnitude increase in the number of compartments to 5000.

In this report, primary emphasis is placed on the Lake 1 model. As such, a detailed review of the kinetics employed in the models is given below for the biological and chemical sub-systems. The systems diagram for the Lake 1 model is shown in Figure 5. The Lake 2 model includes those variables for Lake 1 and also includes a representation of the carbon cycle.

#### PHYTOPLANKTON CHLOROPHYLL

The basic kinetic interactions, for phytoplankton chlorophyll, ( a measure of biomass) is given for a single volume,  $j$ , as

$$S_{p_j} = V_j (G_p - D_p)_j P_j - V_j \frac{w_{ji}}{H_j} P_j + V_i \frac{w_{ij}}{H_i} P_i \quad (4)$$



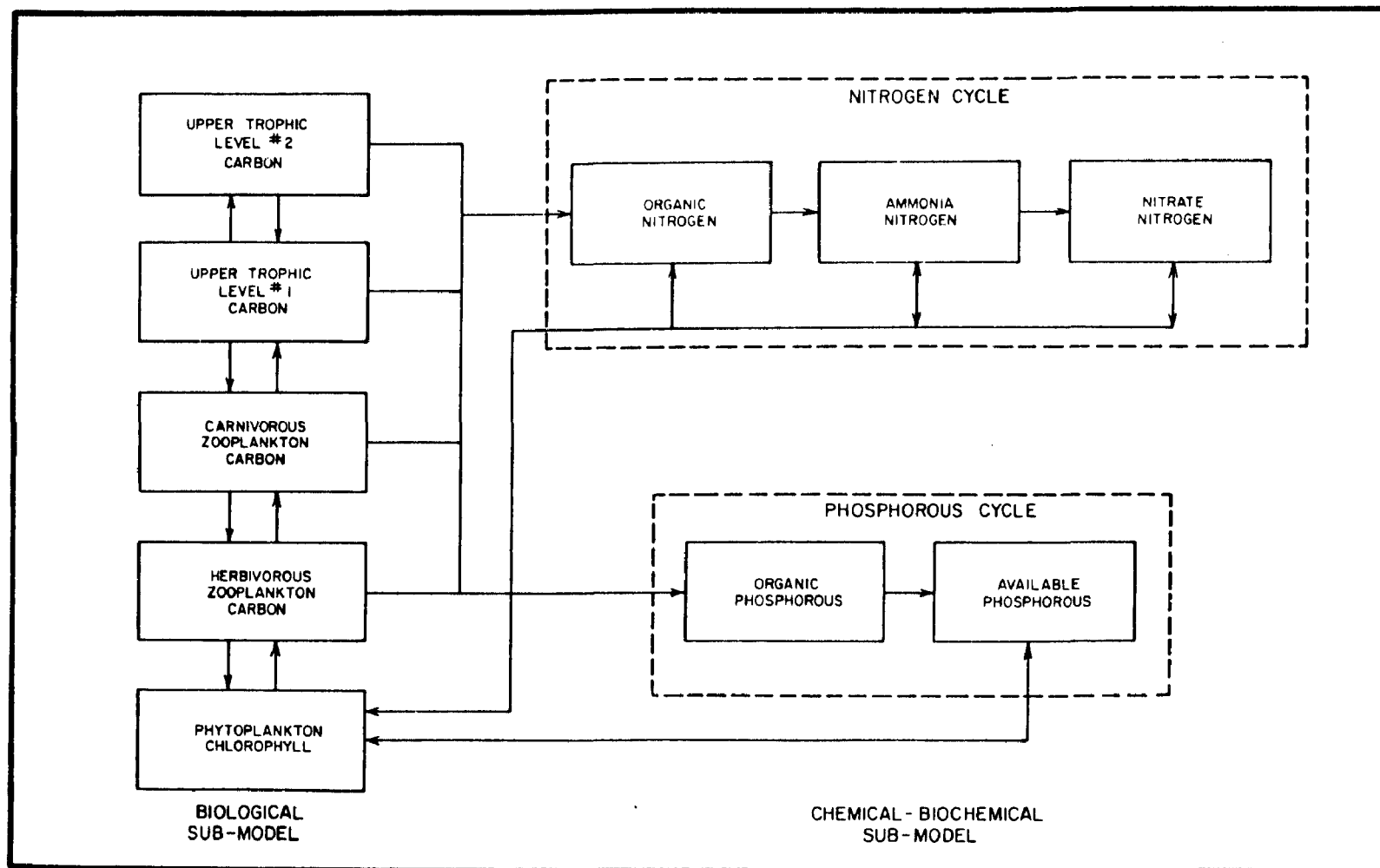


Figure 5. System diagram - Lake 1 model



where P is the phytoplankton chlorophyll ( $\mu\text{g/l}$ ),  $G_p$  and  $D_p$  are the growth and death rate (1/day) respectively and  $w_{ji}$  and  $w_{ij}$  are the sinking velocities of the phytoplankton between segments j and i.

#### Phytoplankton Growth Rate

The growth rate expression is similar to that developed previously (1) and as used in this work is given by

$$G_{pj} = G_1(G_{\max}, T) \cdot [I(I_a, I_s, k_e, P, H)] \cdot ([N'(K_{mn}, N_2, N_3)] [(K_{mp}, p_2)])$$

= (Temperature effect) . (Light effect) . (Nutrient effect) (5)

where  $G_{\max}$  is the maximum growth rate, T is water temperature,  $I_s$  is light intensity at  $G_{\max}$ ,  $I_a$  is incoming solar radiation,  $k_e$  is the extinction coefficient, H is the depth of the segment,  $k_{mn}$  is the half-saturation constant for total inorganic nitrogen,  $N'$ ,  $N_2$  is ammonia nitrogen,  $N_3$  is nitrate nitrogen,  $K_{mp}$  is the half-saturation constant for phosphorus and  $p_2$  is the available phosphorus. The temperature effect is given by Eppley<sup>4</sup> as:

$$G_1(T) = G_{\max} (1.066)^T \quad (6)$$

where Eppley reports  $G_{\max}$  at 0.587 (1/day). This form permits phytoplankton growth at low temperature and at 20°C, results in a growth rate of 2.1/day.

The function form for the light effect is as given in previous work<sup>(1)</sup> and incorporates vertical extinction of solar radiation and self-shading effects.

The form is

$$I = \frac{2,718f}{k_e H} (e^{-\alpha_1} - e^{-\alpha_0}) \quad (7)$$

where

$$k_e = k'_e + 0.0088P + 0.054P^{0.66}$$

$$\alpha_1 = \frac{I_a}{I_s} e^{-k_e H}$$

$$\alpha_0 = \frac{I_a}{I_s}$$



and  $k'_e$  is the light extinction coefficient at zero chlorophyll and  $f$  is the photoperiod. All pertinent variables are functions of  $j$ , the segment location.

The nutrient effect makes use of product Michaelis - Menten kinetics and is given by

$$N'p = \frac{N_2 + N_3}{k_{mn} + (N_2 + N_3)} \cdot \frac{P_2}{k_{mp} + P_2} \quad (8)$$

The range of values for  $K_{mn}$  and  $K_{mp}$ , the half-saturation constants for nitrogen and phosphorus respectively, has been documented previously <sup>(1)</sup>. More recent other work (5,6) tends to support the original range; namely  $K_{mn}$  in the range 5-50  $\mu\text{g N/l}$  and  $K_{mp}$  in the range 1-10  $\mu\text{g/l}$ . There is an obvious species dependence of this constant as well as a possible dependence on the eutrophic state of the lake. In the Lake 1 model,  $K_{mn}$  is used at 25  $\mu\text{g N/l}$  and  $K_{mp}$  of 1 and 10  $\mu\text{gP/l}$  is used as a range.

At the present time, silica limitation is not used in this model. Goering et al <sup>7</sup> and Paasche <sup>8</sup> have estimated the half-saturation value for silica at about .02 - .08  $\text{mg Si/l}$  for marine species. Under peak growing conditions in Lake Ontario, surface silica values are about 0.1-0.2  $\text{mg Si/l}$  which tends to indicate that silica may not have a significant effect on the growth rate. Work is in progress, however, to include this nutrient since at the lower concentration and higher Michaelis levels, it could be important.

The complete growth rate expression,  $G_{pj}$  is then given by the product of (6), (7) and (8). Although there is no a priori reason for using a product formulation, various experiments (see(1)) have tended to support the approach. Another expression has been proposed



on the grounds that Eq. (5) is too severe in reducing growth due to the product term. The alternate construct is (9):

$$G'_p = G_l \cdot \frac{3}{1/I + 1/N' + 1/p} \quad (9)$$

or in general

$$G'_p = G_i \cdot \frac{k}{\sum_i 1/\mu_i} \quad (10)$$

where  $k$  is a normalization factor and  $\mu_i$  represent the general reduction factors. In general, from (5) and (10):

$$G'_p > G_p$$

the extent of the inequality depending on  $\mu_i$ . Undoubtedly then, Eq. (5) will result in increased growth at least at some times; however, due to the coupling to the nutrient pool, such increased growth will in turn be more severe in its impact on the nutrients. Eq. (10) therefore appears to be less severe than Eq. (5), but only with respect to phytoplankton growth. In the final analysis, the validity of any of these formulations rests on the ability to reproduce observed data, barring any real theoretical reasoning. This has been done at least for the product nutrient terms in early work by Ketchum in 1934 (cited in (1)) and more recently by DiToro<sup>10</sup> for the flask experiments. The Lake 1 model, was modified to test the sensitivity of the solutions to Eq. (5) or Eq. (10) and to determine which expression seems to be more appropriate. The results of the comparison are discussed more fully below.

It can also be noted that the gross growth rate of the phytoplankton biomass,  $G_{pj}P_j$  is equivalent to the daily average productivity in the



jth segment. Thus,

$$v_j = a_{cc} G_{pj} P_j H_j \quad (11)$$

where  $v_j$  is the average rate of carbon fixation ( $\text{mgC/m}^2\text{-day}$ ) and  $a_{cc}$  is the carbon to chlorophyll ratio (range 20-100 $\text{mgC/mg Chlor}$ ).

#### Phytoplankton Death Rate

The expression for the death rate of the phytoplankton includes two primary effects: endogeneous respiration and predation by herbivorous zooplankton. The death rate is given by

$$D_{pj} = K_2 (1.08)^{T-20} + C_g Z_j \quad (12)$$

where  $K_2$  is a constant ( $1/\text{day}$ ),  $C_g$  is the grazing rate of the herbivorous zooplankton ( $\text{liters/day} - \text{mg zooplankton carbon}$ ) and  $Z$  is the carbon concentration of the herbivorous zooplankton. As noted below for the zooplankton observed in Lake Ontario, a filtering rate of .03 - .06  $\text{liters/mgC-day-}^\circ\text{C}$  appears appropriate and at  $20^\circ\text{C}$ , represents about 2-6 ml filtered per individual per day.

#### Phytoplankton Sinking

In Eq. (4), the sinking of phytoplankton from one segment to another segment can be a potentially significant sink or source of phytoplankton and associated nutrients. This phenomena is a complex one incorporating vertical turbulence effects, the density structure and the physiological state of different species of phytoplankton. For example, the generation of gelatinous sheaths by phytoplankton has been shown to be of importance in settling (11) and apparently the settling velocity of nutrient rich cells is somewhat less than cells that are nutritionally deficient (12).



Published values of the sinking velocity of phytoplankton, mostly in quiescent laboratory conditions range from 0.07 - 18 meters/day. In some instances, the settling velocity is zero or negative.

Burns and Pashley<sup>(13)</sup> have investigated the settling velocity profile of particulate organic carbon in Lake Ontario with an ingenious in situ measuring device. Their results show a general decrease of settling velocity with depth and a marked seasonal variation of settling velocity. For example, on July 19, 1972 settling velocity in the thermocline (about 10 m) was estimated at about - 0.3m/day, while at 50 meters depth, the settling velocity was about + 1.3m/day. But in March 1973, the velocity profile was all positive ranging from 0.9m/day at 20 meters to 0.1m/day at 140 meters. Overall, the values given by Burns and Pashley varied between - 0.4 and + 2.0m /day. These results and others tend to indicate that the settling velocity should be related in some way to the state of the phytoplankton biomass (e.g. actively growing versus declining phase) and/or vertical velocity variations. In this work however, the vertical settling velocity has been treated as a constant. As such, this effect is only approximately modeled and accordingly, the settling velocity has been treated as a constant over a range from .05m/day to 0.5m/day. The sensitivity of the results to the phytoplankton settling velocity is discussed below.

### Zooplankton Carbon

The measure of the herbivorous zooplankton population  $z^{(1)}$  is taken as the carbon content of the biomass and all sources of food for  $z^{(1)}$  are the phytoplankton chlorophyll. The general expression for a single volume  $j$  is therefore:

$$S_{z_j}^{(1)} = V_j (G_z^{(1)} - D_z^{(1)})_j z_j^{(1)} \quad (13)$$



where  $G_z^{(1)}$  and  $D_z^{(1)}$  are the growth and death rates respectively of  $Z^{(1)}$ . The form of  $G_z^{(1)}$  is

$$G_z^{(1)} = a_{zp} C_{gzp} K_g \frac{P}{K_g + P} \quad (14)$$

where  $a_{zp}$  is the zooplankton carbon to phytoplankton chlorophyll efficiency,  $C_{gzp}$  is the grazing rate of the herbivorous zooplankton and  $K_g$  is the half-saturation concentration of phytoplankton at which the growth of  $Z^{(1)}$  is half of maximum growth. This latter effect reflects the limiting growth of zooplankton at higher phytoplankton populations.

The mortality of the herbivorous zooplankton is given by two terms; endogenous respiration and grazing by the next highest trophic level.

Therefore:

$$D_z^{(1)} = K_z^{(1)}(T) + C_{g21}(T) Z^{(2)} \quad (15)$$

where  $K_z^{(1)}$  is the endogenous respiration rate as a function of temperature (1/day-°C),  $C_{g21}$  is the grazing rate (liters/day-mgC-°C) and  $Z^{(2)}$  is the next highest trophic level, designated by superscript (2).

Expressions for all trophic levels above the herbivorous zooplankton arranged in a linear food chain are similar to Eqs. (13) and (14).

Thus:

$$S_{z_j}^{(2)} = V_j (G_z^{(2)} - D_{z_j}^{(2)} Z_j^{(2)}) \quad (16)$$



where

$$G_z^{(2)} = a_z C_{g21} Z^{(1)} \quad (17)$$

and

$$D_z^{(2)} = K_z^{(2)}(T) + C_{g21}(T) Z^{(3)}$$

These expressions are an obvious oversimplification of a complex food web and reflect only a "linear" type of food chain (See Fig. 5). Indeed the effect of the zooplankton on the phytoplankton as formulated above is to always decrease the population, yet it has been shown (14) that zooplankton can also increase phytoplankton population or have no effect. The mechanism for an increase in the population is apparently through the passage of gelatinous green algae through the zooplankton gut with subsequent break-up of the colonies and regrowth after excretion. The smaller species are generally decreased in numbers by zooplankton grazing, specifically smaller diatoms and *Asterionella formosa*, which are characteristic of Lake Ontario.

The zooplankton of Lake Ontario are dominated by the crustaceans specifically of order copepoda and cladocera. Most hauls are made over 0-50 meter depth range. Principal cupepoid species given by Patalas<sup>15</sup> are *Cyclops bicuspidatus* and *Tropocyclops prasinus* and of the cladocerans: *Daphnia retrocurva* and *Bosmina longirostris*. In Patalas' work in 1967, these four species accounted for 91% of the total zooplankton and averaged about 60/liter from June - October.

Others (16, 17, 18) generally show values in a similar range in some cases up to a maximum of almost 200/liter. For use in biomass computations, conversions must be made to equivalent carbon. Such



conversion depends on age and accompanying weight of the animal and can therefore vary over a wide range. Watson et al<sup>18</sup> in their conversions used weights of species to arrive at total biomass and equivalently averaged about 2.8 $\mu$ g dry weight/ind.

The results using an average of 40% carbon by dry weight show peak values general in August at lakewide averages of between 0.07 - 0.12mg carbon/liter.

At the average dry weight of about 1-5 $\mu$ g/ individual grazing rates of about 0.8 - 2ml/ind - day are appropriate<sup>1,19</sup>. Indeed the rate for *Bosmina long.*, a dominant species in Lake Ontario has been given as 1-3ml/ind-day<sup>11</sup>. Grazing rates expressed as liters per mg zooplankton carbon per day have been assumed to be linearly related to temperature and have been used in the range of .03-.06 (l/mgC-day-<sup>o</sup>C) corresponding to the reported grazing ranges at 20°C.

#### NITROGEN SYSTEM

The basic equations for the nitrogen sub-system follow previous work (2,3) and include non-living organic nitrogen,  $N_1$ , ammonia nitrogen,  $N_2$  and nitrate nitrogen,  $N_3$ . The equation for the source - sink term for organic nitrogen is:

$$S_{N_{1,j}} = \frac{a_1}{a_c} \sum D_z Z + \frac{a_1}{a_c} P_j \left(1 - \frac{a_{zp} K_g}{K_g + P_j}\right) C_{gzp} Z^1 + a_1 D_p P - K_1 (T) N_1 \quad (18)$$

where  $a_1$  is nitrogen to chlorophyll ratio, and  $a_c$  is the carbon to chlorophyll ratio and  $K_1$  is the overall decay of  $N_1$ .



The first and third terms represent organic nitrogen released through endogenous respiration by the zooplankton and phytoplankton respectively and the second term represents the organic nitrogen of the grazed but unassimilated phytoplankton. The last term represents the decomposition, settling and other effects that contribute to the decay of organic nitrogen.

For ammonia,

$$S_{N_2j} = K_{12}(T)N_2 - K_{22}(T)N_2 - a_1 \alpha G_p P \quad (19)$$

where  $K_{12}$  is the rate of production of ammonia from organic nitrogen,  $K_{22}$  is the rate of oxidation of ammonia to nitrate, and  $\alpha$  is a preference factor given by

$$\alpha = \frac{N_2}{N_2 + N_3} \quad (20)$$

or is alternately set equal to one-half for an "indifferent" uptake of nitrogen. The last term represents the uptake of ammonia for phytoplankton growth. For nitrate,

$$S_{N_3,j} = K_{23} N_2 - a_1 (1-\alpha) G_p P \quad (21)$$

where  $K_{23} = K_{22}$ , the production of nitrate by ammonia oxidation.

#### PHOSPHORUS SYSTEM

The equations for the phosphorus cycle used in the models are as previously developed (2,3) and include non-living organic phosphorus and phosphorus available for phytoplankton growth. For organic phosphorus, the equation for the source and sink for  $p_1$  is:



$$S_{p1,j} = \frac{a_p}{a_c} \Sigma D_z Z + \frac{a_p}{a_c} P_j \left(1 - \frac{a_p K_g}{K_g + P_j}\right) C_g Z^{(1)} - K_1 P_1 \quad (22)$$

where  $a_p$  is the phosphorus to chlorophyll ratio and  $K_1$  represents a general decay of organic forms.

For the inorganic phosphorus, assumed as phosphorus available to the phytoplankton, the source-sink equation for  $p_2$  is:

$$S_{p2,j} = K_{12} (T) P_1 - a_p G_p P - K_{22} (T) P_2 \quad (23)$$

where  $K_{12}$  represents the rate of decomposition of organic phosphorus to forms available for phytoplankton utilization and  $K_{22}$  represents an overall loss of inorganic phosphorus.



## CHEMICAL MODELS - DISSOLVED CARBON DIOXIDE

The inclusion of chemical reactions into models of Great Lakes water quality, by contrast to the biochemical and biological reactions considered above, poses a new set of problems by virtue of the rapid rates and the highly non-linear forms of the governing reactions. Nevertheless, it appears that the problems can be handled nicely within the context of conservation of mass equations.

The investigation of purely chemical equilibrium models has been underway for quite some time. An altogether satisfactory presentation of these results is available.<sup>(20)</sup> Application of certain of these models to Great Lakes waters chemistry has been undertaken by Kramer in a series of important papers.<sup>(21,22)</sup> From this work it is clear that the biological reactions affect the chemical systems primarily via the assimilation of dissolved carbon dioxide during phytoplankton growth. From the point of view of the eutrophication problem, at issue are the purely chemical reactions which phosphorus undergoes; for example precipitation or dissolution of phosphate minerals. These reactions may be of practical importance in terms of the overall dynamics of the phosphorus in the lakes. The other chemically active phytoplankton nutrient, silica, may also be affected by purely chemical reactions involving the alumino-silicate minerals. Thus there are possible practical consequences of these purely chemical reactions so that their inclusion, at least on a preliminary basis, is warranted.

The presentation given below is based on the carbon dioxide - bicarbonate - carbonate equilibria primarily because of its importance as the major buffer system of the lakes, and because it can serve



as a prototype for all other such reactions. In fact the procedure is the same for the inclusion of all such reactions within the context of conservation of mass equations.

### Equilibrium Analysis

The carbonate equilibria is treated in the conventional way.<sup>(20,24)</sup> The major species considered are aqueous or dissolved  $[\text{CO}_2]$  (the concentration of hydrated  $\text{CO}_2$  being small), bicarbonate,  $[\text{HCO}_3^-]$ , and carbonate,  $[\text{CO}_3^{=}]$ , ion, together with the hydrogen,  $[\text{H}^+]$ , and hydroxyl,  $[\text{OH}^-]$ , ions. At first glance one is tempted to write mass balance equations for each of these species. However this is complicated by the fact that they undergo reversible ionization reactions, e.g.  $\text{CO}_2 + \text{H}_2\text{O} = \text{H}^+ + \text{HCO}_3^-$  which occur very rapidly relative to the time scales of mixing and gas transfer.<sup>(23)</sup> In fact it is clear that the individual species are each extremely reactive so that a direct mass balance formulation results in equations which are non-linear and numerically quite badly behaved.

The very fact that the ionization reactions are rapid leads to a much more tractable formulation in terms of quantities which are conservative relative to the ionization reactions. A formal mathematical discussion is given subsequently. However, it is easy to see the principle involved. Consider the total inorganic carbon concentration.

$$C_T = [\text{CO}_2] + [\text{HCO}_3^-] + [\text{CO}_3^{=}] \quad (24)$$

It is clear that any reversible ionization reaction will not affect the  $C_T$  of the system (we assume no carbonate precipitates are forming or dissolving.) Thus a mass balance equation for  $C_T$  can ignore the



ionization reactions since they are neither sources nor sinks of  $C_T$ .

The electroneutrality requirement can be used to obtain a second conservative quantity. Let  $\{M\}$  and  $\{L\}$  be the concentration in equivalents of the metal ions and ligands, e.g.  $N_a^+$ ,  $K^+$ ,  $C_a^{++}$ , ..., and  $Cl^-$ ,  $SO_4^{=}$  ..., which are present and assumed not to react appreciably with the carbonate or hydrogen-hydroxide species. Then it is clear that a charge balance equation:

$$\{M\} - \{L\} = [HCO_3^-] + 2[CO_3^{=}] + [OH^-] - [H^+] \quad (25)$$

is unaffected by ionization reactions so that the quantity called alkalinity

$$[Alk] = \{M\} - \{L\} \quad (26)$$

is also conservative in the sense that a mass balance equation for Alk need not consider ionization sources or sinks. It can be shown there are no other independent conservative quantities for this system, the other common conservative quantities<sup>(20)</sup> are linear combinations of  $C_T$  and A.

If  $C_T$  and Alk are known, the concentration of all the species being considered is easily obtained. In fact, using the equilibrium equations<sup>(20,24)</sup>

$$\begin{aligned} [H^+] [OH^-] &= K_W \\ [H^+] [HCO_3^-] &= K_1 [CO_2] \\ [H^+] [CO_3^{=}] &= K_2 [HCO_3^-] \end{aligned} \quad (27)$$



it is true that<sup>(24)</sup>

$$\text{Alk} = \alpha(\text{H}) C_{\text{T}} + \gamma(\text{H}) \quad (28)$$

where

$$\alpha(\text{H}) = \frac{1 + 2K_2/[\text{H}^+]}{1 + [\text{H}^+]/K_1 + K_2/[\text{H}^+]} \quad (29)$$

and

$$\gamma(\text{H}) = K_{\text{W}}/[\text{H}^+] - [\text{H}^+] \quad (30)$$

It does not seem to have been noticed that if the alkalinity concentration is large relative to  $\gamma(\text{H}) = [\text{OH}^-] - [\text{H}^+]$ , which is the common situation then, eq. (28) becomes

$$\frac{\text{Alk}}{C_{\text{T}}} = \alpha(\text{H}) \quad (31)$$

so that only the ratio of alkalinity to total inorganic carbon is important in determining the resulting pH whenever  $\text{Alk} \approx \text{Alk} + [\text{H}^+] - [\text{OH}^-]$ . Using tabulated values of  $K_1$  and  $K_2$  for pure water Figure 6 illustrates the pH,  $\text{Alk}/C_{\text{T}}$  relationship as a function of temperature. These figures are most useful since they represent the carbonate equilibria completely as a function of the ratio of the critical conservative quantities. Taken together with the conventional log concentration plot of the species versus pH, they provide a complete picture of the behavior of the equilibria.



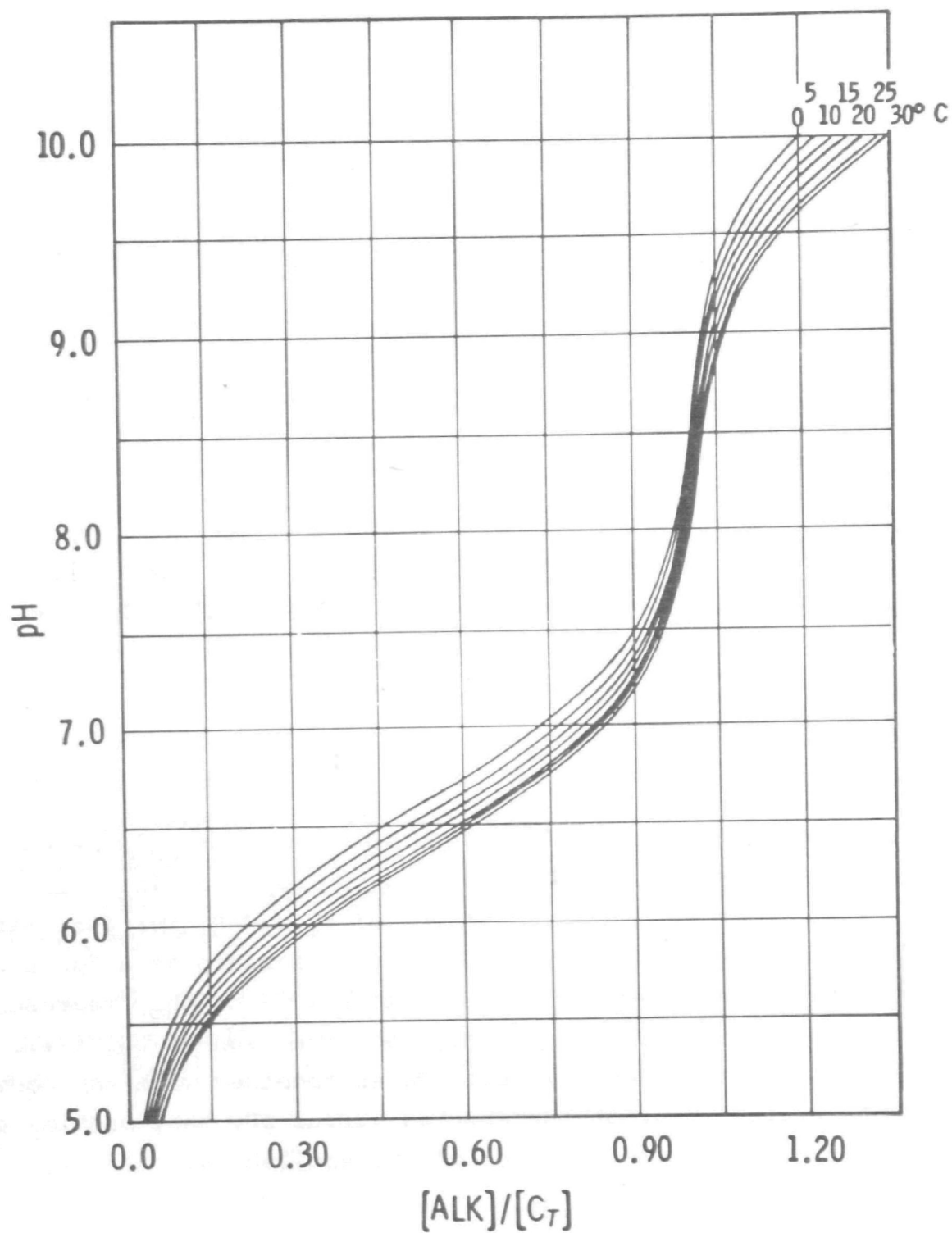


Figure 6. Relationship of pH and the ratio,  $Alk/C_T$



The equations which govern the distribution of Alk and  $C_T$  are available as mass balances, independent of the ionization reactions. For example, in a one dimensional vertical model the equations would be

$$\frac{\partial [\text{Alk}]}{\partial t} - \frac{1}{A} \frac{\partial}{\partial z} (EA \frac{\partial [\text{Alk}]}{\partial z}) = S_{\text{Alk}} \quad (32)$$

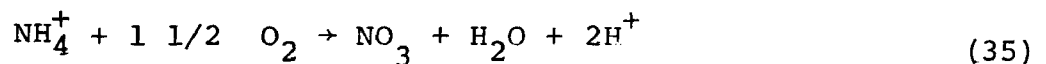
$$\frac{\partial [C_T]}{\partial t} - \frac{1}{A} \frac{\partial}{\partial z} (EA \frac{\partial [C_T]}{\partial z}) = S_{C_T} \quad (33)$$

with a zero mass flux boundary condition at  $z=0$  for alkalinity and an air-water exchange condition for  $C_T$  :

$$-EA \frac{\partial [C_T]}{\partial z} = K_L (CO_2(g) - CO_2(aq)) \quad (34)$$

representating the exchange of carbon dioxide. The difficulty in solving these equations is due to this non-linear boundary condition since  $CO_2(aq)$  is a non-linear function of the dependent variables of the problem:  $[\text{Alk}]$  and  $[C_T]$ , so that a numerical procedure is required.

The internal sources and sinks of alkalinity and inorganic carbon are due to biological reactions. For example, the nitrification reaction (if bacterial synthesis is ignored) can be represented as:



so that as ammonia is oxidized to nitrate, alkalinity is consumed (i.e.  $H^+$  is produced) and a term representing this sink of alkalinity would be included in the expression of  $S_{\text{Alk}}$ .



Similarly as phytoplankton grow they utilize inorganic carbon and this sink would be included in  $S_{C_T}$ . These mass balance equations would then be solved in conjunction with the equations for the other species of interest.

### Linear Approximation

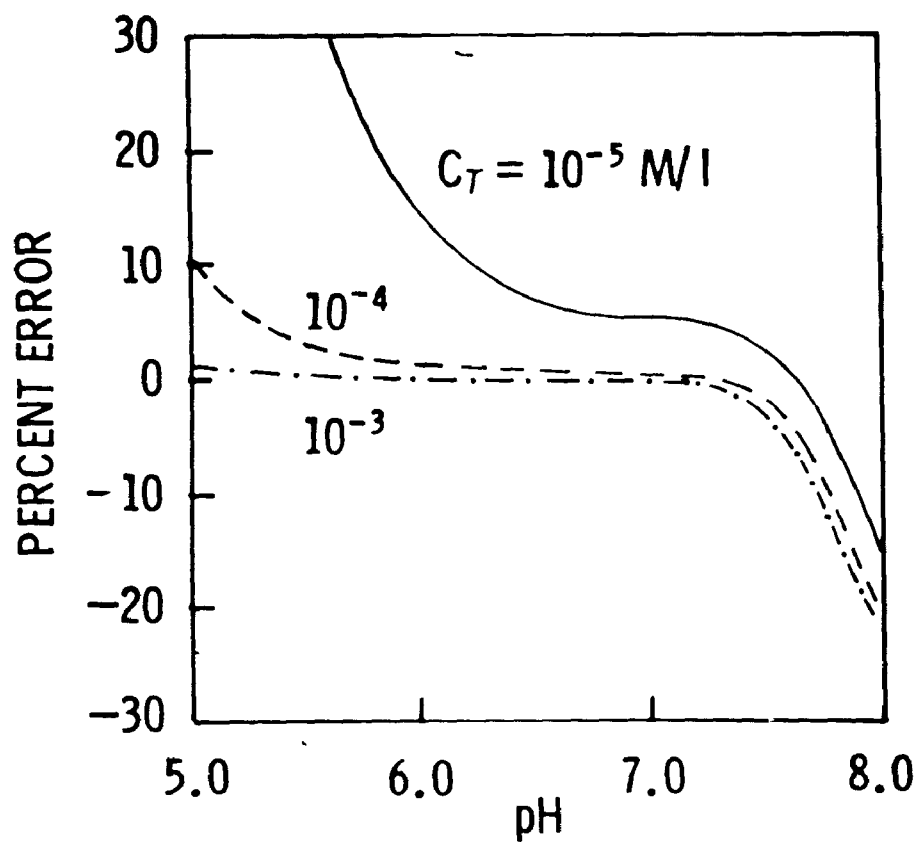
It is clear that mass balance equations which ignore the ionization reactions are only correct if the dependent variable is conservative relative to these reactions. Consider the conservative quantity  $[C_T] - [Alk] = [CO_2 - Acidity]$ . Clearly it is conservative since it is the difference of conservative quantities. From eqs. (24), (25) and (26), it is the case that

$$[CO_2 - Acy] = [CO_2] + [H^+] - [CO_3^{=}] - [OH^-] \quad (36)$$

But this equation implies that over a certain range of pH and  $C_T$ , the major component of  $CO_2$ -acidity is  $[CO_2]$  itself. Figure 7 presents the % error in the approximation  $[CO_2 - Acy] \approx [CO_2]$ . The chemical reasoning which leads to the same conclusion begins with the observation that in the above pH range, the alkalinity is primarily bicarbonate ion. If a source introduces only carbon dioxide, this does not change the alkalinity; therefore the concentration of bicarbonate remains constant. Hence the introduced  $CO_2$  does not ionize to  $HCO_3^-$  and  $H^+$  but rather remains as  $CO_2$ . Hence ionization reactions can be ignored. Thus from eqs. (32) and (33) the mass balance equation for  $CO_2$ -Acidity is

$$\frac{\partial [CO_2 - Acy]}{\partial t} - \frac{1}{A} \frac{\partial}{\partial z} \left( EA \frac{\partial [CO_2 - Acy]}{\partial z} \right) = S_{C_T} - S_{Alk} \quad (37)$$





Percent error: 
$$\frac{\text{CO}_2(\text{approx}) - \text{CO}_2}{\text{CO}_2} 100$$

Error in approximation:

$$[\text{CO}_2(\text{aq})] = [\text{CO}_2 - \text{acidity}]$$

Figure 7. Per cent error in assuming  
 $[\text{CO}_2 - \text{Acy}] \approx [\text{CO}_2]$



and the reaeration source of  $[\text{CO}_2\text{-Acy}]$  can be approximated as  $K_L ([\text{CO}_2]_{\text{sat}} - [\text{CO}_2 - \text{Acy}])$  so that within the errors in Fig.

7 the equation for  $[\text{CO}_2\text{-Acidity}]$  is linear. And since the alkalinity equation is also linear, simple analytical solutions are available and superposition can be applied to buildup a solution when many sources and sinks are active. This is in contrast to the non-linear  $C_T$  equation which must be solved with all sources and sinks at once, a situation which is quite inconvenient. Unfortunately this linear region does not include the pH range typically encountered in the Great Lakes so that this simplification is not available. However, for more acid situations this simplification provides a useful and direct avenue for the solution of the inorganic carbon - alkalinity mass balance equation.

#### Temperature Dependence of the Equilibrium Constants

The equilibrium constants of the dissolved carbon system are rather strong functions of temperature so that this effect must be taken into account. The implimentation of this dependency poses no serious problem since standard curve fitting techniques can be applied to the experimental data. However, such an approach lacks a certain elegance and generality. It turns out, however, that for the temperature ranges encountered in natural waters there is an entirely satisfactory solution available based on the thermodynamic constants of the reactions.

It is well known that the equilibrium constant,  $K$ , of a reversible reaction is related to the change in Gibbs free energy of the reaction at standard state,  $\Delta G_r^\circ$  via the equation:

$$\ln K = - \frac{\Delta G_r^\circ}{RT} \quad (38)$$



where

$$\Delta G_r^\circ = \sum_{\text{products}} \Delta G_f^\circ - \sum_{\text{reactants}} \Delta G_f^\circ$$

$\Delta G_f^\circ$  = the Gibbs free energy of formation

R = universal gas constant

T = temperature °K

and further that the free energy change is related to the change in enthalpy,  $\Delta H_r^\circ$  and entropy,  $\Delta S_r^\circ$  as follows:

$$\Delta G_r^\circ = \Delta H_r^\circ - T \Delta S_r^\circ \quad (39)$$

Hence the equilibrium constant is given by:

$$\ln K = -\frac{\Delta H_r^\circ}{RT} + \frac{\Delta S_r^\circ}{R} \quad (40)$$

This equation is strictly true at any temperature; the difficulty is that  $\Delta H_r^\circ$  and  $\Delta S_r^\circ$  are also functions of temperature. The conventional temperature at which they are available is 298.15 °K or 25°C. Table 5 presents the relevant thermodynamic properties for the carbonate system and Table 6 gives the properties for the reactions of interest.

Two approximations are investigated:

- (1) Assume that  $\Delta H_r^\circ$  and  $\Delta S_r^\circ$  are constants over the temperature range of interest (20)
- (2) Apply a correction which attempts to evaluate the change in the specific heat as a function of temperature (26)



TABLE 5 -  
THERMODYNAMIC PROPERTIES AT 25°C

Compound	$\Delta H_f^\circ$ (kcal/mole)	$\Delta G_f^\circ$ (kcal/mole)	$\Delta S_f^\circ$ (cal/deg mole)
CO <sub>2</sub> (g)	-94.051	-94.254	51.06
H <sub>2</sub> CO <sub>3</sub> (aq)*	-167.22	-148.94	44.8
HCO <sub>3</sub> <sup>-</sup>	-165.39	-140.26	21.8
CO <sub>3</sub> <sup>=</sup>	-161.84	-126.17	-13.6
H <sup>+</sup>	0	0	0
H <sub>2</sub> O	-68.315	-56.687	16.71
OH <sup>-</sup>	-54.970	-37.594	-2.57

Source: Wagman, 1968 (25)

\* H<sub>2</sub>CO<sub>3</sub>(aq) = H<sub>2</sub>CO<sub>3</sub> + CO<sub>2</sub>(aq); [H<sub>2</sub>CO<sub>3</sub>(aq)] ≈ [CO<sub>2</sub>(aq)]

TABLE 6  
THERMODYNAMIC PROPERTIES AT 25°C

Reaction	$\Delta H_r^\circ$ (kcal/mole)	$\Delta S_r^\circ$ (cal/deg mole)
1. H <sub>2</sub> O = H <sup>+</sup> + OH <sup>-</sup>	13.345	-19.28
2. CO <sub>2</sub> (g) + H <sub>2</sub> O = H <sub>2</sub> CO <sub>3</sub>	-4.854	-22.97
3. H <sub>2</sub> CO <sub>3</sub> = H <sup>+</sup> + HCO <sub>3</sub> <sup>-</sup>	1.830	-23.0
4. HCO <sub>3</sub> <sup>-</sup> = H <sup>+</sup> + CO <sub>3</sub> <sup>=</sup>	3.55	-35.4



The equation for the second approximation is:

$$\ln K = \frac{1}{RT} [-\Delta H_r^\circ + \tau(T) \Delta S_r^\circ] \quad (41)$$

where

$$\tau(T) = T_r - \frac{\theta}{w} [1 - e^{(T-T_r)/\theta}] \quad (42)$$

and

$$\begin{aligned} T_r &= 298.15 \text{ }^\circ\text{K} \\ \theta &= 219. \\ w &= 1.00322 \end{aligned}$$

These approximations are compared to the experimental equilibrium constants in Table 7. As can be seen the approximations are quite good with the non-linear relationship giving somewhat better results at the lower temperatures. Thus to within a few percent these approximations are quite adequate.

#### Simple Equilibrium Models - Exploratory Calculations:

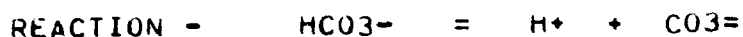
In order to explore the computational feasibility of including chemical reactions in water quality models a series of computations have been performed utilizing the Rand Chemical Composition Program<sup>(27)</sup>. It is expected that this computer program will form the basis for the chemical submodel calculations to be included in Great Lakes water quality models.

The computations are for the system  $\text{CO}_2 - \text{H}_2\text{O}$  for which the partial pressure of  $\text{CO}_2(\text{g})$  is fixed and varying amounts of acidity and alkalinity are added. The results are computed for the temperature range  $0^\circ$  to  $30^\circ\text{C}$  using the linear approximation for the temperature



TABLE 7

## TEMPERATURE DEPENDENCE COMPARISON



ENTHALPY OF REACTION = 3550.0000 CAL/MOLE  
 ENTROPY OF REACTION = -35.4000 CAL/DEG-MOLE

TEMP (°C)	EXPERIMENTAL PK	METHOD 1 <sup>(20)</sup> PK	PER CENT ERROR	METHOD 2 <sup>(26)</sup> PK	PER CENT ERROR
0.0	10.6250	10.5770	-.45	10.6181	-.07
5.0	10.5570	10.5260	-.29	10.5523	-.04
10.0	10.4900	10.4767	-.13	10.4917	.02
15.0	10.4300	10.4292	-.01	10.4360	.06
20.0	10.3770	10.3832	.06	10.3852	.08
25.0	10.3290	10.3389	.10	10.3389	.10
30.0	10.2900	10.2959	.06	10.2970	.07



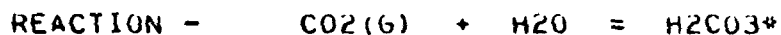
ENTHALPY OF REACTION = 1830.0000 CAL/MOLE  
 ENTROPY OF REACTION = -23.0000 CAL/DEG-MOLE

TEMP (°C)	EXPERIMENTAL PK	METHOD 1 <sup>(20)</sup> PK	PER CENT ERROR	METHOD 2 <sup>(26)</sup> PK	PER CENT ERROR
0.0	6.5790	6.4908	-1.34	6.5175	-.93
5.0	6.5170	6.4645	-.81	6.4816	-.54
10.0	6.4640	6.4391	-.38	6.4489	-.23
15.0	6.4190	6.4146	-.07	6.4191	.00
20.0	6.3810	6.3909	.16	6.3922	.18
25.0	6.3520	6.3681	.25	6.3681	.25
30.0	6.3270	6.3459	.30	6.3466	.31



TABLE 7

## TEMPERATURE DEPENDENCE COMPARISON (continued)



ENTHALPY OF REACTION = -4854.0000 CAL/MOLE

ENTROPY OF REACTION = -22.9700 CAL/DEG-MOLE

TEMP (°C)	EXPERIMENTAL PK	METHOD 1 <sup>(20)</sup> PK	PER CENT ERROR	METHOD 2 <sup>(26)</sup> PK	PER CENT ERROR
0.0	1.1100	1.1364	2.37	1.1630	4.78
5.0	1.1900	1.2062	1.36	1.2233	2.80
10.0	1.2700	1.2735	.28	1.2832	1.04
15.0	1.3200	1.3385	1.40	1.3430	1.74
20.0	1.4100	1.4013	-.62	1.4026	-.53
25.0	1.4700	1.4620	-.54	1.4620	-.54
30.0	1.5300	1.5207	-.61	1.5214	-.56



ENTHALPY OF REACTION = 13345.0000 CAL/MOLE

ENTROPY OF REACTION = -19.2800 CAL/DEG-MOLE

TEMP (°C)	EXPERIMENTAL PK	METHOD 1 <sup>(20)</sup> PK	PER CENT ERROR	METHOD 2 <sup>(26)</sup> PK	PER CENT ERROR
0.0	14.9435	14.8911	-.35	14.9134	-.20
5.0	14.7338	14.6991	-.24	14.7135	-.14
10.0	14.5346	14.5140	-.14	14.5221	-.09
15.0	14.3463	14.3352	-.08	14.3390	-.05
20.0	14.1669	14.1626	-.03	14.1636	-.02
25.0	13.9965	13.9958	-.01	13.9958	-.01
30.0	13.8330	13.8344	.01	13.8350	.01



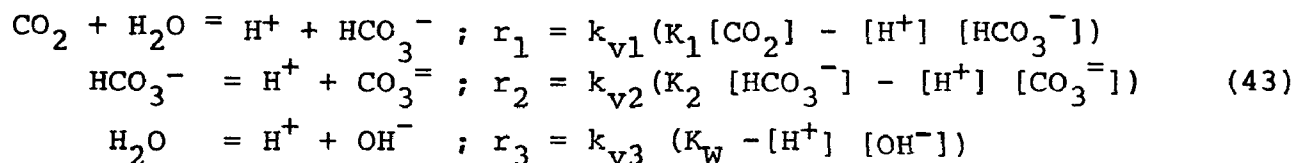
dependence of  $\Delta G_r^\circ$  for the three reactions of interest. Fig. 8(a) gives the total inorganic carbon that is in equilibrium with an atmosphere for which the partial pressure of  $\text{CO}_2(\text{g})$  is  $10^{-3.5}$  atmospheres. As alkalinity is added the  $C_T$  increases and it is approximately true that  $[C_T] \approx [\text{Alk}]$  with the pH in the range 7.5 to 8.5. The temperature effects change the pH of the resulting solutions by approximately 0.25 pH units as shown in Fig. 8(b).

For varying partial pressures of  $\text{CO}_2(\text{g})$  and  $\text{Alk}=0$ , the results are shown in Fig. (8)c and (8) d. A substantial temperature effect occurs with the  $C_T$  in solution varying by a factor of two over the range of interest, whereas the pH variation is smaller, due to its logarithmic units.

Computation time for the numerical solution of one set of conditions is on the order of 0.1 sec. of cpu time on a CDC 6600. Thus for daily evaluations of the chemistry for a year simulation for ten layers would consume on the order of 300 seconds, which is not excessive so that the computation is feasible.

### Theoretical Considerations

A formal derivation of equations (32) and (33) requires that ionization reactions be considered explicitly as sources and sinks of the components. Assume that the following three reactions are the mechanisms by which hydration and ionization take place:





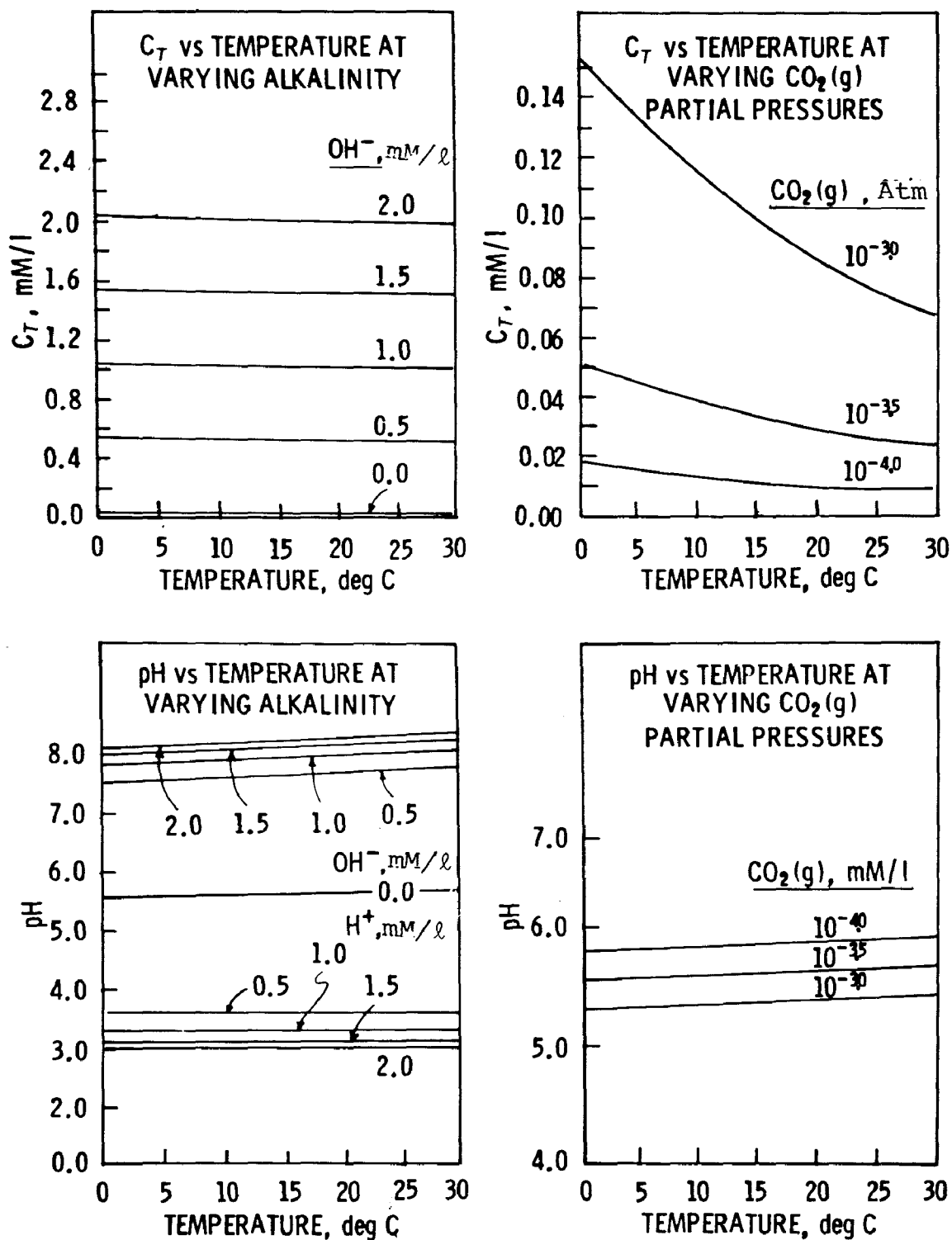


Figure 8. Computations for  $\text{CO}_2$  -  $\text{H}_2\text{O}$  system



and that the law of mass action correctly describes the rates of reaction as indicated. For notational convenience let  $D$  denote the mass transport differential operator, i.e. the lefthand side of eqs. (32) and (33) are denoted by  $D[\text{Alk}]$  and  $D[C_T]$ . The conservation of mass equations for each species is obtained by equating mass transport to sources and sinks:

$$D[\text{CO}_2] = -r_1 + S_{\text{CO}_2} \quad (44)$$

$$D[\text{H}^+] = r_1 + r_2 + r_3 + S_{\text{H}} \quad (45)$$

$$D[\text{HCO}_3^-] = r_1 - r_2 + S_{\text{HCO}_3} \quad (46)$$

$$D[\text{CO}_3^{=}] = r_2 + S_{\text{CO}_3} \quad (47)$$

$$D[\text{OH}^-] = r_3 + S_{\text{OH}} \quad (48)$$

The  $S$ 's are whatever direct sources of the species exist, and the  $r$ 's are the rates associated with the assumed reactions. It is, of course, possible in principle to solve these simultaneous nonlinear differential equations numerically. The values chosen for the  $k_v$ 's would be large enough so that the solution is unaffected by their magnitude. This procedure has been tried and found to be quite unstable numerically, the cause being the "stiffness" of the equations due to the large reaction rates which makes convergence difficult to achieve. Also the  $k_v$ 's are, in a sense, artifacts of the formulation since they are present only to introduce the ionizations correctly in a formulation that requires such reactions to be included as kinetic expressions. Therefore it would be convenient to obtain equations which are devoid of the reaction rates entirely. This can be done by defining new



variables which are appropriate sums of the species in such a way that the reaction terms cancel out. Thus if  $C_T = [\text{CO}_2] + [\text{HCO}_3^-] + [\text{CO}_3^{=}]$  then by adding eqs. (44), (46) and (47) the result is

$$DC_T = S_{\text{CO}_2} + S_{\text{HCO}_3} + S_{\text{CO}_3} \quad (49)$$

The other variable is, of course,

$$\text{Alk} = [\text{HCO}_3^-] + 2 [\text{CO}_3^{=}] + [\text{OH}^-] - [\text{H}^+] \quad (50)$$

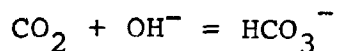
and since D is a linear operator,

$$D[\text{Alk}] = D[\text{HCO}_3^-] + 2D[\text{CO}_3^{=}] + D[\text{OH}] - D[\text{H}^+] \quad (51)$$

and using eqs. (45), (46), (47), and (48) the result is eq.(32) as before, with the r's cancelling out in a satisfying way.

So far no approximations have been made; the equations for Alk and  $C_T$  are exact, regardless of the magnitude of the  $k_v$ 's. They are the invariants of the reactions<sup>(28)</sup> in the sense that their values are unchanged by the kinetics. The approximation, and it is an excellent one for this application, is to compute the concentrations of the species from the equilibrium expressions, eq. (27), rather than the differential equations (44-48)

There is a slight theoretical flaw in the above derivation since the explicit forms are assumed for the reactions considered and a reaction of the form.



was not explicitly considered. It is a simple matter to verify that



the inclusion of this reaction does not affect the validity of the resulting equations for  $Alk$  and  $C_T$  but no guarantee has been presented that such a reaction does not exist. This can be done (28) although it requires some results from linear vector space theory. The crux of the demonstration lies in showing that the subspace spanned by the reactions implied by the equilibrium equations is orthogonal to the subspace spanned by the invariant quantities,  $Alk$  and  $C_T$ , and that the dimension of the orthogonal subspace is two which implies that no other independent invariant quantities exist, and that the dimension of the reaction subspace is three, indicating that all the possible reactions have been taken into account for the five quantities of interest

The theoretical framework and a theorem which indicates that the invariant quantities are always easy to find has been structured. (29) The results are essentially a generalization of the previous derivations.



## SECTION V

### REFERENCES

1. DiToro, D.M., D.J. O'Connor and R.V. Thomann. "A dynamic model of the phytoplankton population in the Sacramento - San Joaquin Delta," Advances in Chemistry No. 106, pp.131-180. American Chemical Society, Washington, D.C. 1971.
2. Hydrosience, Inc. Limnological Systems Analysis of the Great Lakes. Prepared for Great Lakes Basin Commission. Westwood, N.J. 474 pp. 1933.
3. Thomann, R.V., D.M. DiToro and D.J. O'Connor. "Preliminary model of Potomac Estuary phytoplankton," Journal of Environmental Engineering Division, ASCE 100(SA3):699-715. 1974.
4. Eppley, R.W. "Temperature and phytoplankton growth in the sea," Fishery Bulletin 70(4):1063-85. 1972.
5. Caperon J. and J. Meyer. "Nitrogen-limited growth of marine phytoplankton - II. Uptake kinetics and their role in nutrient limited growth of phytoplankton," Deep Sea Research 19:619-32. 1972.
6. Hendrey, G.R. and E. Welch. The Effects of Nutrient Availability and Light Intensity on the Growth Kinetics of Natural Phytoplankton Communities. Presented at 36th Meeting of the American Society of Limnology and Oceanography, Salt Lake City, Utah. June 1973.



7. Goering, J.J., D.N. Nelson and J.A. Carter. "Silicic acid uptake by natural populations of marine phytoplankton, "Deep Sea Research 20(9):777-89. 1973.
8. Paasche, E. "Silicon and the ecology of marine plankton diatoms, I. *Thalassiosira pseudomona* (Cyclotella Nana) grown in a chemostat with silicate as limiting nutrient," Marine Biology 19:117-126. 1973.
9. Bloomfield, J.A., R.A. Park, D. Scavia and C.S. Zahorcak. "Aquatic modeling in the eastern deciduous forest biome, U.S.," in Modeling the Eutrophication Process (E.J. Middlebrooks, H. Falkenborg and T.E. Maloney, editors), pp.139-158. Workshop proceedings of the International Biological Program. Utah Water Res. Lab., Logan. 1973.
10. DiToro, D.M. An evaluation of phytoplakton kinetic behavior in flask experiments. In preparation. 1974.
11. Hutchinson, G.E. A Treatise on Limnology, Vol. II: Introduction to Lake Biology and the Limnoplankton. J. Wiley & Sons, N.Y. 601 pp. 1967.
12. Yentsch, C.S. "Marine plankton," in Physiology and Biochemistry of Algae (R.A. Lwein, editor), pp.771-797. Academic Press, N.Y. 1962.
13. Burns, N.M. and A.E. Pashley. "In situ measurement of the settling velocity profile of particulate organic carbon in Lake Ontario," Jour. Fish Res. Bd. of Canada 31(3):291-297. 1974.



14. Porter, K.G. "Selective grazing and differential digestion of algae by zooplankton," Nature 244(5412):179-180. 1973.
15. Patalas, K. "Composition and horizontal distribution of crustacean plankton in lake ontario," Jour. Fisheries Res. Bd. of Canada 26(8):2135-2164. 1969.
16. Glooschenko, W., J.E. Moore and R.A. Vollenweider. "The seasonal cycle of phaeo-pigments in Lake Ontario with particular emphasis on the role of zooplankton grazing," Limn. & Ocean. 17(4):597-605. 1972.
17. McNaught, D.C. and M. Buzzard. "Zooplankton production in Lake Ontario as influenced by environmental perturbations," in First Annual Reports of the EPA/IFYGL Projects, NERC-ORD, EPA-660/3-73-021, pp.28-70. U.S. Environmental Protection Agency, National Environmental Research Center, Corvallis, Oregon. 1973.
18. Watson, N.H.F. and G.F. Carpenter. "Seasonal abundance of crustacean zooplankton and net plankton biomass of Lakes Huron, Erie and Ontario," Jour. Fish. Res. Bd. of Canada 31(3):309-317. 1974.
19. Kibby, N.V. "Effects of temperature on the feeding behavior of *Daphnia Rosea*," Limn. & Ocean 16(3):580-581. 1971.



20. Stumm, W. and J.J. Morgan. Aquatic Chemistry. Wiley-Interscience, New York. 1970.
21. Kramer, J.R. "Theoretical model for the chemical composition of fresh water with application to the Great Lakes," in Pub. No. 11, pp.149-160. Great Lakes Research Division. 1964.
22. Kramer, J.R. "Equilibrium models and composition of the Great Lakes," in Equilibrium Concepts in Natural Water Systems, Adv. in Chemistry Series No. 67, pp.243-254. American Chemical Society, Washington, D.C. 1967.
23. Kern, D.M. "The hydration of carbon dioxide," J. Chem 37(1):14-22. 1960.
24. Trussell, R.R. and J.F. Thomas. "A discussion of the chemical character of water mixtures," J.AWWA 63(1):49-51. 1971.
25. Wagman, D.C., W.H. Evans, V.B. Parker, I. Halow, S.M. Bailey and R.H. Schumm. "Selected values of chemical thermodynamic properties," Technical Note 270-3. National Bureau of Standards. Jan. 1968.
26. Helgeson, H.C. "Thermodynamics of complex dissociation in aqueous solution at elevated temperatures," J. Phys. Chem. 71:3121-3136. 1967.
27. Shapley, M. and L. Cutler. Rand's Chemical Composition Program: A Manual. Report R-495-PR, Rand Corp., Santa Monica, California. June 1970.



## REFERENCES (Continued)

28. Shapiro, N. Analysis by Migration in the Presence of Chemical Reaction. Report, P. 2596, Rand Corp., Santa Monica, California. June 1962.
29. DiToro, D.M. "Combining Chemical Equilibrium and Water Quality Models." Manhattan College, Bronx, N.Y. Oct. 1974.



## SECTION VI

### LAKE 1 MODEL

#### BASIC STRUCTURE AND EQUATIONS

Because of the complexity of the overall modeling structure, a simplified version of the lake has been developed to explore the kinetic behavior in greater detail. This is indicated in the modeling strategy of Fig. 4. The simplified model, designated Lake 1, assumes that Lake Ontario is well mixed horizontally and gradients are allowed to develop only in the vertical dimension. Such a simplification obviously does not permit near-shore vs. open-lake comparisons or the effect of the Rochester or Toronto discharges on the local lake environment. However, an inspection of the data on nutrients and chlorophyll does not appear to indicate substantial horizontal gradients although variations do exist in certain areas. (Lake Ontario can be contrasted in this regard to Lake Huron with marked horizontal gradients from Saginaw Bay or Lake Erie with important horizontal gradients from the Western Basin to the Eastern Basin.)

Because of the complexity of the interactive systems and most importantly, the computational time involved in obtaining solutions, the horizontally well-mixed assumption appears to offer a reasonable starting point for understanding the dynamic behavior of Lake Ontario. Fig. 9 is a schematic of the Lake 1 model and shows the three vertical segments that comprise the basis geometry. The principal physical features included are (a) horizontal transport, (b) vertical dispersion between the epilimnion and hypolimnion and



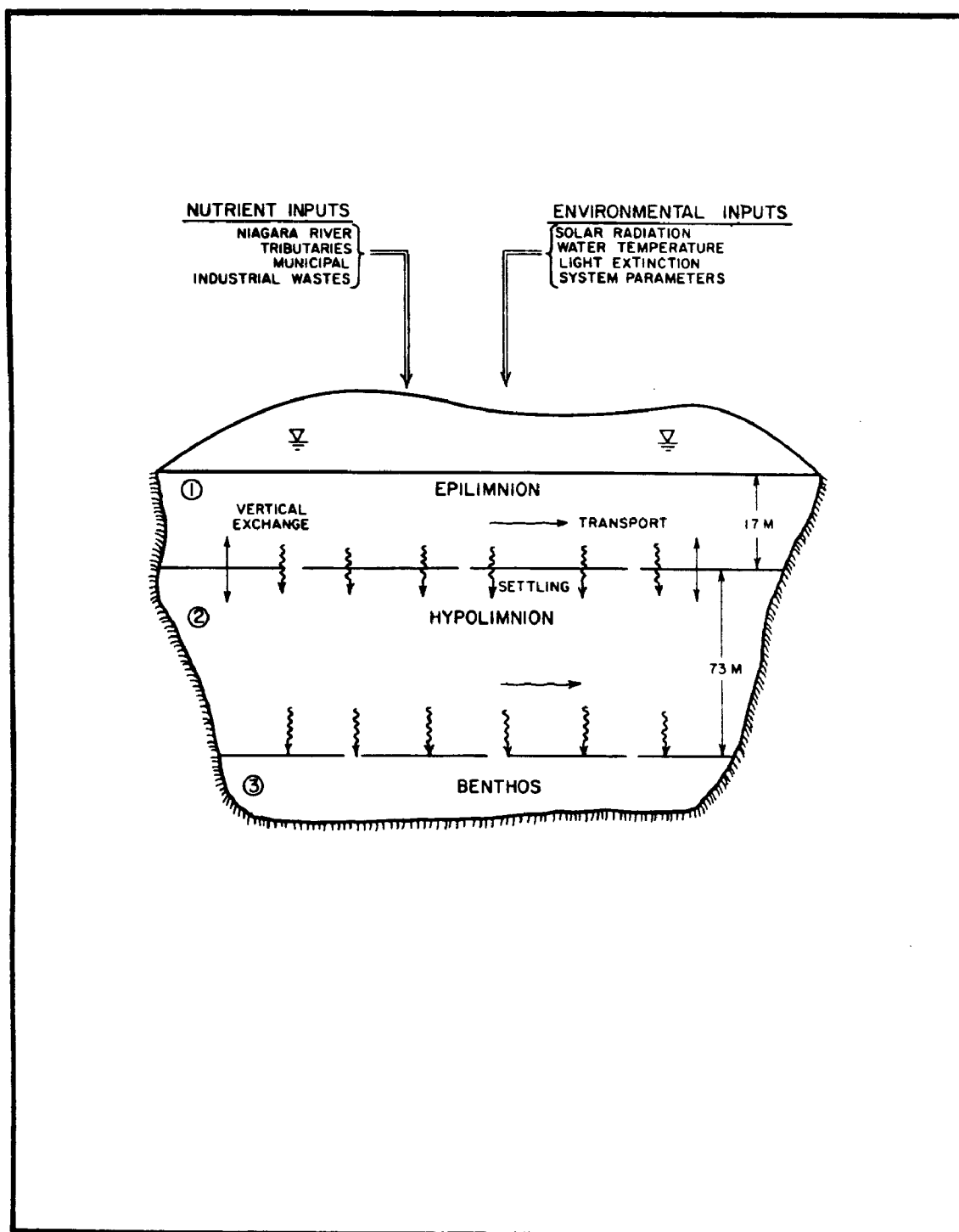


Figure 9. Major physical features included in Lake 1 model



TABLE 8

## BASIC PHYSICAL DATA OF THE LAKE 1 MODEL

Segment No.	Segment Interface	Volume ( $\text{m}^3 \times 10^6$ )	%	Depth (m)	Surface Area ( $\text{m}^2$ )	cfs	Flow $\text{m}^3/\text{sec}$	%
1		297,000	19	17		43,500	1232	19
	1-2				$1.64 \times 10^{10}$			
2		1,373,000	81	73.3		188,500	5323	81
	2-3				$0.89 \times 10^{10}$			
3 (sediment)		-		0.15*				

Note: Vertical dispersion coefficient between segments No. 1 and 2  
varied from 0-90  $\text{cm}^2/\text{sec}$  (0-778  $\text{m}^2/\text{day}$ )

\* Segment #3 depth is arbitrary



(c) vertical settling of the phytoplankton. The Lake shown in Fig. 9 has a defined epilimnion depth of 17 meters and a hypolimnetic depth of 73.3 meters. The Lake 1 model is well-mixed in the winter and spring, stratifies during summer and then goes through a fall over turn. The effects are simulated by control of the vertical mixing. Table 8 presents the physical data of the Lake 1 model.

With the vertical segmentation as given in Fig. 9 and Table 8 and using the general Eq. (3), the equations for Lake 1 are:

Segment No. 1 - Epilimnion:

$$V_1 \frac{ds_{1k}}{dt} = (Qs_k)_{B1} - Q_{1E}s_{1k} + \left[\frac{EA}{\Delta z}\right]_{12} (s_2 - s_1)_k \pm V_1 S_{1k} \quad (52)$$

Segment No. 2 - Hypolimnion:

$$V_2 \frac{ds_{2k}}{dt} = (Qs_k)_{B2} - Q_{2H}s_{2k} + \left[\frac{EA}{\Delta z}\right]_{12} (s_1 - s_2)_k \pm V_2 S_{2k} \quad (53)$$

Segment No. 3 - Sediment:

$$V_3 \frac{ds_{3k}}{dt} = \pm V_3 S_{3k} \quad (54)$$

where  $s_{k,B1}$  and  $s_{k,B2}$  are the concentrations of the kth system inputted into the epilimnion and hypolimnion respectively,

$Q_{B1}$  and  $Q_{B2}$  are the flows into segments 1 and 2,  $V_i$  is the volume



of segment  $i$ ,  $E_{12}$  is the vertical turbulent exchange,  $A_{12}$  is the cross-sectional area between the epilimnion and hypolimnion and  $\bar{\Delta z}$  is the average depth of the two segments. As shown in Fig. 5 the Lake 1 model consists of 10 systems ( $k=1 \dots 10$ ). The kinetics are as given previously in Section V. A review of the Lake 1 computer program is given in Appendix A together with a listing of all system parameters, inputs and sample outputs.

#### MODEL CALIBRATION AND VERIFICATION

Several ways have been used to test the validity of the basic model structure as given in Lake 1. First, a series of runs were made to test the general behavior and sensitivity of the model. This is followed by inspection of the model output to determine the general order of magnitude of the response of each of the variables. The comparisons are made between the observed data and the computed output for data collected during years prior to IFYGL. These comparisons are qualitative in the sense that an assessment of the degree to which the computed output agrees with observed data is left to the analyst. It should also be noted that other checks can be used in the model verification; specifically variables that can be constructed from the model output and compared subsequently to field measurements. The total verification then includes both the primary variables as given in the systems diagram (Fig. 5) and secondary variables constructed for the behavior of the model. The variables examined therefore for calibration and verification are:

- 1) Phytoplankton chlorophyll "a" -  $\mu\text{g}/\ell$
- 2) Primary productivity -  $\text{mg carbon}/\text{m}^2 - \text{day}$
- 3) Total zooplankton carbon -  $\text{mgC}/\ell$
- 4) Bottom deposition rate -  $\text{mg carbon}/\text{m}^2 - \text{year}$



- 5) Total phosphorus - mg/l
- 6) Available phosphorus (orthophosphate) mg/l
- 7) Total Kjeldahl nitrogen - mg/l
- 8) Ammonia nitrogen - mg/l
- 9) Nitrate nitrogen - mg/l

The approach was to examine past data (principally from the years 1967-1971), run the Lake 1 model under different parameter settings consistent with reported values and compare to the observed data. The results of this sensitivity and calibration analysis are given below. It should be noted however, that even with variable parameter settings (such as zooplankton grazing rate) the results are generally always consistent with the observed data. The results of the comparison to observed data are presented after the results of the preliminary sensitivity and calibration runs.

#### Preliminary Runs and Sensitivity Analysis

A finite difference scheme is used to solve the equations using explicit time-space differencing. For the Lake 1 model, a time step of 0.5 days is used. For a one-year simulation, the central processing unit (CPU) time required for execution is about 7 seconds on a CDC 6600 computer. Total CPU time required however is 30 seconds with additional overhead converted to equivalent CPU time being 115 seconds. The CPU time excluding overhead is equal to about 1.4 milliseconds per compartment step. A number of preliminary runs were made using the Lake 1 model structure to 1) test program elements 2) study the behavior of the system and its sensitivity to various system parameters and inputs and 3) prepare a preliminary verification of the Lake 1 model using data collected prior to IFYGL. These early runs therefore



represent a type of "tuning" of the model using past data as a basis for additional verification of the IFYGL data. The Lake 1 model has been used to examine several areas including, for example variable levels of spring and fall vertical mixing, and settling velocities for phytoplankton in addition to zooplankton grazing rate, and effect of half-saturation constant for phosphorus, Some of the output from these areas is discussed below.

### Variable Vertical Mixing

Vertical mixing plays an important role in the dynamics of phytoplankton population in lakes. Several paths were followed in order to obtain an estimate of the vertical dispersion in Lake Ontario. A survey of the literature on vertical mixing indicated that generally the vertical dispersion coefficient is several orders of magnitude lower than the horizontal coefficient. Oceanic vertical dispersion coefficients are in the range of  $10\text{--}100\text{ cm}^2/\text{sec}$  and generally decrease with depth. Recently, during IFYGL, Murthy et al<sup>1</sup> estimated values from  $0.1\text{ cm}^2/\text{sec}$  to  $22\text{ cm}^2/\text{sec}$  depending on effects such as wind conditions and density stratification. In the Lake I work, the vertical dispersion was therefore treated as a parameter and sensitivity analyses made under an expected range from complete stratification (no mixing) throughout the year to variable mixing up to  $90\text{ cm}^2/\text{sec}$ . More extensive analysis of vertical mixing was carried out in the Lake 2 and 3 models using temperature as a tracer variable. The details of these analyses are given in Section VI.

Figure 10 shows the effect of vertical dispersion on chlorophyll a. The runs include a sinking velocity of  $0.05\text{ m/day}$ . A bimodal distribution of phytoplankton occurs in all cases due to the interaction of the two higher zooplankton levels used in



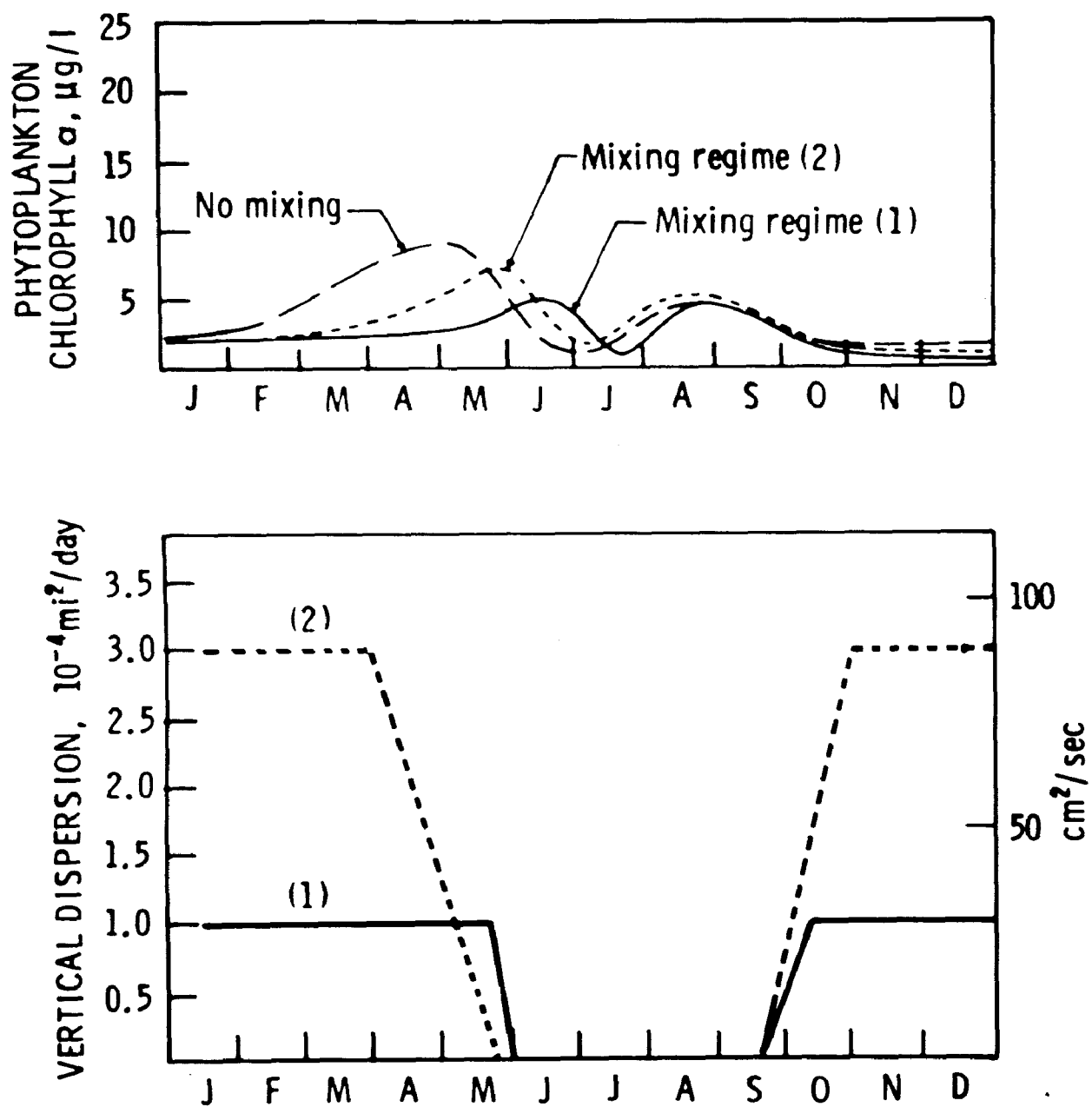


Figure 10. Effect of vertical mixing



these runs. As populations build up in the spring, the herbivorous zooplankton increase. This together with nutrient depletion decreases the phytoplankton population and at about the same time, the carnivorous zooplankton prey on the next lowest trophic level. The phytoplankton can then increase again in the late summer.

As shown in Fig. 10, the main effect of vertical mixing is in the spring where populations increase more rapidly when no mixing is allowed and reach a peak earlier. With mixing, the first peak is delayed and reduced in magnitude. The results in the summer and early fall are generally comparable under the different dispersion regimes although the timing of maximum and minimum is changed.

#### Variable Phytoplankton Settling Velocity

A number of analyses using the Lake 1 model have been made to examine the behavior of the phytoplankton population under different settling velocities. The reported values for phytoplankton sinking in quiescent waters (see Section III) are apparently too high to support adequate growth in the Lake 1 model. This is due in part, to the crude vertical definition and the interaction between the sinking of phytoplankton and their physiological state. The settling velocity has been treated as a parameter ranging from 0 to 0.5 meters/day.

Figure 11 summarizes the results from several analyses using different sinking velocities. For these runs, zooplankton grazing was set at 0.06 l/mg carbon-day-°C, no vertical mixing was used and the Michaelis constants were 25µg/l and 10 µg/l for nitrogen and phosphorus respectively. At a velocity of 0.5 m/day phytoplankton populations never exceed about 3µg chlor/l



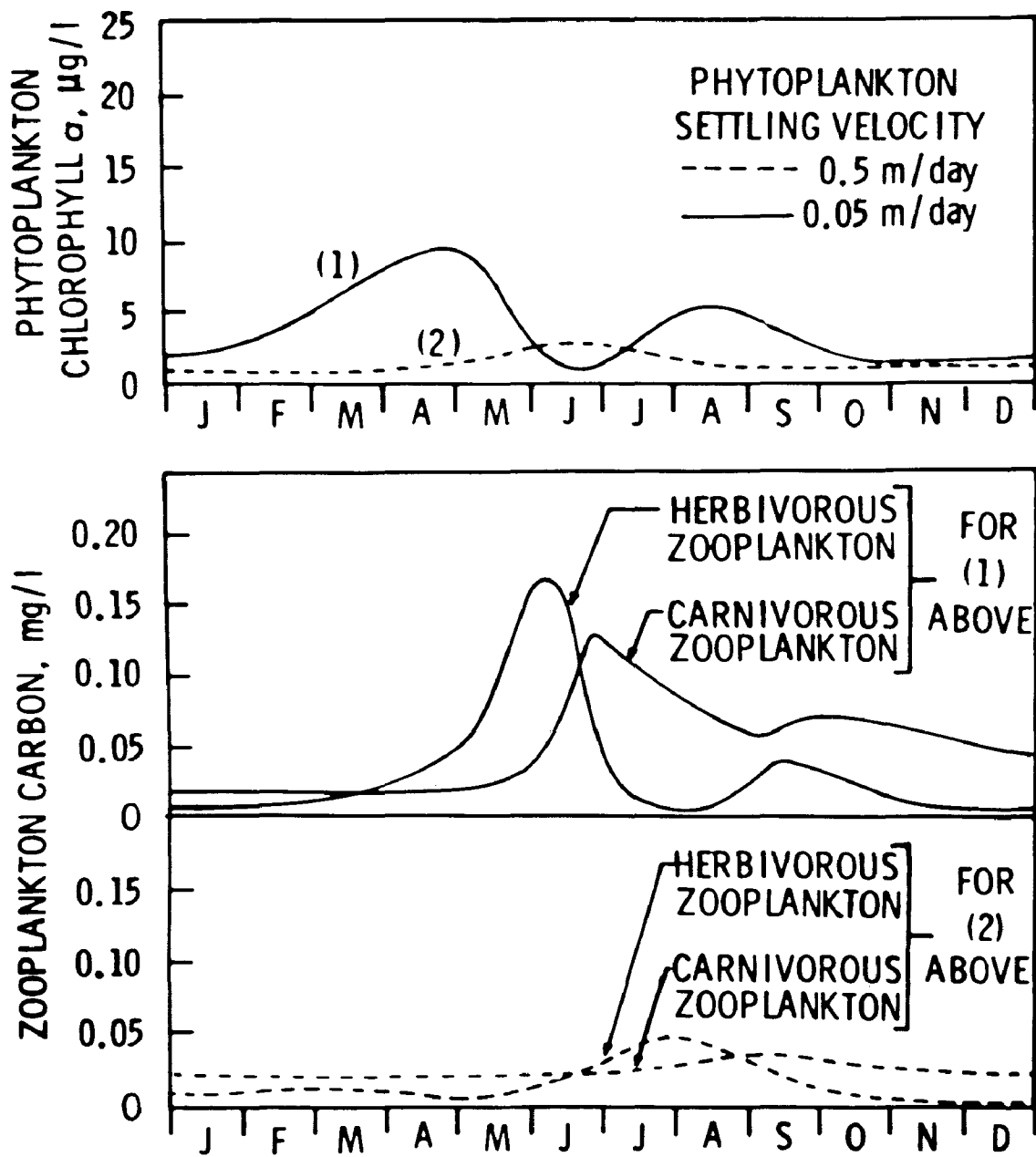


Figure 11. Effect of phytoplankton settling velocity,

$$K_{mp} = 10\mu\text{g/l}$$



and total zooplankton carbon (Figure 8) never exceeds about 0.08 mg Carbon/l. Both values are less than observed. The reason for the low levels is that under a settling velocity of 0.5 m/day (which for the 17 meter depth of the epilimnion represents a "decay" coefficient of .03/day), the phytoplankton are not retained in the upper layer long enough to undergo net growth. As a consequence, zooplankton levels are also low and the nutrient concentrations remain high and are not reflective of observed nutrient depletion. Using a velocity of 0.05m/day, the behavior of the phytoplankton biomass is quite different as shown in Figure 11. Now, the lower trophic level has a chance to grow and a reasonable predator-prey relationship begins to develop.

The half-saturation constant for phosphorus,  $K_{mp}$ , has an important effect however. An order of magnitude reduction in this coefficient to  $1\mu\text{g}/\ell$  does permit growth of the phytoplankton at the higher settling velocity of 0.5m/day. Figures 11 and 12 show this effect and indicate the trade-off between a population adapted to low phosphorus concentration and settling velocity. These results also tend to indicate the possible interaction of settling velocity and the active growth phase of the population.

The sinking velocity of phytoplankton also has an important effect on the nutrient uptake as shown in Fig. 13, which is a plot of the nitrate and available phosphorus concentrations calculated under the conditions of  $K_{mp} = 10\mu\text{g}/\ell$ . In addition, Fig. 13 shows the nitrogen and phosphorus limitation terms, i.e., the ratio of total inorganic nitrogen to total inorganic nitrogen plus the Michaelis for nitrogen and similarly for available phosphorus (see Eq.8). It can be seen that nutrient uptake and growth



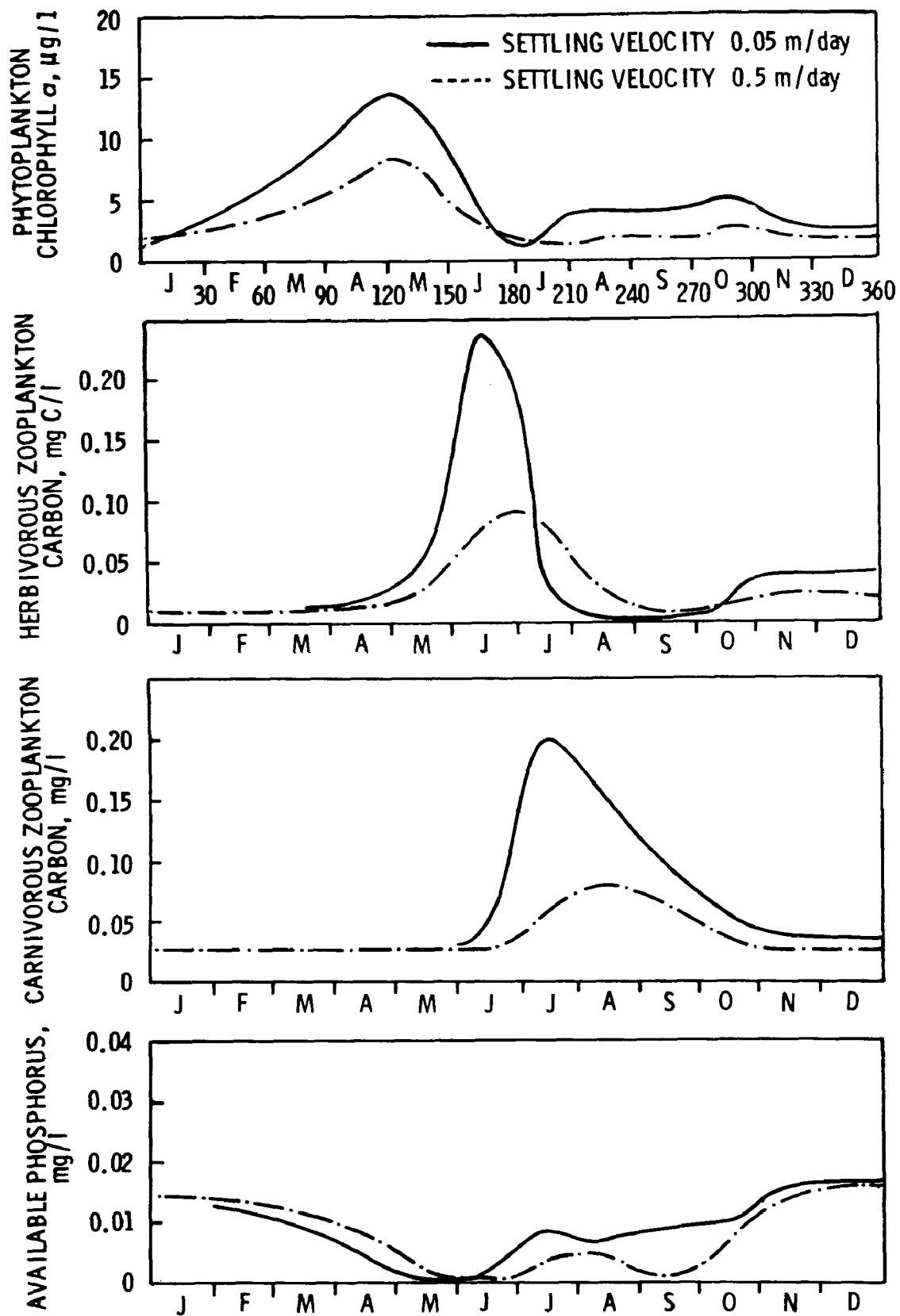


Figure 12. Effect of phytoplankton settling velocity,  
 $K_{mp} = 1\mu\text{g/l}$



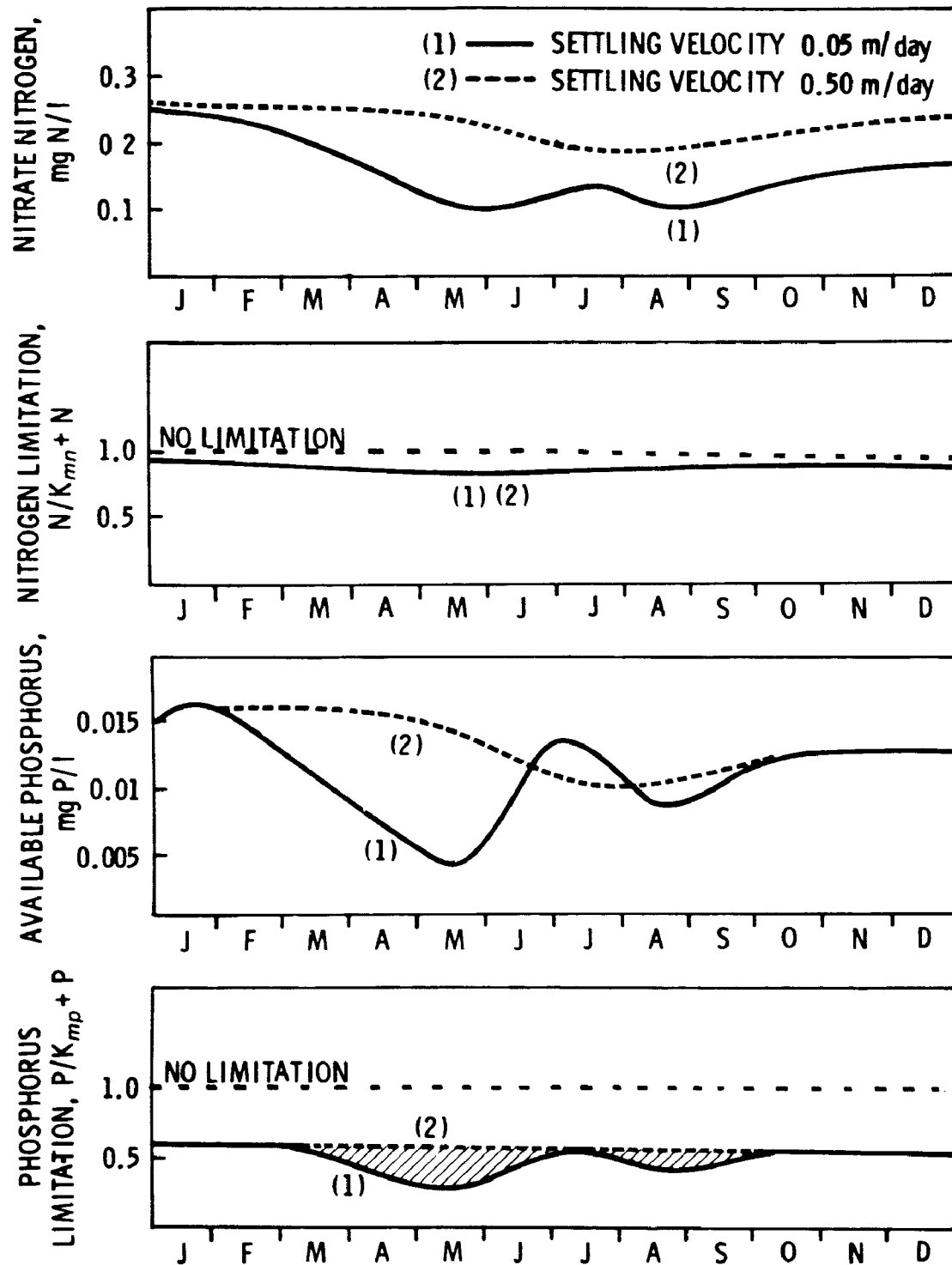


Figure 13. Effect of phytoplankton settling velocity on nutrients and nutrient limitation,  $K_{mp} = 10\mu\text{g}/\ell$



limitation is minimal for the case of sinking velocity = 0.5m/day. This is a result of the minimal phytoplankton growth. At the lower sinking rate, however, nitrate uptake is increased but as indicated in the upper curves of Fig. 13 nitrogen does not significantly limit growth for the case of  $K_{mp} = 10\mu\text{g}/\ell$ .

The lower curves representing the phosphorus dynamics however do exhibit a limiting effect. If attention is directed to the phosphorus limitation term, it is seen that for both settling velocity cases, levels of phosphorus are such that a limitation of .50 - 0.60 prevails during the early and later parts of the year. However, substantial differences occur in the spring and late summer. At day 135, a minimum value of about 0.2 is calculated indicating that phosphorus is acting as a significant limiting factor in the phytoplankton growth. This helps explain the decrease in phytoplankton biomass beginning at day 120, (see Fig.11). Two effects are occurring: a) herbivorous zooplankton are growing rapidly and b) phosphorus levels are being depleted to below the half-saturation constant thereby acting to reduce the growth rate. It is interesting to note then that a biomodal distribution in phytoplankton can be obtained without a species differentiation. The latter is often offered as the explanation for the observed two peaks in the phytoplankton. In order to accomplish this, however, at least two trophic levels must be included above the phytoplankton. This permits a higher order predation, e.g. carnivorous zooplankton which reduces the lower zooplankton level. The reduction permits phytoplankton to grow again in late summer. This is explored in greater detail below.



### Effect of Michaelis Constant

As indicated in Eq. ( 5), the growth of the phytoplankton is considered to be limited by a Michaelis Menton product term of total inorganic nitrogen and available phosphorus given by Eq. ( 8 ). The dynamics of growth therefore are affected by the levels of  $K_{mn}$  and  $K_{mp}$ , the half-saturation constants for nitrogen and phosphorus, respectively. Several sensitivity runs have been made therefore specifically examining two levels of  $K_{mp}$ , 1 and 10  $\mu\text{g}/\ell$  both of which encompassed the range of published values. Phosphorus is emphasized because of the waste removal programs presently underway in the Great Lakes Basin.

Figs. 14 and 15 show the results of two computations at an order of magnitude difference in  $K_{mp}$ . For both runs, settling velocity was .05m/day,  $K_{mn}$  (nitrogen half-saturation constant) is 25 $\mu\text{g}/\ell$  and zooplankton are included as before. As seen in Fig.14 at the 1 $\mu\text{g}/\ell$  level, phytoplankton biomass grows earlier more rapidly and reaches a peak value of 14 $\mu\text{g}/\ell$  chlorophyll/l at the end of April. At the 10 $\mu\text{g}/\ell$  value, growth is later, slower and reaches a maximum value of about 9 $\mu\text{g}/\ell$  almost a month later at the end of May. Values in the late summer are comparable. The nutrient plots shown in Fig. 14 indicate that in May, phosphorus is limiting under the 1 $\mu\text{g}/\ell$  case while in August-September, nitrogen appears to be limiting. This is shown more clearly in Fig. 15 - which is a plot of the nitrogen and phosphorus limitation terms under both conditions. It can be noted that at 1 $\mu\text{g}/\ell$  the growth is limited by phosphorus for only a short period in May and the system tends to be nitrogen limited throughout the rest of the growing season. On the other



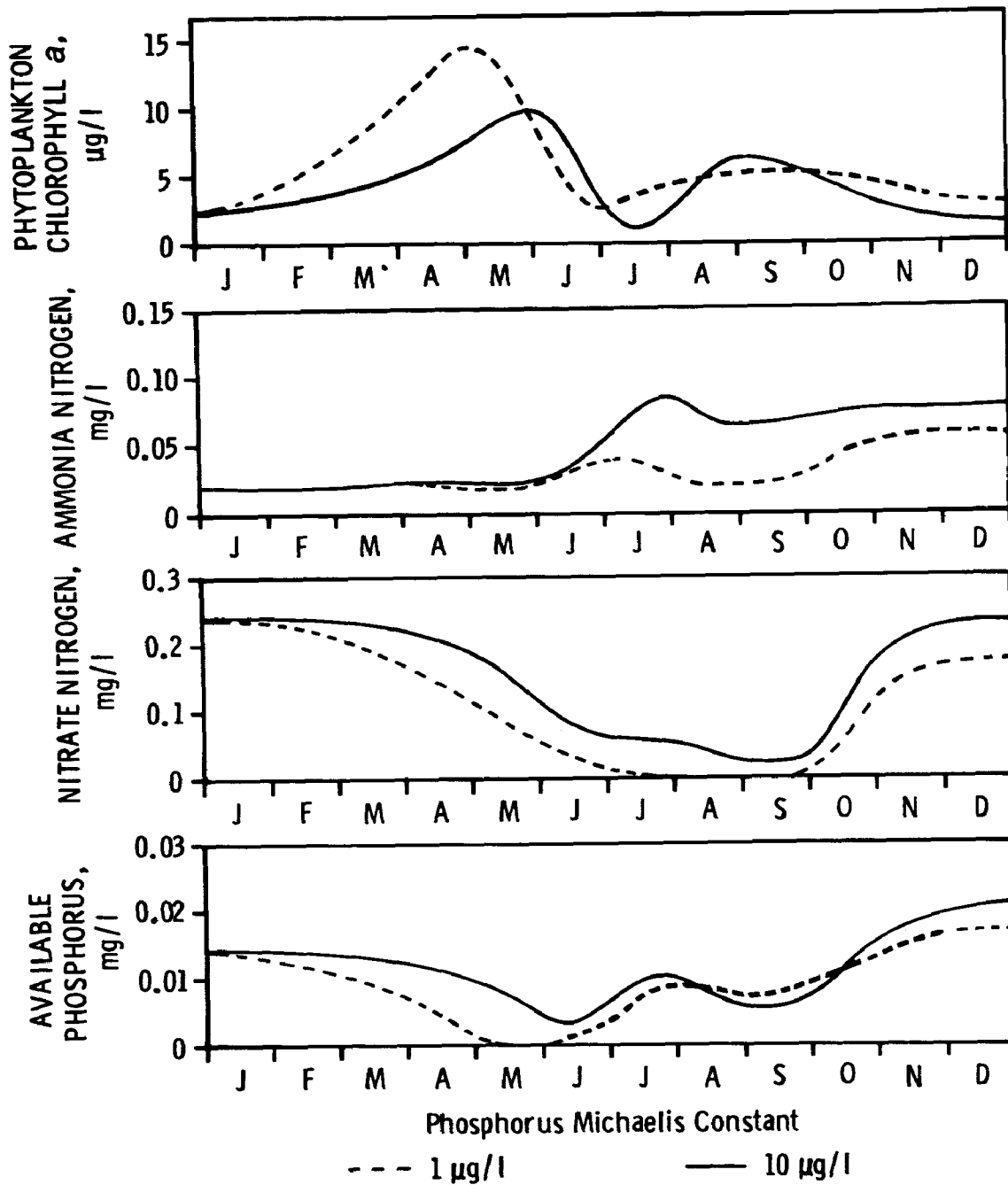


Figure 14. Effect of Michaelis constant for phosphorus on primary variables



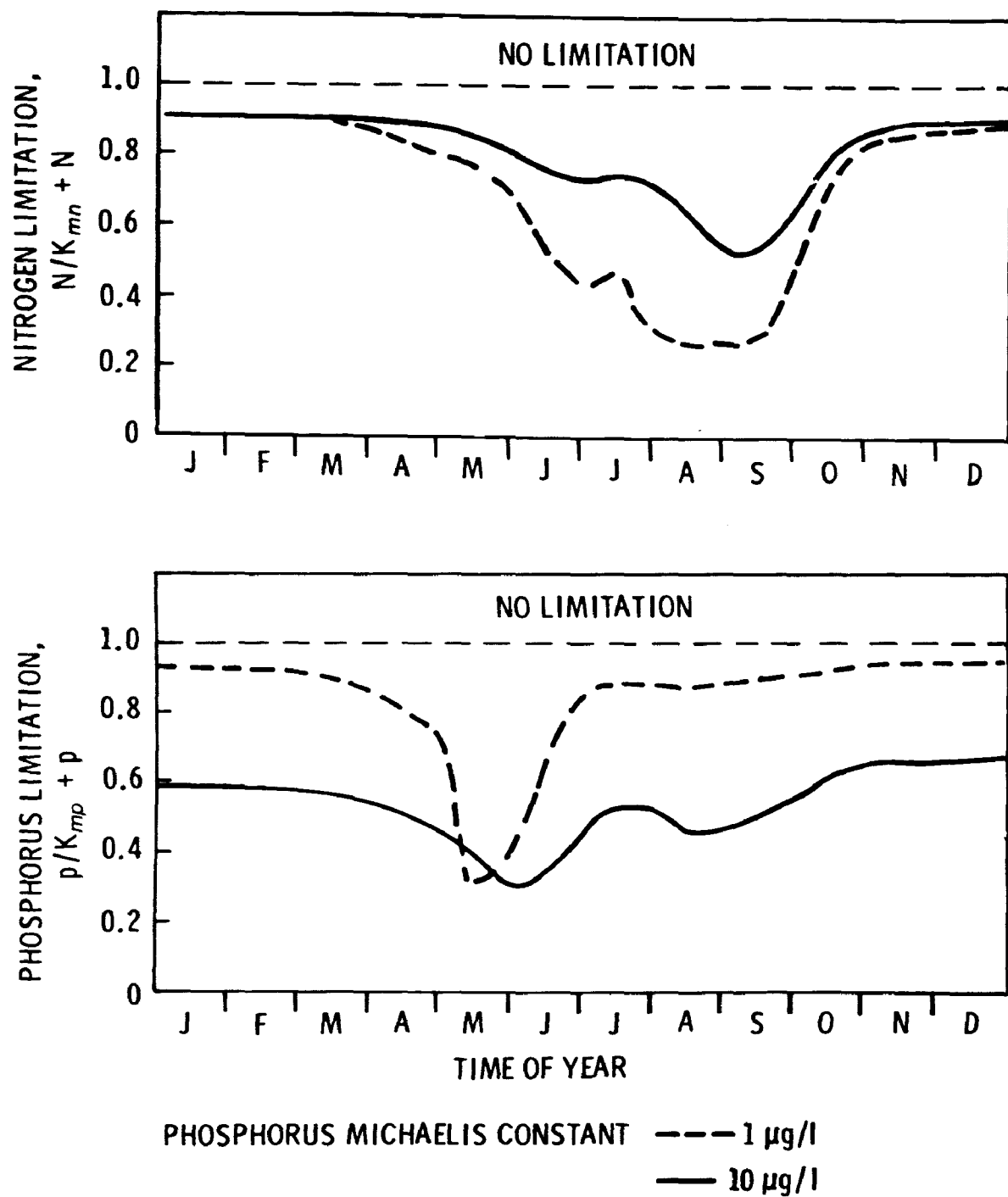


Figure 15. Effect of Michaelis constant for phosphorus on nutrient limitation of nitrogen and phosphorus



hand, at a phosphorus Michaelis constant of  $10\mu\text{g}/\ell$  the system is more phosphorus limited throughout the year although nitrogen is still an important limiting interest in late summer.

The results indicate the importance of reasonably accurate estimates of the half-saturation constant. This will be particularly important during any simulation of nutrient reduction programs. The results also indicate that reliance on a single nutrient as "the limiting nutrient" does not recognize the interaction between nutrients and may be quite misleading in estimating the effects of a control program.

#### Effect of Alternate Growth Formulation

As discussed in Section III, Eqs. (5) and (9) represent different expressions for the growth term in the phytoplankton equation. In order to examine the behavior of the response to each form, the Lake 1 growth kinetics were modified to incorporate Eq. (9). The results for three output variables are shown in Fig. 16. Both runs displayed therein are for identical conditions except for the alternate growth formulation as indicated in the figure.

Eq. (9) results in immediate and rapid growth of the phytoplankton with subsequent total depletion of the phosphorus. The dynamic behavior of the results using the formulation of Eq. (9) do not even approximately agree with observed data. This is especially true for the high levels of phytoplankton in the early and late months of the year and the zero concentration of phosphorus throughout the better part of the year. The dynamic shape is also not consistent with the observed data (see Fig. 3 ). From this one comparison, then, Eq. (5) the original product formulation is still to be preferred.



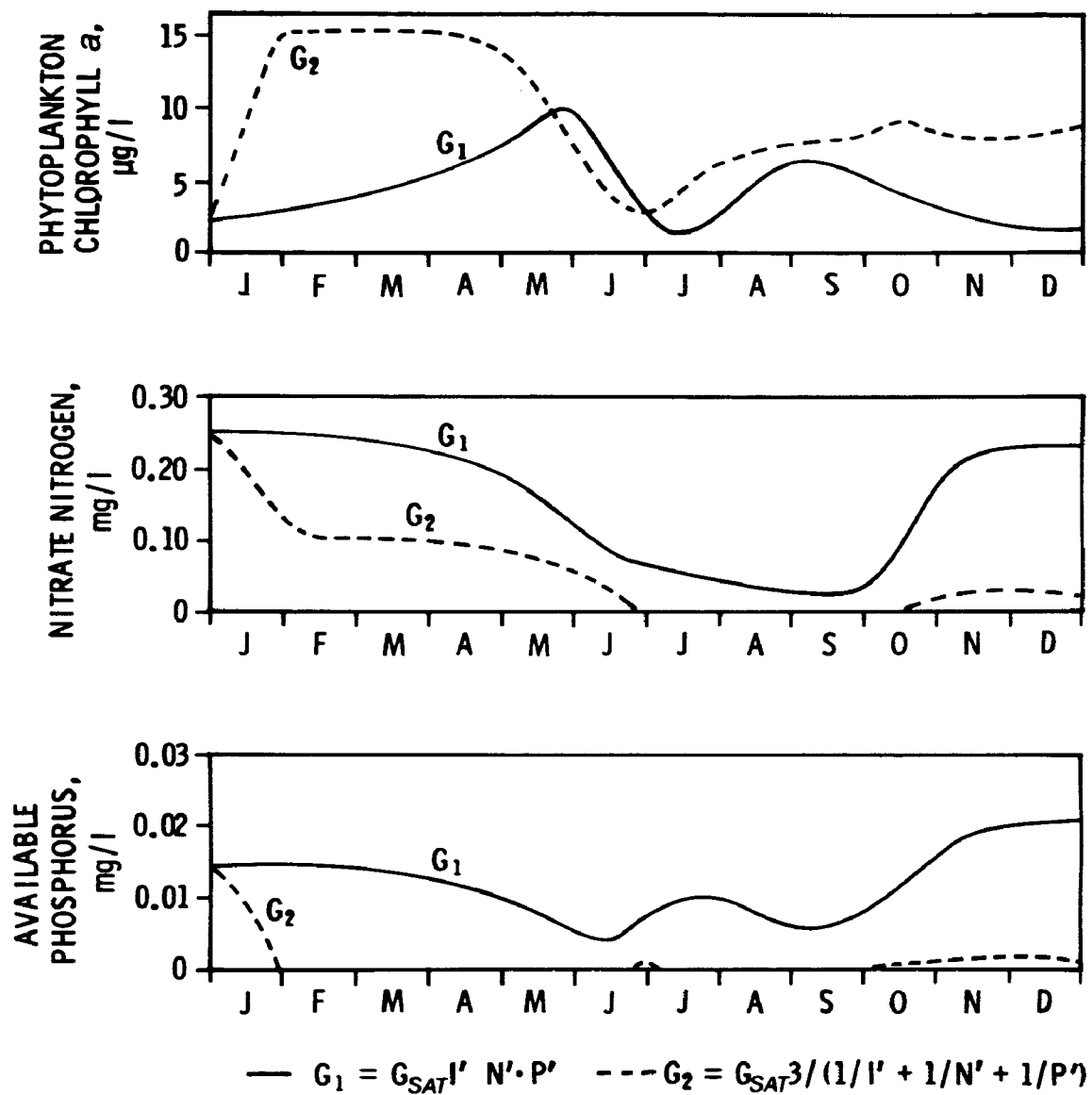


Figure 16. Responses due to two photoplankton growth formulations



### Time to Dynamic Equilibrium

With the relatively long detention time of about 8 years for Lake Ontario, the time to reach a dynamic steady state (i.e. where the solution becomes periodic) is an important management consideration. For a single non-conservative variable in a completely mixed lake, the solution for a mass input of  $W$  is

$$s = \frac{W}{Q+KV} [ 1 - e^{-(k+1/t_o)t} ] + s_o e^{-(k+1/t_o)t} \quad (55)$$

where  $s_o$  is the initial condition of  $s$  and  $t_o$  is the detention time given by  $V/Q$ . For  $K=0$ , the conservative case, the time to reach 95% of a new steady value is about 3 detention times, which for the whole of Lake Ontario is about 24 years. Furthermore, the initial conditions will also take approximately that long to "die down" and not influence the solution. Any solution therefore that is calculated for only one year (as per the previous figures) is dominated by the initial conditions and the effect of the mass input is negligible. For verification purposes, however, a single year run is sufficient to explore the general behavior of the system. For any projections of the effects of reduced inputs, longer runs are needed. Therefore, the solutions must be run for a period of time until the initial conditions for all variables are repeated year by year. With the complex interactions of the Lake 1 model, this time to reach a dynamic equilibrium is not immediately obvious. Accordingly, several long-term runs were prepared to illustrate this effect.

Fig.17 shows a time history plot of 16 years of solution equivalent to two detention times. The conditions are comparable to previous runs but use a Michaelis phosphorus constant of  $10\mu\text{g}/\text{l}$ . As shown,



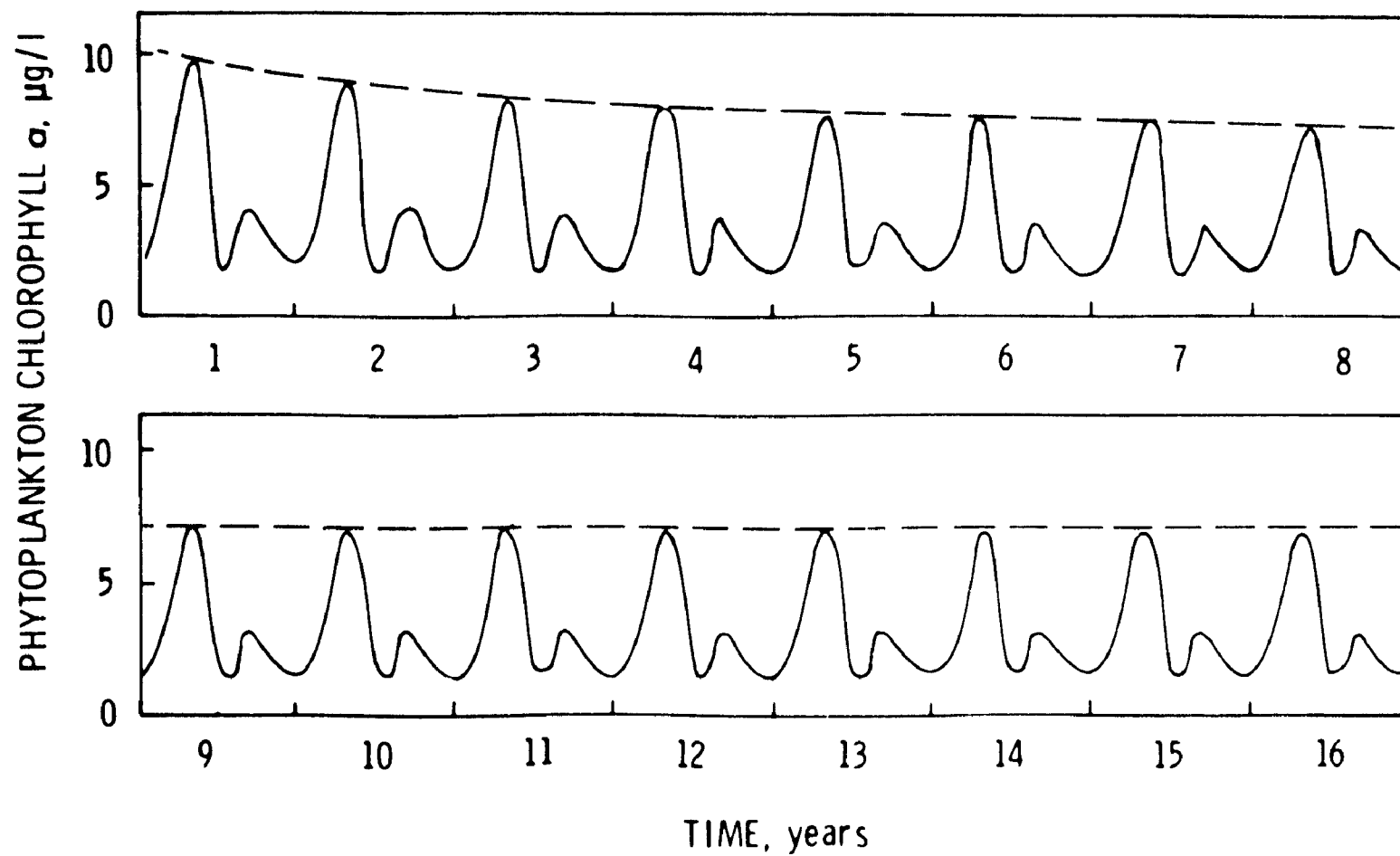


Figure 17. Sixteen year computed output of phytoplankton chlorophyll



peak phytoplankton levels in the spring gradually decrease from greater than  $9\mu\text{g}/\ell$  in the first year to about  $7\mu\text{g}/\ell$  by the eighth year after which time, a dynamic equilibrium has been reached. Thus, a time of about one detention time for Lake Ontario was required for the phytoplankton to reach a steady state. However, due to internal cycling between the various nutrient sub-systems shorter or longer times may be required for some of the nutrient forms. This is shown in Fig. 18 which indicates system response under two phosphorus Michaelis constants. The upper figure indicates a parallel decrease in the phytoplankton maximum under the two conditions and although the two runs began with a peak difference of almost  $3\mu\text{g}/\ell$ , the difference is about half of that at equilibrium.

The lower two plots of Fig. 18 are quite interesting and illustrate further the difference in the dynamic behavior under the two phosphorus Michaelis levels. Under the lower level of  $1\mu\text{g}/\ell$  equilibrium is reached almost immediately in both phosphorus and total inorganic nitrogen. Under an order of magnitude increase in the level to  $10\mu\text{g}/\ell$  dynamic steady state is not reached for the inorganic nitrogen until almost two detention times or 16 years. With the lower level of  $1\mu\text{gP}/\ell$  phytoplankton growth is increased due to the increased ability to utilize low phosphorus concentrations. As a consequence, however, nitrogen utilization is increased and as shown in the middle plot, the system becomes nitrogen limited. The times of the year of the nitrogen and phosphorus limitation are different however as shown in Fig. 15

In essence, then these runs illustrate the need to carry out any simulations of a proposed nutrient reduction program out to about 8-16 years to determine the expected phytoplankton levels under a



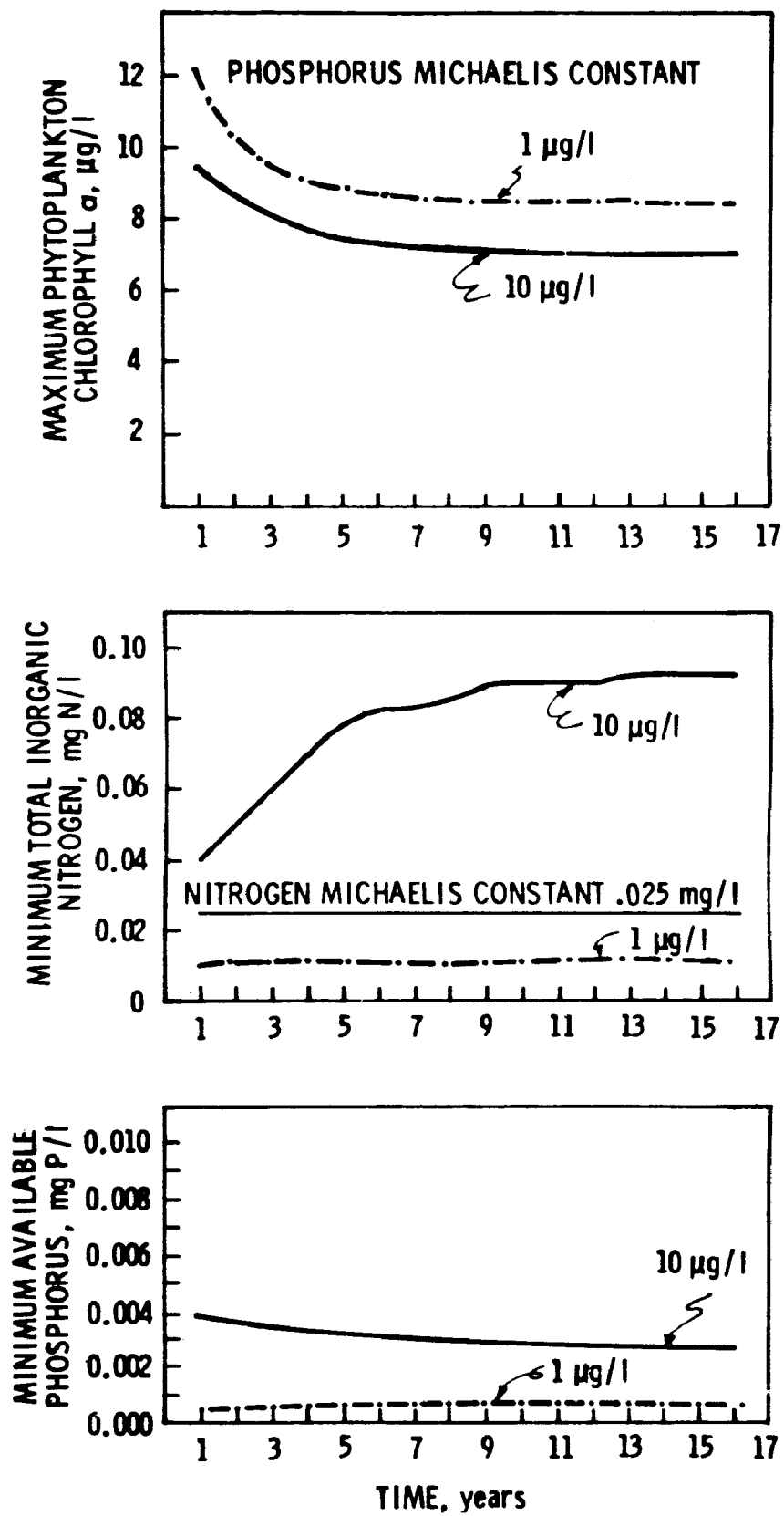


Figure 18. Long term behavior of model components under two phosphorus Michaelis constants



different waste load input. If however, the loads are changing from year to year, as, for example, in a linear increasing or fashion, then even longer times may be required. Indeed, under changing loads, a dynamic equilibrium may never be theoretically possible. For many practical purposes, the system will probably reach steady state in a 10-20 year time horizon after significant changes have been made.

### Preliminary Comparison

Figs.19 and 20 show one of the early comparisons of observed data and model output. The Michaelis constant for phosphorus was  $10\mu\text{g}/\text{L}$  and settling velocity was  $0.05\text{m}/\text{day}$ . In the preliminary comparisons, a variety of similar plots was generated. Figs. 19 and 20 therefore represent a type of a first level of calibration. In general, the overall comparison is quite good and indicates that even with first, approximate analysis, results are obtained from the model that are in general agreement with the observed data. This tends to support the contention that the basic model structure does represent the principal features of the phytoplankton biomass.

Several details of Figs.19 and 20 however remained to be explored in greater depth before a "final" verification could be obtained. For example, in the preliminary runs, the fall peak in phytoplankton is only approximately reproduced and in addition the total zooplankton carbon is generally too high. Finally, the dynamic behavior of the nutrients such as phosphorus and ammonia, while generally satisfactory, could be improved. Using therefore, the sensitivity runs discussed previously and the results of the preliminary comparisons, further verification analyses were conducted to construct a coherent



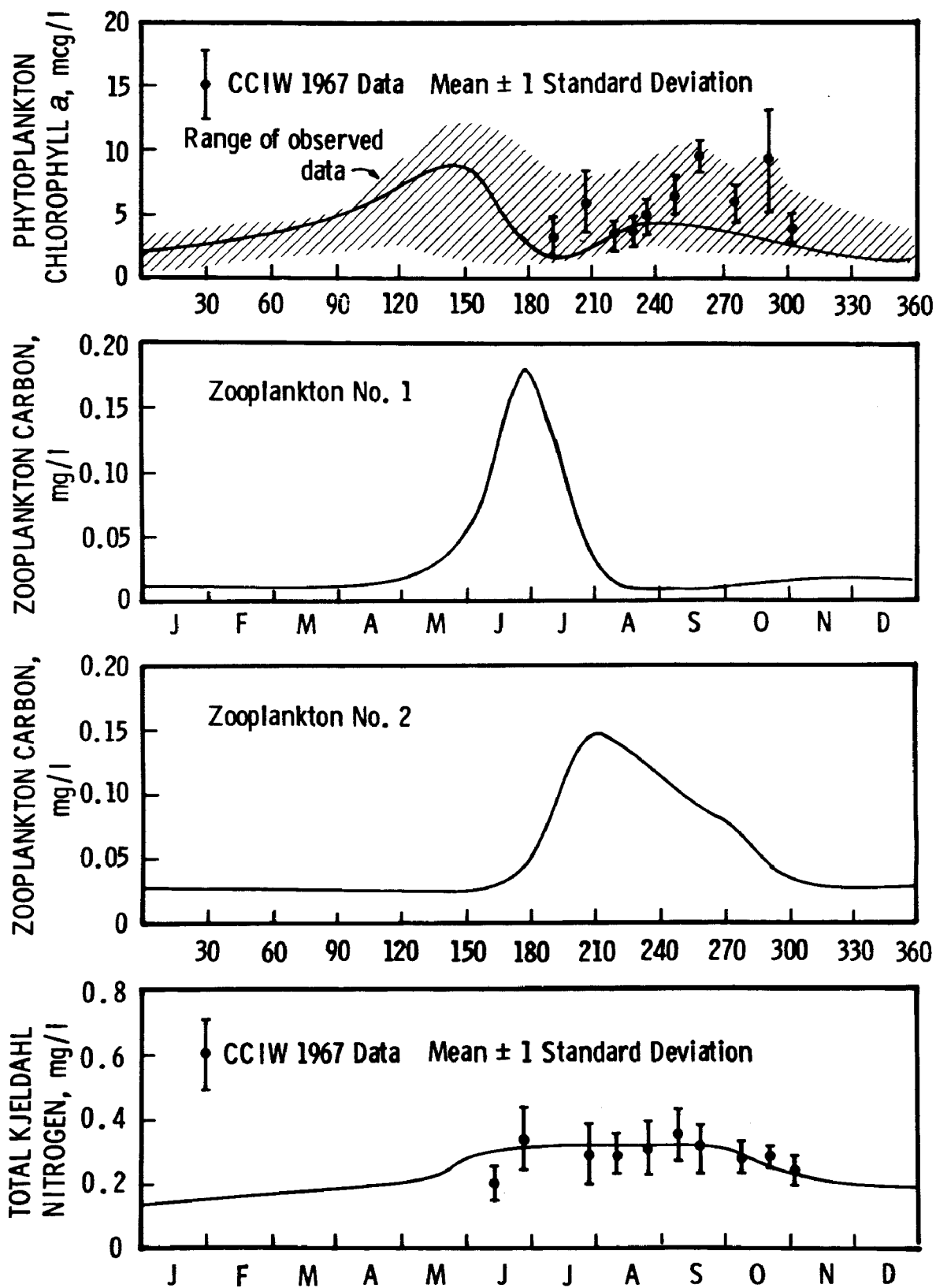


Figure 19. Preliminary comparison of model output and observed data.



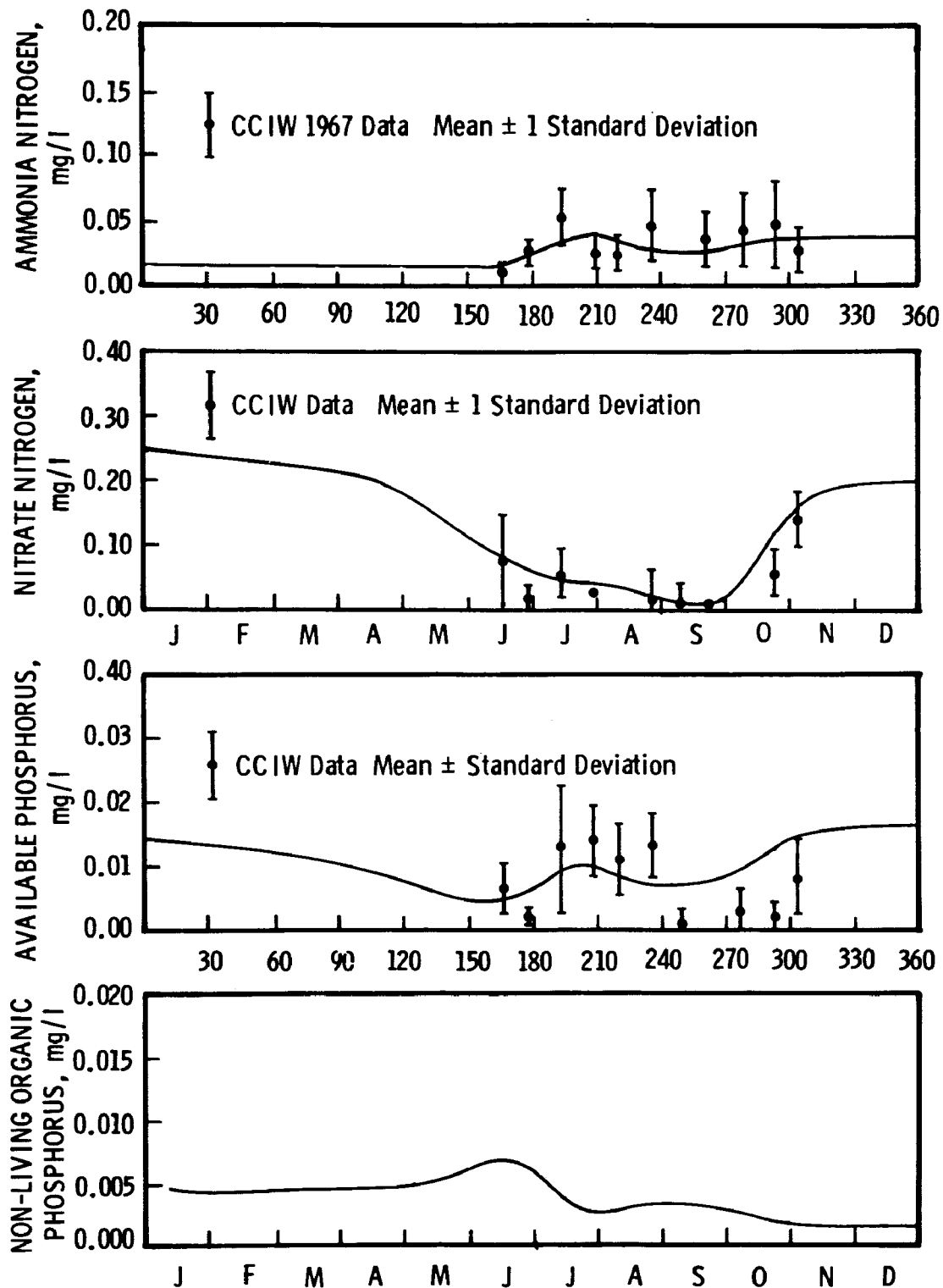


Figure 20. Preliminary comparison of model output and observed data, continued



picture of the dynamics of the lake. The goal then in this final verification phase of Lake 1 model was to produce a set of parameters and accompanying hypotheses that represented as good a comparison as possible to available data.

#### RESULTS OF "FINAL" VERIFICATION ANALYSIS

Data were available for the years 1967-70 collected by the Canadian Centre for Inland Waters for this final verification phase. These data were supplemented by other observations in the literature. Values for the various coefficients, parameters and exogenous variables were obtained from published sources as discussed previously and all values used are within reported ranges in the literature. More than 80 runs have been made of Lake 1 to examine the effects of various phenomena such as settling velocity, vertical mixing, zooplankton predation and half-saturation constants for nitrogen and phosphorus. Out of these runs has emerged a consistent set of parameter values which satisfactorily explains the observed data on a variety of different variables. A plausible explanation for the dynamic behavior of the phytoplankton is therefore possible and is discussed below.

Figs. 21 and 22 show the verification of the Lake 1 model upper layer (0-17 meters) while Fig. 23 shows the verification for the hypolimnion (data in range, 50-150 meters). Table 9 shows the principal coefficients used for the runs. As shown, the verification for plankton in the epilimnion is quite good and satisfactorily duplicates the spring peak, subsequent mid-summer die off and fall bloom. Five other variables in addition to the phytoplankton chlorophyll are satisfactorily verified in the comparison. It should be noted here that it is generally not



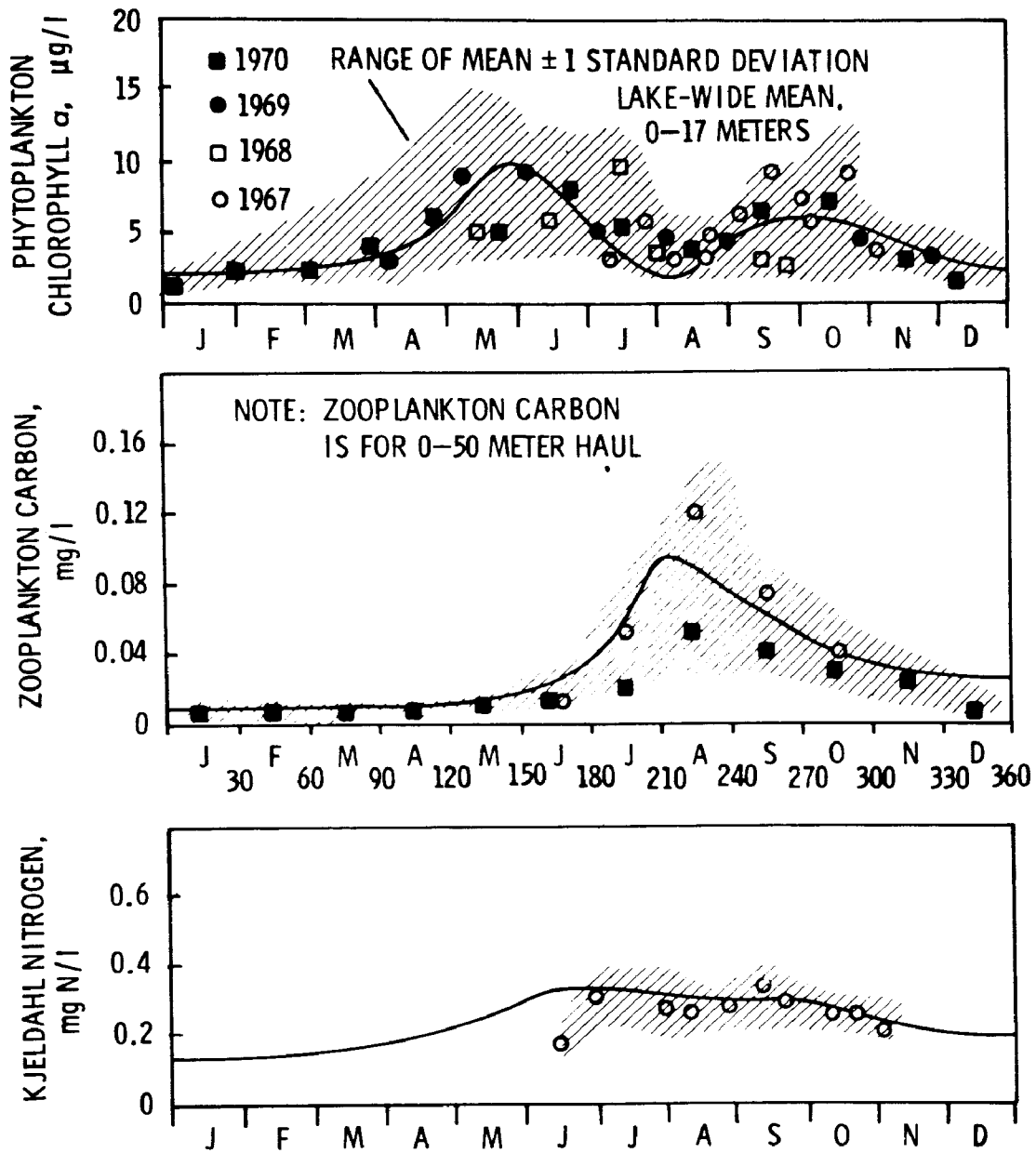


Figure 21. Lake 1 model verification, 0 - 17 meters



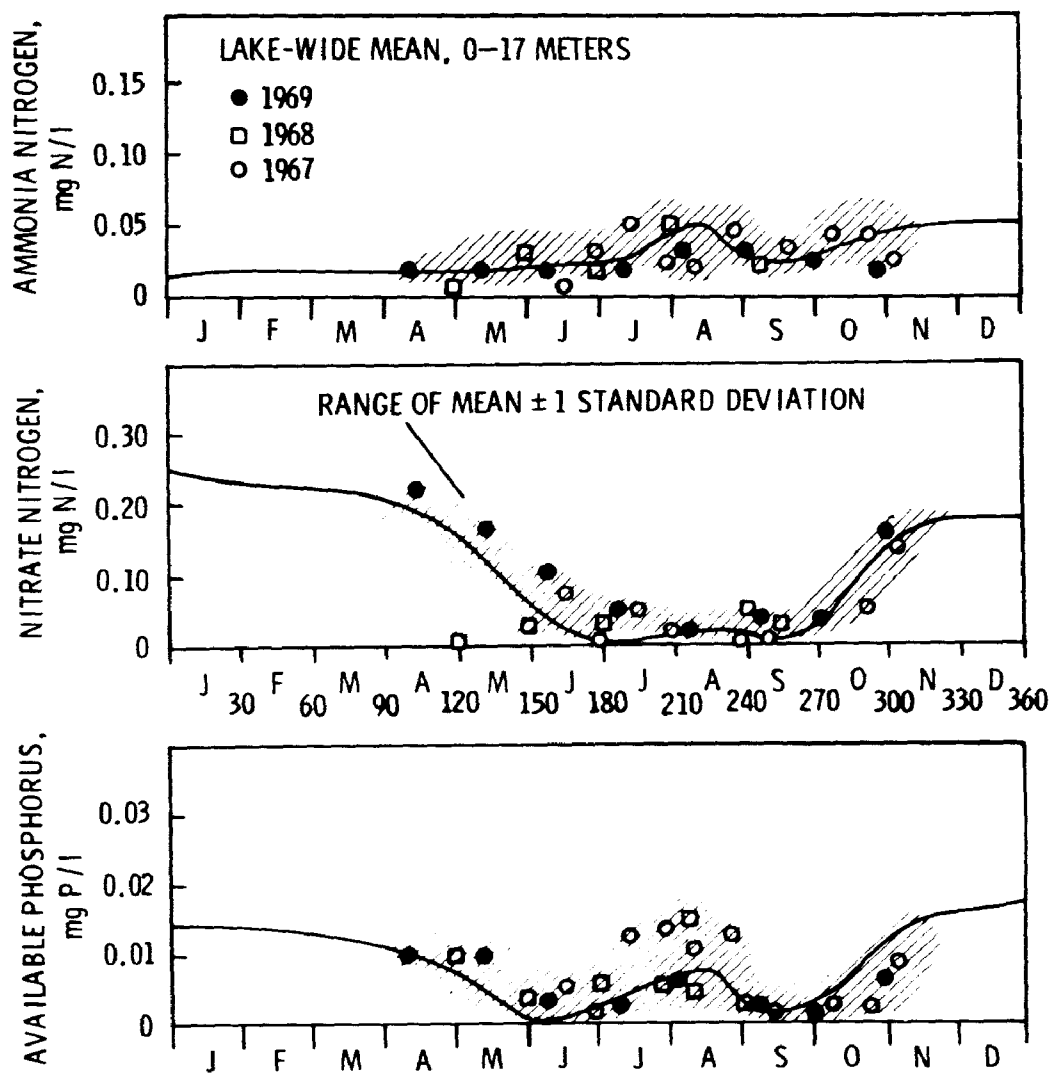


Figure 22. Lake 1 model verification (cont.), 0 - 17 meters



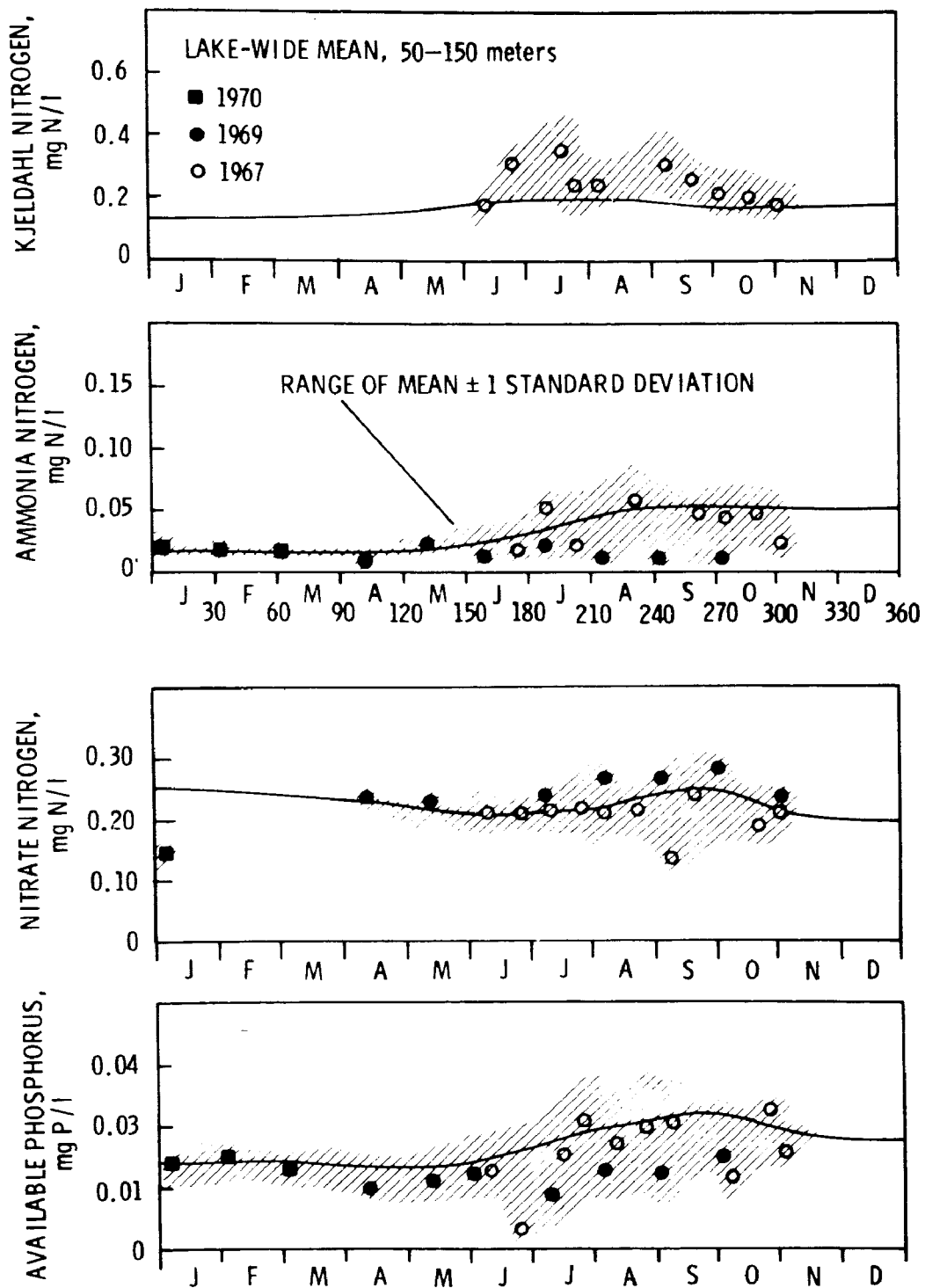


Figure 23. Lake 1 model verification, 50 - 150 meters



TABLE 9. PRINCIPAL PARAMETER VALUES USED IN LAKE 1 MODEL OUTPUT

SHOWN IN FIGURES 21 - 23

8	<u>Notation</u>	<u>Name</u>	<u>Value</u>	<u>Unit</u>
	K <sub>mn</sub>	Half-saturation constant-nitrogen	25	µgN/l
	K <sub>mp</sub>	Half-saturation constant-phosphorus	2	µgP/l
	C <sub>g</sub>	Grazing rate for zooplankton	.06	l/mg C-Day-C°
	K <sub>g</sub>	Half-saturation constant-phytoplankton	10	µg Chlor/l
	K <sub>2</sub>	Endogenous respiration rate-phytoplankton	0.1	days <sup>-1</sup> (@20°C)
	a <sub>zp</sub>	Zooplankton conversion efficiency	0.6	-
	K <sub>z</sub>	Zooplankton endogenous respiration rate	.001	(days - °C) <sup>-1</sup>
	K <sub>1</sub>	Decomposition rate of organic nitrogen	.00175	(day - °C) <sup>-1</sup>
	K <sub>22</sub>	Ammonia to nitrate nitrification rate	.002	(days - °C) <sup>-1</sup>
	K <sub>op</sub>	Decomposition rate of organic phosphorus	.007	(day - °C) <sup>-1</sup>
	a <sub>1</sub>	Nitrogen-chlorophyll ratio	10	µgN/µg chlor
	a <sub>p</sub>	Phosphorus-chlorophyll ratio	1	µgP/µg chlor
	a <sub>c</sub>	Carbon-chlorophyll ratio	50	µgC/µg chlor
	w	Settling velocity of phytoplankton	0.1	m/day



possible to obtain the verification shown in Figs. 21-23 by arbitrary specification of the coefficients, so that the results shown do not simply represent a "curve fitting" exercise. Rather, the results, which are based on the theory discussed earlier, are representative of the observed data in a much more meaningful way than just through arbitrary statistical coefficients. Since the model permits computation of the components of the dynamic behavior, considerable insight can be gained by examining the influence of various phenomena on the growth and death rates of the phytoplankton.

Fig. 24 shows the dynamics of the kinetic growth rate of the phytoplankton ( $G_p$  in Eq.(4)). As shown, maximum growth rate reaches a peak in mid-September in the Lake 1 model at about 1.8/day and then decreases rapidly due to the fall overturn. The reduction in the maximum growth rate due to light is substantial and shifts peak growth to early August. A further reduction in growth rate is due to the nutrient limitation so that the resultant growth rate,  $G_p$  is lowest at the end of May and peaks at about 0.25/day in August. The peak value represents an overall reduction of 90% from saturated growth conditions. Primary productivity values calculated from the growth rate and phytoplankton biomass Eq.(11) give peak values of about 600 mg carbon/m<sup>2</sup>-day at the end of August and values of about 500 mg C/m<sup>2</sup> day at the height of the spring bloom. The former value is in general agreement with Glooshenko<sup>2</sup> while the latter is somewhat lower than the Glooshenko's estimated spring values of 500-1100 mg C/m<sup>2</sup>-day.



## Dynamics of Phytoplankton Growth Rate

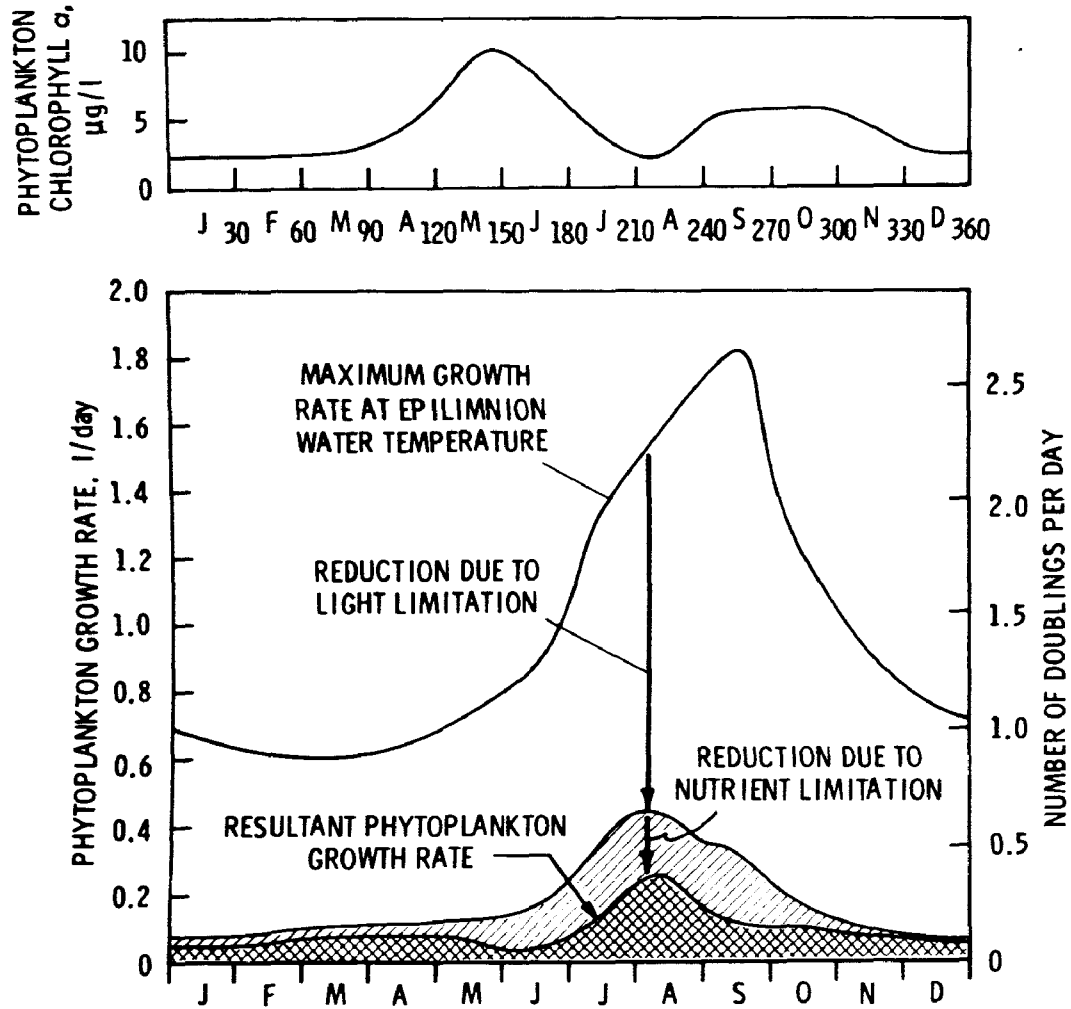


Figure 24. Dynamics of the phytoplankton growth rate



Fig.25 shows the dynamics of the kinetic death rate of the phytoplankton ( $D_p$  in Eq. (4) ). Three effects are to be noted: a) phytoplankton settling, b) water temperature effect on endogeneous respiration and c) effect of zooplankton grazing. Peak resultant death rate is 0.25/day at the beginning of August and is primarily due to zooplankton predation and quantitatively explains the mid-summer decline in phytoplankton biomass.

The dynamics of phytoplankton net production, i.e. chlorophyll/liter-day,  $dP/dt$ , are shown in Fig. 26. Net production here includes the kinetic interactions of growth in Fig.21, death and predation in Fig.25 and the effect of vertical mixing and lake outflow. The results shown in Fig.23 summarize the basic hypotheses of phytoplankton dynamics in Lake Ontario.

The spring growth phase to approximately mid-May is due primarily to increasing light and temperature. There are little zooplankton as yet, so growth continues until nutrient limitation becomes significant in early June. (This is principally phosphorus limitation as discussed below). The spring growth and spring peak are therefore simply described by a nutrient interaction effect with light and temperature dominating the growth and death terms. Following the spring peak however, the situation becomes considerably more complex and indeed a significant effort was devoted to unraveling the complex interactions which lead to a mid-summer decline and subsequent broad full peak.

It is hypothesized as computed in Fig.26, that during mid-summer, and following the nutrient limitation effect, zooplankton grazing



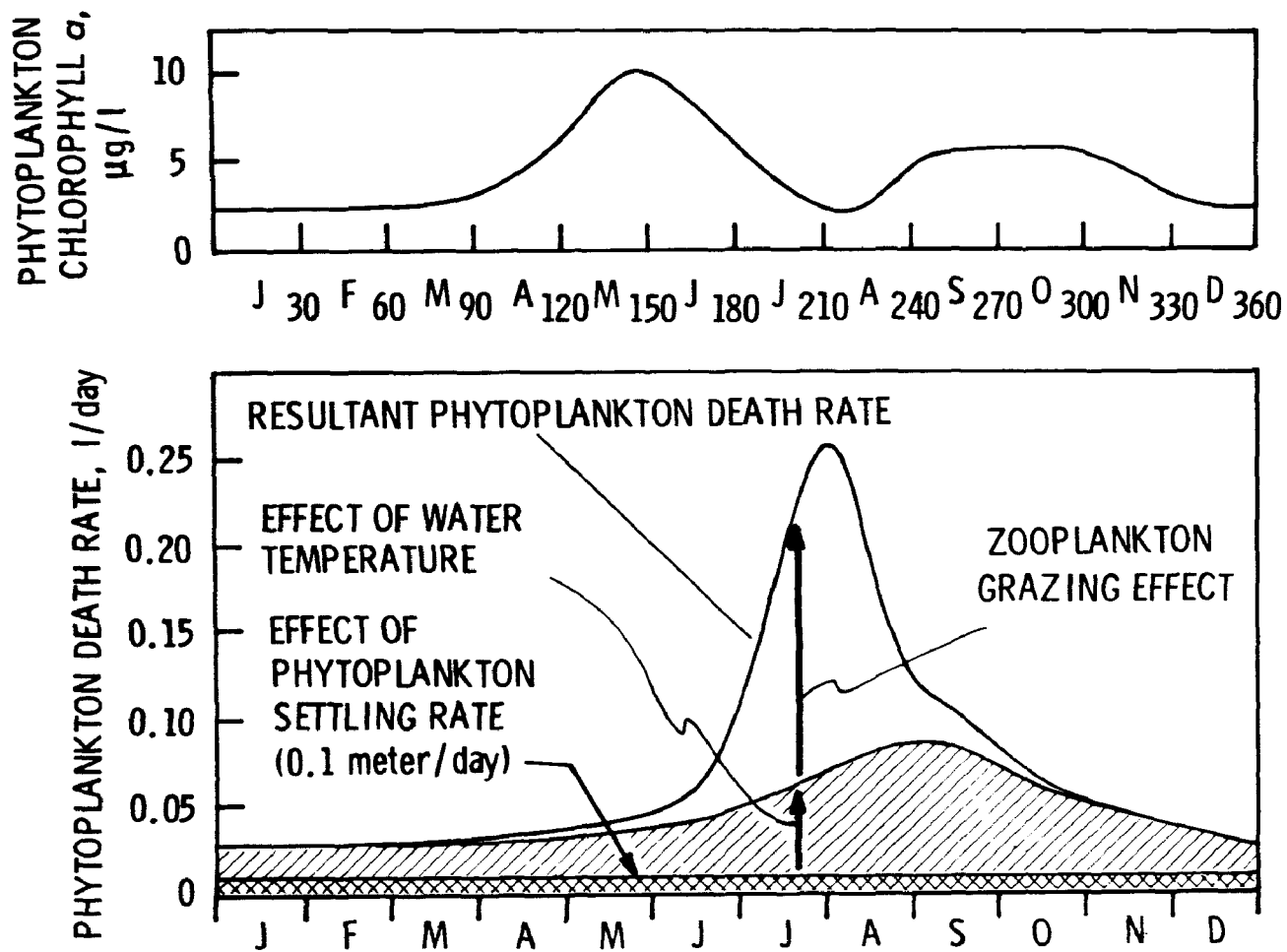


Figure 25. Dynamics of the phytoplankton death rate







becomes increasingly important and accounts for the minimum values of biomass in July. However, at increased zooplankton grazing, biological recycling of nutrients becomes more significant. Nutrients are released back to the epilimnion through excretion as well as phytoplankton endogenous respiration. In late July then, growth exceeds death due to nutrient regeneration and an active growth phase begins again. Nutrients however, are already at low levels so growth is not pronounced and proceeds slowly (as shown by the net production approaching zero in September but not yet entering a negative growth phase). The fall overturn of the lake then reduces the growth of phytoplankton biomass primarily because of mixing with the colder hypolimnion waters.

Figs. 27 and 28 explore these dynamic effects at another level of detail. The model permits calculation of nutrient limitation effects as well as the flux of nutrients due to zooplankton excretion and release of nutrients due to endogenous respiration by the plankton. Fig. 27 shows the nutrient effects. As seen, the spring bloom is halted essentially by a reduction in phosphorus that is quite pronounced and growth is reduced by a factor of about 0.35 due to the low phosphorus levels. At the same time, nitrogen is not limiting and is at a level twice that of the phosphorus. Nitrogen however does become limiting during July and again in September at which time phosphorus also exerts a limiting effect on growth. Fig. 27 shows therefore that the spring peak is primarily phosphorus controlled. The dynamics after the spring peak are however controlled by both nitrogen and phosphorus (as well as zooplankton predation).



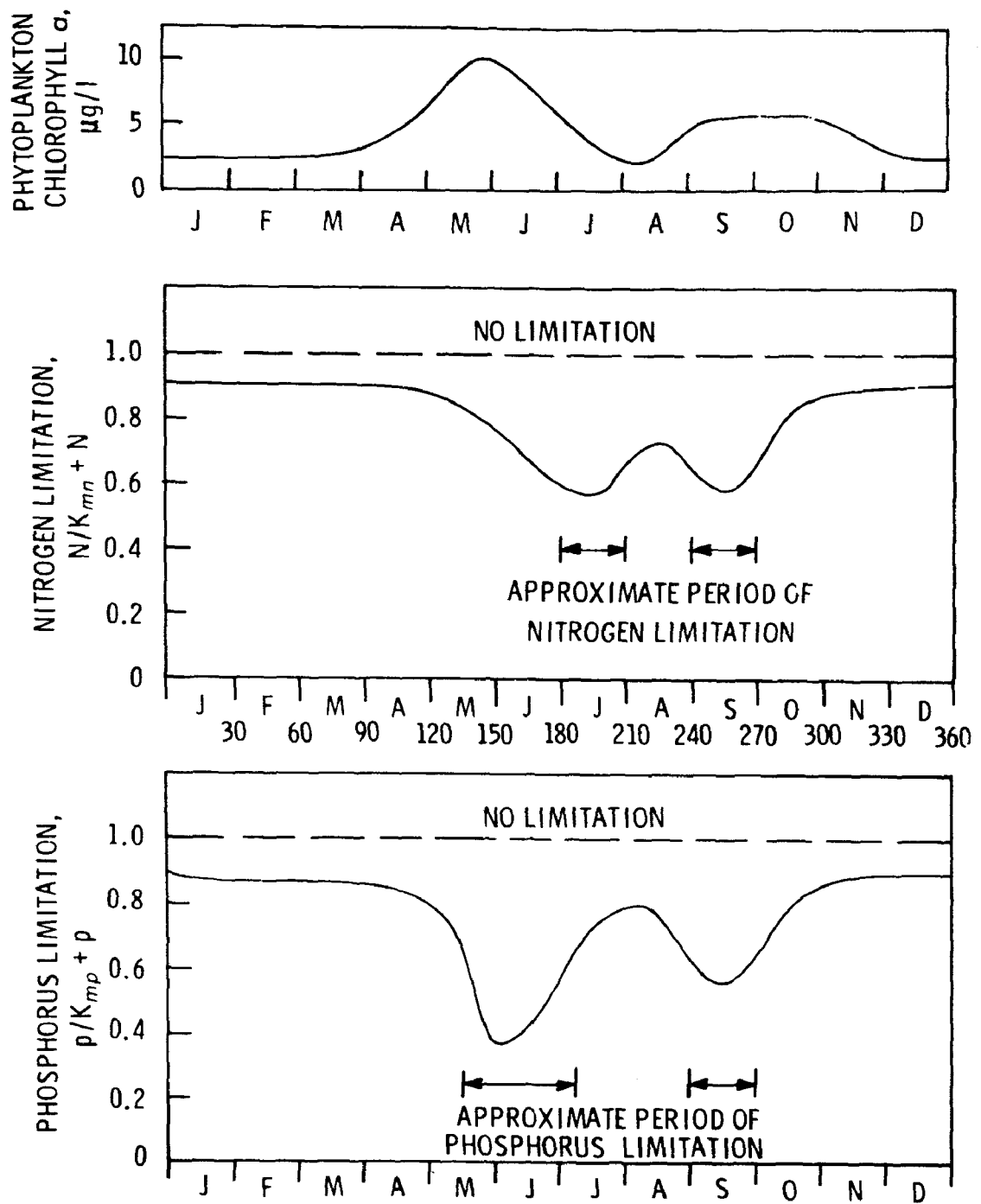


Figure 27. Dynamics of nitrogen and phosphorus limitations

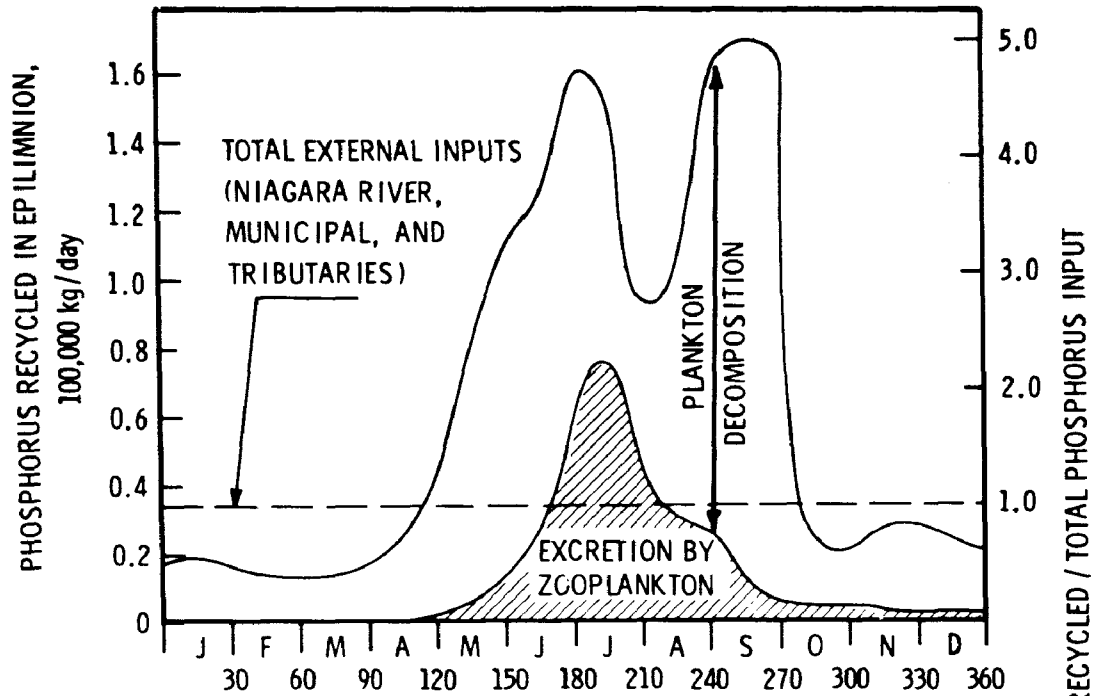


Fig.28 shows the estimated sources of phosphorus recycled to the epilimnion by both biological effects and vertical mixing effects from the hypolimnion. As shown, during early spring the hypolimnion contributes almost twice as much nutrients to the epilimnion as from external inputs and by early summer in June-July, biological recycling reaches almost five times the mass rate of external phosphorus sources due to waste residuals, Niagara River and other contributors. Zooplankton excretion recycles almost twice the input rate and in late summer-early fall, biological recycling reaches another peak but then drops rapidly due to fall overturn. The flux of nutrients from the more nutrient rich hypolimnion during October is not sufficient to offset the drop in water temperature in the epilimnion. Biological recycling therefore drops rapidly in October and the phytoplankton biomass declines (see Fig.21). The results shown in Fig.28 indicate quantitatively the significance of biological recycling and vertical mixing relative to the level of external nutrient inputs. A reduction in input phosphorus load therefore may not necessarily result in a concomitant reduction in biomass. Further, the time to reach a new equilibrium biomass level will extend beyond a single year due, in part, to the recycling effects discussed previously, and long detention times in Lake Ontario.

In summary, the Lake 1 modeling effort, to date, has indicated that a considerable degree of quantitative insight into the behavior of phytoplankton biomass can be obtained with a spatially simplified model that consists of an epilimnion, hypolimnion and sediment but is horizontally well mixed. The model, using acceptable ranges for plankton growth parameters, verifies observed data on phytoplankton, zooplankton and nutrient levels and as such can form a first basis for estimating the lake-wide effects



## Biological Recycling



## Hypolimnetic Recycling

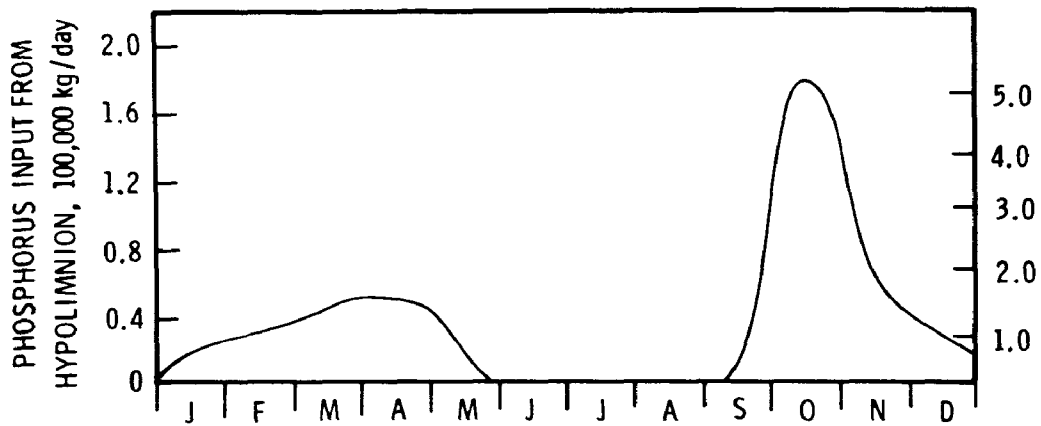


Figure 28. Biological and hypolimnetic recycling of phosphorus



of a nutrient reduction program.

The results indicate that the spring growth phase and peak phytoplankton biomass are primarily controlled by increasing light and temperature and phosphorus limitation. The mid-summer minimum in phytoplankton is estimated to be due principally to zooplankton grazing and nitrogen limitation. The broad fall peak in phytoplankton is a complex interaction of nutrient regeneration (up to five times the external nutrient inputs), subsequent nutrient limitation and then fall overturn. Both nitrogen and phosphorus are important nutrients in this dynamic succession.

From a water quality viewpoint, peak values of biomass in the spring are important, and are generally limited by phosphorus concentrations which reduce the nutrient growth rate by 35%. Nitrogen also has an additional effect of about a further 10% drop in growth rate. In the later summer months, it appears that the system is nitrogen limited as well as phosphorus limited. There may be important implications of this hypothesis; to wit, nutrient removal programs aimed solely at phosphorus may not achieve a sought-after objective especially in the late summer recreation months. This is especially relevant when one recognizes that generally this period of the year is dominated by the green and blue-green algae, which have greater potential for water use interference than do the diatoms.

A period of 10 - 20 years may be necessary for Lake Ontario to reach a new level of dynamic equilibrium in phytoplankton biomass after a nutrient reduction program is instituted. The long detention times, recycling effects and large store of nutrients in the hypolimnion are the principal reasons for this long response



Therefore, the Lake Ontario presently being observed represents conditions of about 10-20 years ago and since loads into the upper basin (e.g. Lake Erie) have been increasing steadily over the years, Lake Ontario is obviously in a "slowly" varying state from year to year. Thus, the effects of a waste removal program may not be apparent for approximately one-two decades and if some residual loads are allowed to continue to grow, significant changes in Lake Ontario quality may "never" be apparent. This also implies that a detailed program of sampling of effluents and tributaries and concurrent lake wide sampling are correlated only through an approximate ten year lag. The results also indicate that surveillance of large lake systems such as Lake Ontario may best be accomplished in a time scale of perhaps once every five years rather than year to year.

All of these observations on response times apply to the lake as a whole. The more detailed Lake 3 model which includes horizontal detail will obviously reflect more localized situations which may (or may not) reach dynamic equilibrium in shorter times.



## SECTION VI

### REFERENCES

1. Murthy, C.R., G. Kullenberg, H. Westerberg, and K.C. Miners. "Large scale diffusion studies," in IFYGL Bull. No. 10, pp.22-49. NOAA, Rockville, Md. May 1974.
2. Glooshenko, W.A., J.E. Moore, M. Munawar and R.A. Vollenweider. "Primary production in Lakes Ontario and Erie: A comparative study," Journal of Fisheries Research Board of Canada. 31(3):253-263. 1974.



## SECTION VII

### LAKE 2 ANALYTICAL INVESTIGATIONS

#### INTRODUCTION

As illustrated in Fig. 4 a strategy of essentially parallel investigations has been pursued in the development of Lake Ontario phytoplankton models. The Lake 2 investigation has resulted in a theoretical analysis, as opposed to numerical investigations, of the vertical interactions in phytoplankton populations. Two specific areas are addressed: the behavior of the asymptotic population growth rate and the effect of vertical settling velocity.

The form of the equations for a quantitative theory of the distribution of phytoplankton biomass have been known for some time<sup>(1)</sup> and their applications to various Great Lakes problem settings is ongoing<sup>(2,3,4)</sup>. An analyses of the conditions required for temporal steady state accompanied their introduction; however no time varying analysis of their general properties has been made.

The condition under which a population can maintain itself against transport loss<sup>(5)</sup> are related to the analysis to be presented insofar as an eigenvalue problem results, which gives the bounds on the parameter groups that result either in population increase or decrease. What has not been recognized is that if the population does increase it asymptotically approaches a condition which is a substantial simplification of the general solution of the biomass conservation equation. In particular, it can be shown that there exists an asymptotic population growth rate,  $\mu$ , which is independent of position, and an asymptotic population distribution, which completely



characterize the solution to the biomass equation. The asymptotic solution depends on the kinetic and transport parameters and to find these dependencies it is necessary to make some simplifying assumptions. However, the general existence of the asymptotic solution follows directly from the assumption of temporally constant parameters. It is shown subsequently that in fact this prediction is born out by observed phytoplankton biomass distributions.

The specific spatial setting for the analysis presented subsequently is in the vertical dimension. The motivation for the investigation is a desire to calculate the effects of vertical settling velocity on phytoplankton population development; in particular, what are the important dimensionless parameter groups. Depending on the question to be addressed a series of dimensionless plots are presented which give quantitative answers to the importance of the various parameters. In this way an economy is realized so that the complexity of even these idealized situations is kept to a manageable level.

A final product of this analysis is a demonstration that mathematical theory and biological fact can be brought into accord if the complexities of the latter are aggregated in such a way that the larger scale relationships are susceptible to a necessarily simplified mathematical treatment. The use of biomass as the primary dependent variable is a biological example; the use of a dispersion coefficient is a physical example. The result is a tractable mathematical problem which yields an array of information that can then be checked against observation. In this case, the prediction is the existence of an asymptotic population growth rate which is independent of position.



## THEORETICAL CONSIDERATIONS

The conservation of phytoplankton biomass in the presence of vertical transport processes requires that the rate of change of the biomass with respect to time is the result of the balance between the kinetic source and sink of biomass and the vertical transport, the effect of which is to remove biomass from the euphotic zone. The equation is quite well known:

$$\frac{\partial P}{\partial t} - \frac{\partial}{\partial z} \left( E \frac{\partial P}{\partial z} \right) + \frac{\partial}{\partial z} (wP) = (G - D) P \quad (56)$$

where

- $E$  = vertical dispersion coefficient
- $w$  = settling velocity, positive downward
- $G$  = growth rate
- $D$  = death rate
- $P(z,t)$  = phytoplankton biomass

In the absence of vertical transport, the population of each depth would either grow exponentially if  $G(z) > D(z)$  or decay exponentially if  $G(z) < D(z)$ . In fact, for  $E = w = 0$  it is clear that the solution is of the form:

$$P(z,t) \sim \exp [G(z) - D(z)]t \quad (57)$$

so that  $G-D$  is the net growth or decay rate of the population in a kinetic reactor with conditions comparable to those at depth  $z$ . The magnitude of  $G$  is quite well known <sup>(6,7)</sup> from numerous short term growth experiments. For the case of excess nutrients and constant



optimal light intensity,  $G$  is in the range of  $1.5-2.5 \text{ day}^{-1}$  at  $20^\circ\text{C}$ . The decay rate,  $D$ , for a population isolated from a light source is on the order of  $0.05$  to  $0.2 \text{ day}^{-1}$  at  $20^\circ\text{C}$ <sup>(1)</sup>. Thus, in the absence of vertical transport and with excess nutrients present, there should exist a depth at which the population is growing at a rate on the order of  $1.0 \text{ day}^{-1}$  so that in ten days the population at this depth increases by approximately 22,000 times. At large depths, however, the population should, in ten days, decrease to approximately 37% of its initial concentration. Such explosive growth does occasionally occur (patch blooms) but the more normal course of events is a much slower growth of the entire population until either nutrient exhaustion, zooplankton predation, or self-shading reduces  $G-D$  to a point at which population growth ceases. The question of interest is how does the population growth rate depend on the kinetic parameters,  $G$  and  $D$ , the transport parameters,  $E$  and  $w$ , and the variation of growth rate with depth due to light extinction.

If conditions are such that the population does increase with time, and for a period the transport and kinetic parameters are constant in time, then there are mathematical reasons, given subsequently, to expect that after a relatively short time, the population distribution will be of the form

$$P(z,t) \approx P(z)e^{\mu t} \quad (58)$$

that is, the entire population will be growing at an asymptotic population log growth rate,  $\mu$ , independent of depth. The asymptotic population growth rate and the asymptotic population distribution as a function of depth,  $P(z)$ , aside from a constant multiple, are independent of the initial biomass



distribution  $P(z,0)$  at the time of the start of the population growth (arbitrarily taken as  $t=0$ ). They depend only on the kinetic and transport parameters which characterize the period of population growth. This is a substantial simplification of what, in general, are complex and difficult solutions to the biomass equation, and from this simplification follows substantial insights into the behavior of phytoplankton populations during their growth phase.

#### ASYMPTOTIC POPULATION GROWTH RATES

To establish that, in fact, phytoplankton biomass behaves as predicted by the mathematical analysis, a series of plots of  $\log P(z,t)$  vs. time at various depths are presented in Figs. 29 through 32.

During the winter and spring the horizontally averaged phytoplankton biomass in Lake Ontario increases quite slowly but the increase is approximately exponential as shown in Fig. 29. The data collected during the 1973 IFYGL cruises shows this population growth and in particular, it is approximately the same for all depths to 50 meters. Since the population growth rate is quite small, and the time for the development of the asymptotic distribution is on the order of  $1/\mu$ , in this case approximately 100 days, it is not surprising that the lower layers have not yet responded in the predicted manner.

During the intensive Project Hypo study of Central Lake Erie (8) the phytoplankton population increased approximately five fold in 35 days. As shown in Fig. 30 the asymptotic population growth rate was  $\mu \approx 0.043 \text{ day}^{-1}$  and again the population increased at this



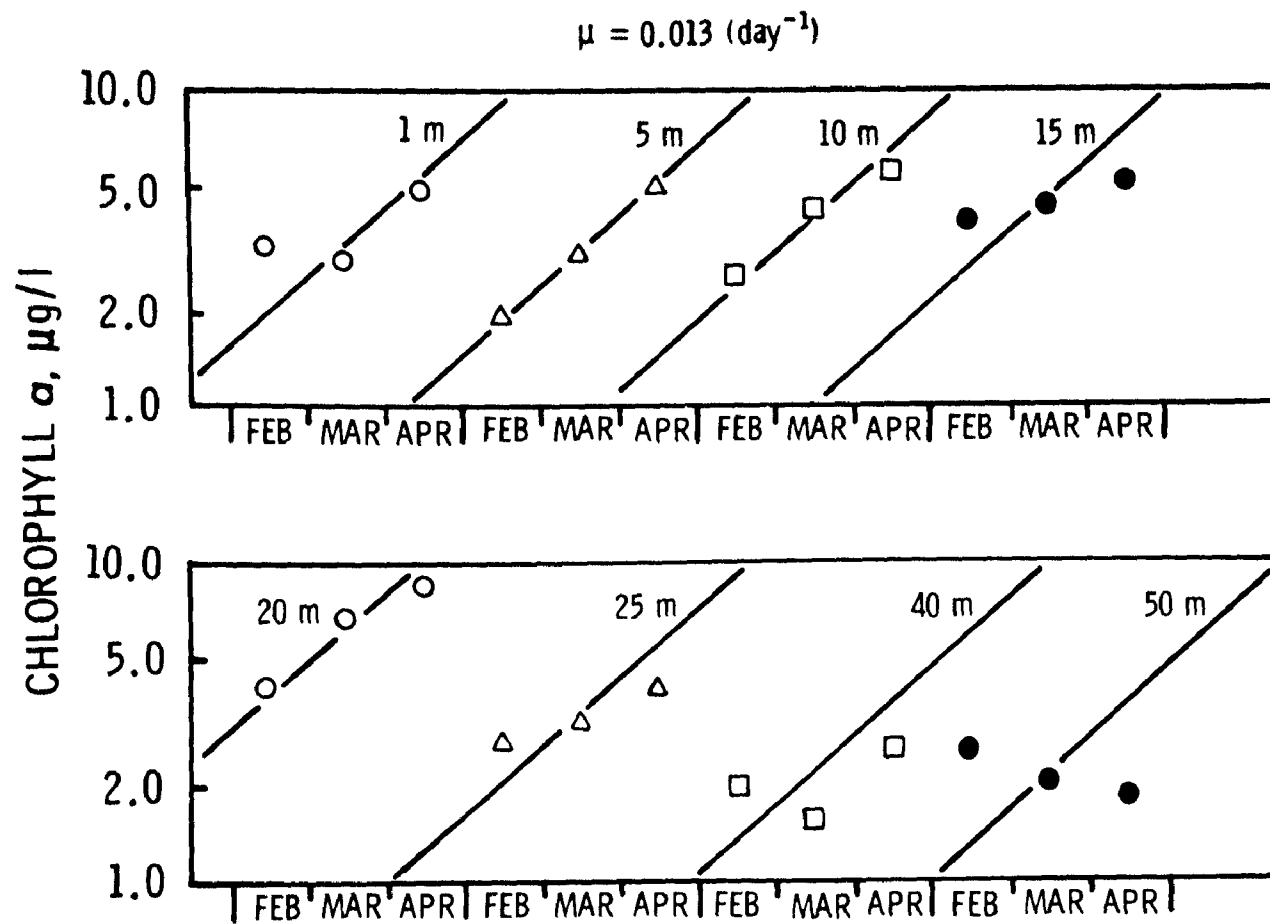


Figure 29. Lake Ontario Phytoplankton Biomass, horizontal averages 1973.  
IFYGL



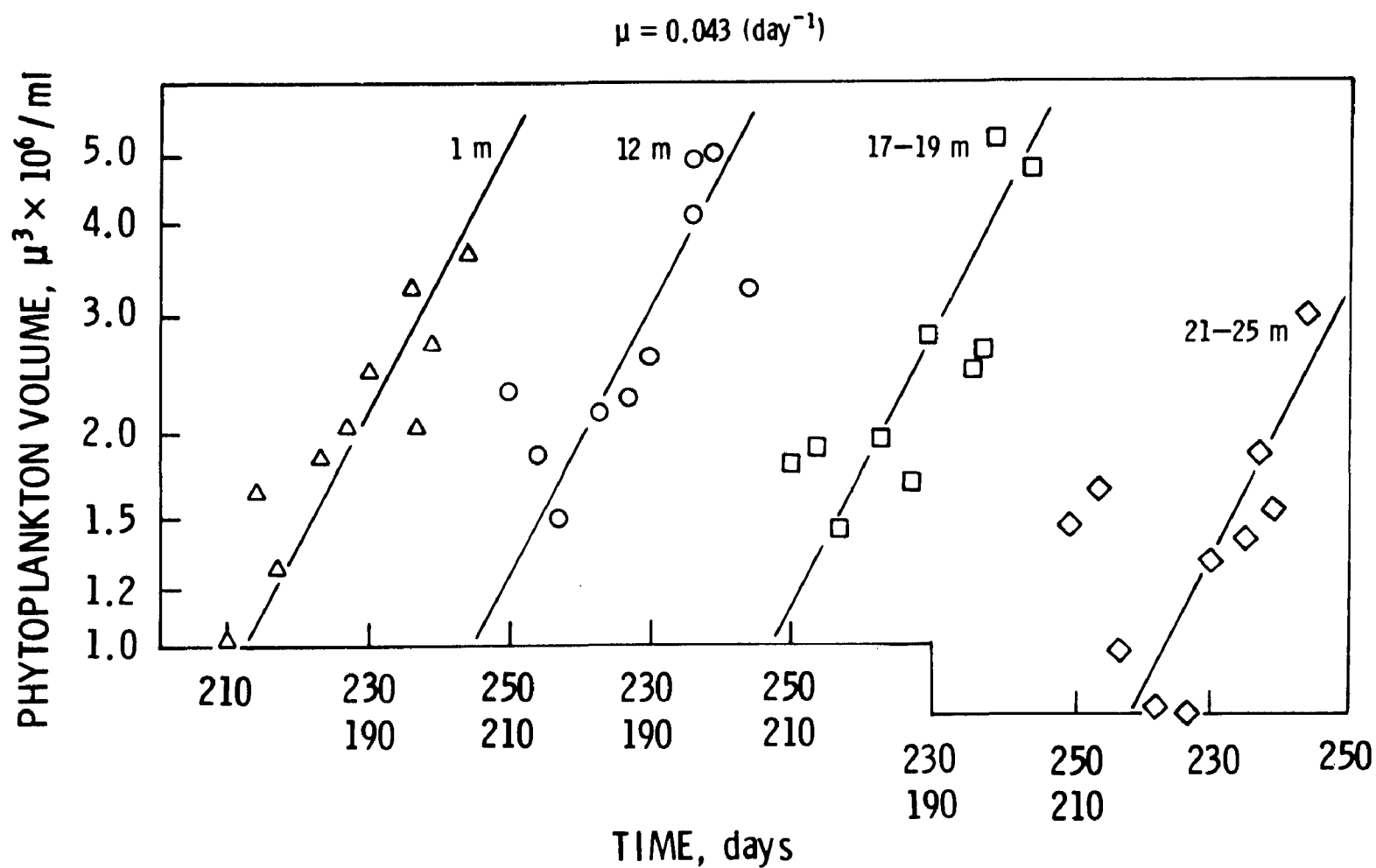


Figure 30. Central Lake Erie Phytoplankton Biomass, four station log averages. 1970.  
Project Hypo



exponential rate at 1,12 and 17-20 meters, with the population in the deeper layers (21-25 m) acquiring this growth rate near the end of the sampling period. The time to achieve the asymptotic distribution in this case is on the order of 25 days.

Onondaga Lake is a small ( $12\text{km}^2$  surface area, 20 m maximum depth), highly eutrophic lake in New York State<sup>(9)</sup>. The duration of the growth period for the phytoplankton population is 150 days during which the population increases one thousand fold to concentrations of  $10^5$  cells/ml corresponding to a population growth rate of  $\mu=0.048\text{ day}^{-1}$ . As shown in Fig. 31 the population growth rate is approximately the same at the four depths sampled even though there is almost an order of magnitude less biomass in the deeper layers.

St. Margaret's Bay is a coastal inlet on the southern shore of Nova Scotia<sup>(10)</sup>. Similar behavior is observed during the period of exponential growth. The population growth rates is  $0.16\text{ day}^{-1}$ , substantially larger than those of the previous examples. The deviations from the predicted constant population growth rates in the lower layers cannot be attributed to the time it takes to achieve the asymptotic distribution since at this large  $\mu$ , 10 days should be quite sufficient. It appears that self-shading is causing the growth rate in the lower layers to decrease as the population increases in the top layers, thus violating the assumption that the parameters are constant in time.

Taken as a whole, the data presented strongly suggests that during the exponential growth of a population, if the kinetic and transport parameters are constant, an asymptotic population growth rate occurs which characterizes the growth of the entire population,



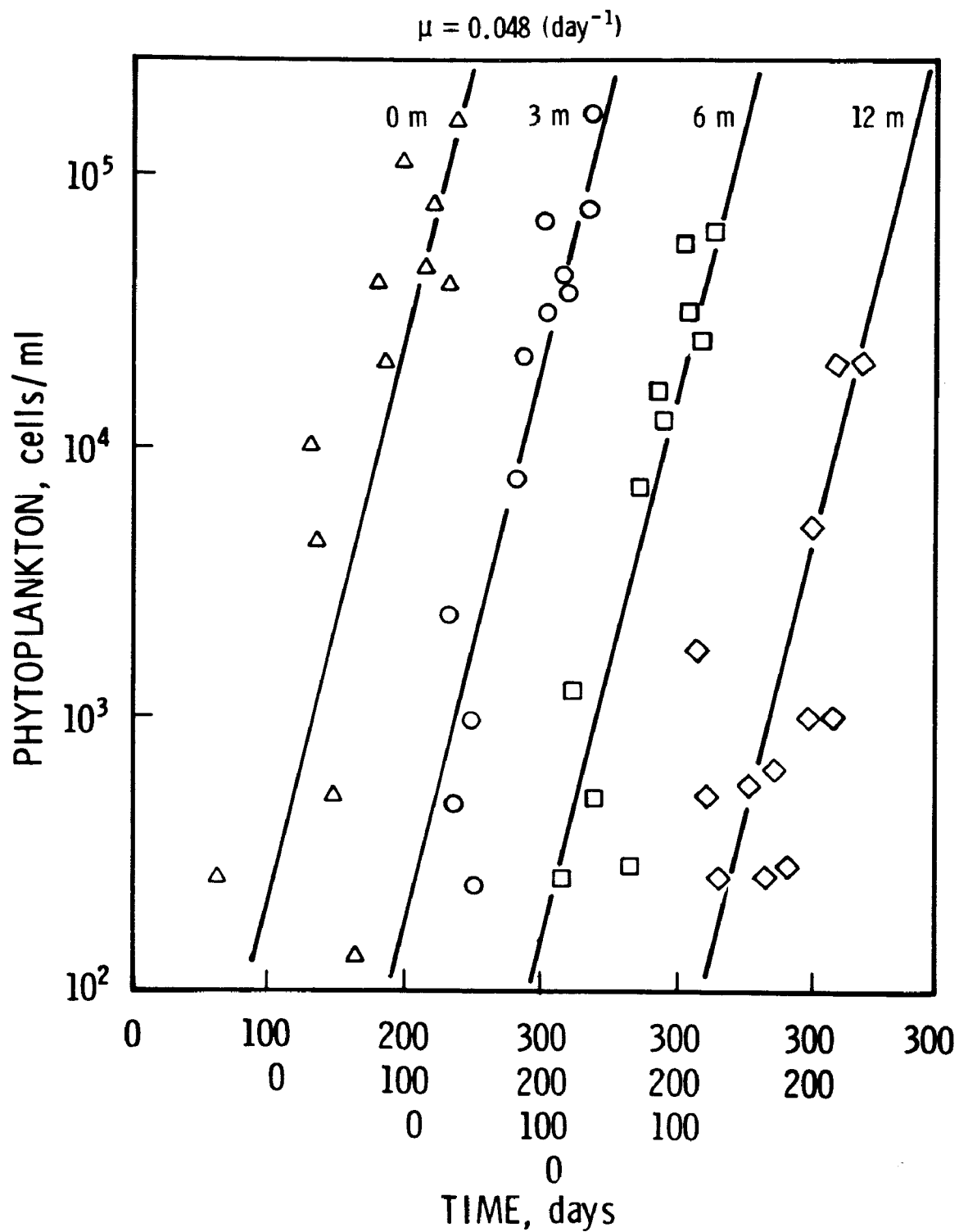


Figure 31. Onondaga Lake Phytoplankton Biomass, two stations.  
1969.



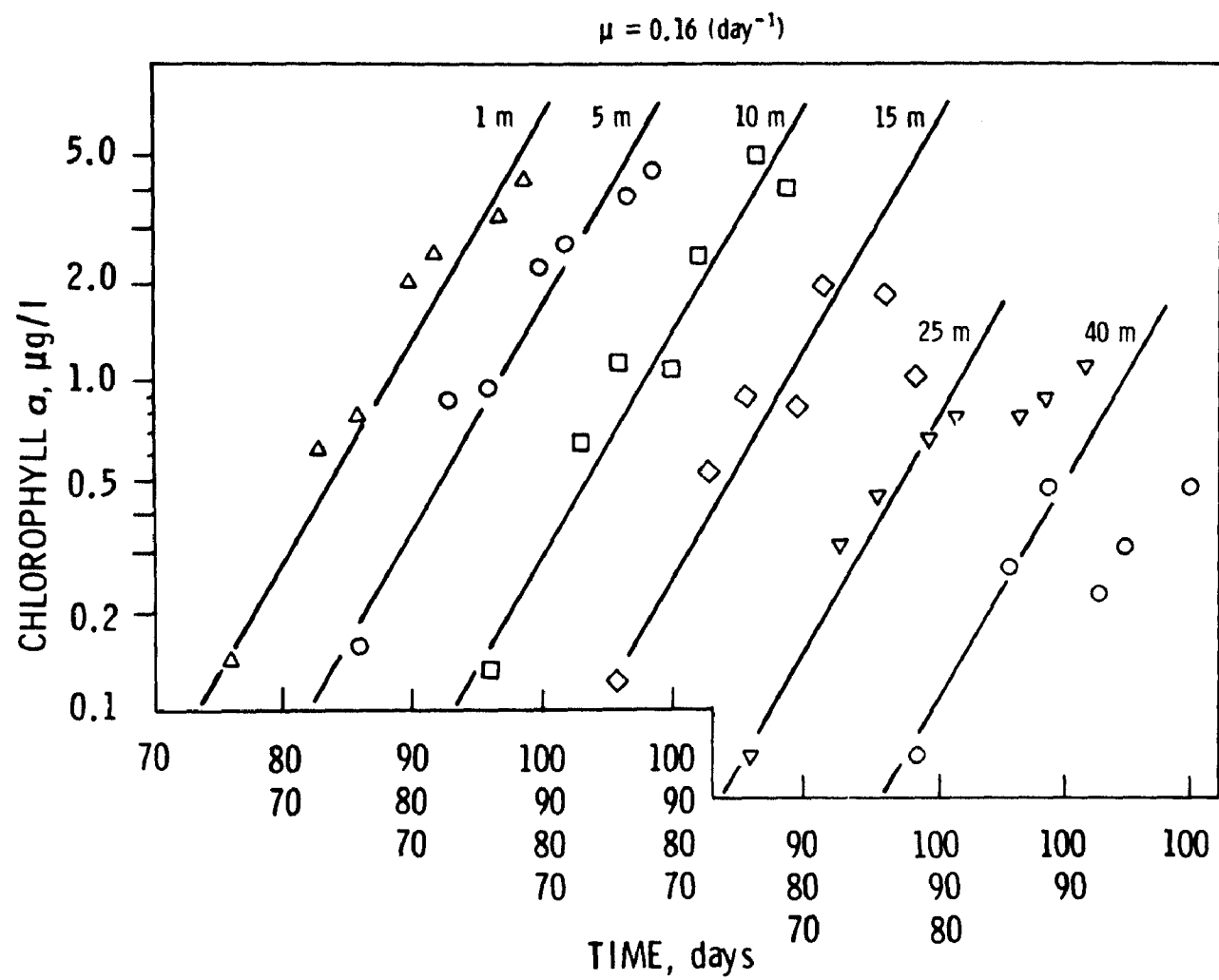


Figure 32. St. Margaret's Bay Phytoplankton Biomass, station A, 1969.



independent of position.

#### SOLUTIONS FOR SPECIFIC CASES

The existence of an asymptotic population growth rate, independent of depth for temporally constant parameters, is a consequence of the properties of the general mass balance equation. In order to investigate the relationship between this growth rate and the parameters of the equation, it is necessary to make certain assumptions concerning the variations in depth of the kinetic and transport parameters. In particular, assume (not very realistically for some cases) that all the parameters, save the growth rate, are constant. For the growth rate, two forms lend themselves to analytical solutions:

a two layer approximation:

$$\begin{aligned} G(z) &= G & 0 < z < L \\ &= 0 & L < z \end{aligned} \quad (59)$$

and an exponential approximation:

$$G(z) = G e^{-z/L} \quad (60)$$

The solution proceeds directly using the asymptotic solution (eq.58). Substituting it into the conservation of mass equation (56) yields:

$$-E \frac{d^2 P}{dz^2} + w \frac{dP}{dz} = [G(z) - (D+\mu)]P \quad (61)$$

This equation is solved together with the boundary condition at the water surface:

$$-E \frac{dP}{dz} + wP = 0 \quad \text{at} \quad z=0 \quad (62)$$

which requires that no biomass cross the air-water interface, and



the boundary condition at infinite depths, for which we require that the biomass remain finite. The result is an eigenvalue problem to find  $\mu$  and  $P(z)$  for the above ordinary differential equation with the homogenous boundary conditions.

For the exponential case the differential equation (56) becomes:

$$-E \frac{d^2 P}{dz^2} + w \frac{dP}{dz} = [G e^{-z/L} - (D+\mu)] P \quad (63)$$

which has a solution (11)

$$P(z) = e^{\pi z/2L} J_{\nu} (2\lambda e^{-z/2L}) \quad (64)$$

where  $\nu = \sqrt{\pi^2 + 4\lambda^2/\kappa}$

$$\kappa = G/(D+\mu)$$

$$\pi = wL/E$$

$$\lambda = L \sqrt{G/E}$$

and  $J_{\nu}(z)$  is a Bessel function of the first kind. At large depths, the solution becomes

$$P(z) \approx \exp \left[ \left( 1 - \sqrt{1 + \frac{4\lambda^2}{\pi^2 \kappa}} \right) \frac{\pi z}{2L} \right] \quad (65)$$

which approaches zero exponentially. The eigenvalue equation is obtained from the boundary condition at  $z = 0$  (eq. 62):

$$J_{\nu}(2\lambda) \left( 1 + \frac{\nu}{\pi} \right) \frac{\pi}{2\lambda} = J_{\nu+1}(2\lambda) \quad (66)$$

A multiplicity of  $\mu$ 's are solutions for the equation; the one of interest is that which is largest and, more important, positive since it is the asymptotic population log growth rate. For



certain sets of  $\pi$  and  $\lambda$  no positive  $\mu$  exists. For such situations no population increase is possible.

For the two layer case, the solution is obtained in two parts, a sinusoidal solution in the euphotic zone,  $0 < z < L$ , and a decreasing exponential thereafter. The eigenvalue equation is:

$$\pi = \frac{\tan^{-1} \left( \frac{1}{\beta} \right) + \tan^{-1} \left( \frac{\sqrt{1+4n}}{\beta} \right)}{\beta/2} \quad (67)$$

where  $\beta = \sqrt{4n(\kappa-1) - 1}$

$$n = (D+\mu) E/w^2$$

and  $\kappa = \bar{G}/(D+\mu)$

The solutions of these eigenvalue equations is shown in Fig. 33 in terms of the dimensionless ratio of growth rate of the sum of death rate and population growth rate  $G/D+\mu$ ; a penetration depth  $L\sqrt{G/E}$  which characterizes the size of the euphotic zone in terms of the growth rate and the dispersion coefficient; and a piclet number  $wL/E$ , which is the ratio of advective transport to dispersive transport. The values for the exponential case are given in Table 10. It is interesting to note that the shapes and magnitudes of the results are comparable, indicating that the details of the vertical distribution of the growth rate are not critical to the conclusions that can be drawn. As an example of their utility consider the effect of settling velocity for the range of  $G/D+\mu$  encountered in practice,  $G/D+\mu < 10$ , it is clear that a peclet number,  $wL/E$ , of greater than 0.1 is required to affect the growth rate of the population.



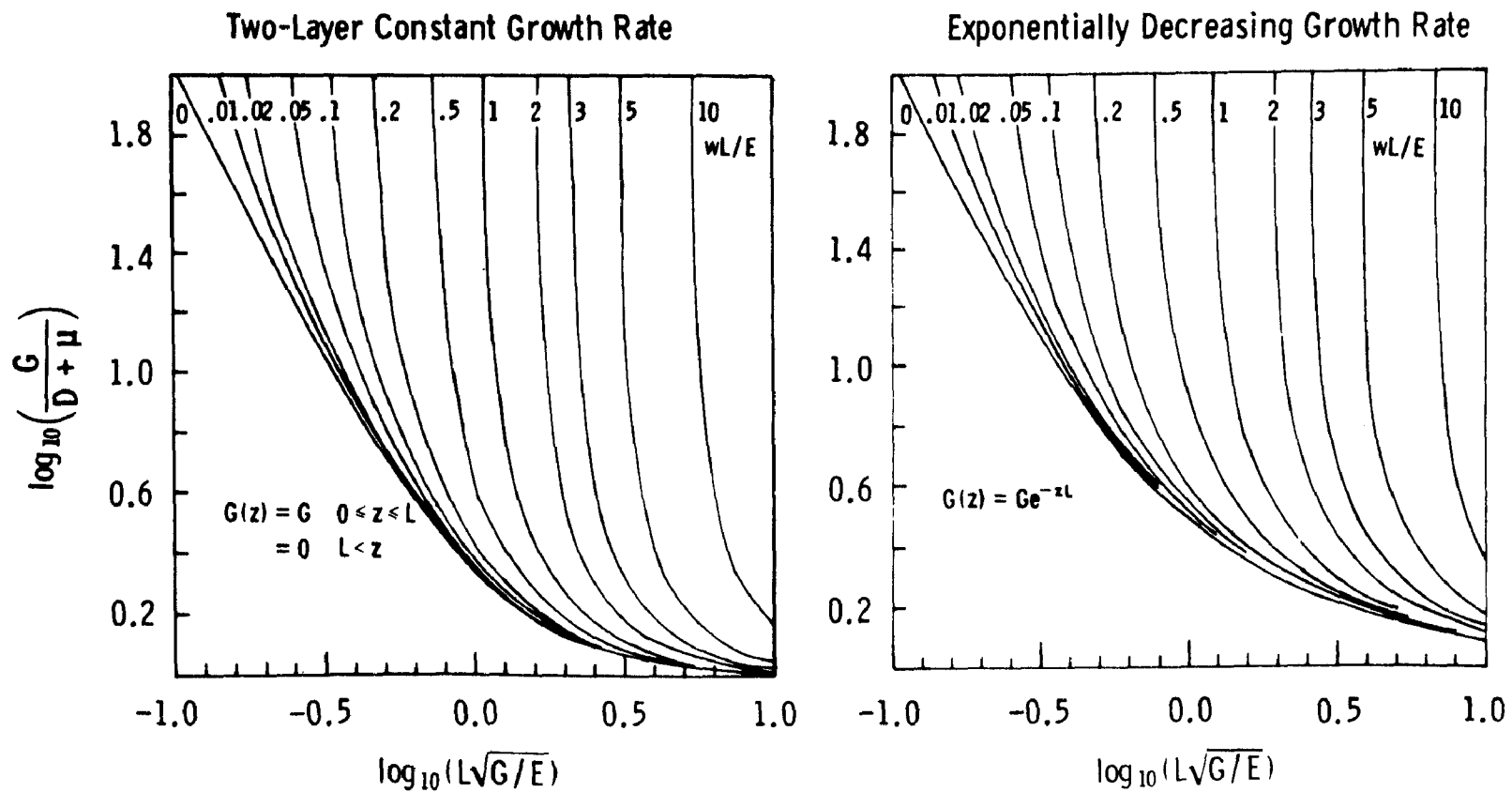


Figure 33. Eigenvalue equation solutions for constant growth layer and exponentially decreasing growth rate cases.



TABLE 10

FOR EXPONENTIALLY DECREASING GROWTH RATE

LOG <sub>10</sub> (G/D+μ) FOR EXPONENTIALLY DECREASING GROWTH RATE											
Log 10 <sup>(λ)</sup>	π	-1.0	-0.9	-0.8	-0.7	-0.6	-0.5	-0.4	-0.3	-0.2	-0.1
0.50											2.2281
0.20									1.7007	1.0358	0.7731
0.10								1.4158	1.0455	0.8251	0.6681
0.05						1.9903	1.4123	1.1192	0.9129	0.7536	0.6263
0.02				2.3352	1.7515	1.4364	1.2021	1.0115	0.8519	0.7172	0.6038
0.01			2.2545	1.8509	1.5721	1.3456	1.1512	0.9816	0.8337	0.7059	0.5966
0.00		2.0170	1.8226	1.6325	1.4484	1.2724	1.1068	0.9542	0.8166	0.6951	0.5897

$\pi$	$\text{Log}_{10}^{(\lambda)}$	0.0	0.1	0.2	0.3	0.4	0.5	0.6	0.7	0.8	0.9
5.00								1.2401	0.5484	0.3512	0.2479
3.00							0.7034	0.4394	0.3106	0.2322	0.1795
2.00					1.4192	0.6510	0.4352	0.3186	0.2440	0.1920	0.1540
1.00			1.4778	0.7376	0.5114	0.3842	0.3002	0.2401	0.1950	0.1602	0.1327
0.50		0.9140	0.6411	0.4880	0.3856	0.3113	0.2548	0.2106	0.1754	0.1469	0.1235
0.20		0.6083	0.4908	0.4020	0.3326	0.2771	0.2322	0.1953	0.1649	0.1395	0.1183
0.10		0.5486	0.4545	0.3789	0.3175	0.2670	0.2253	0.1906	0.1615	0.1372	0.1167
0.00		0.4994	0.4228	0.3580	0.3034	0.2575	0.2187	0.1860	0.1583	0.1349	0.1150



It is this kind of order of magnitude analysis for which the analytical expressions are most suited. For more realistic investigations of detailed properties of the population, resort to direct numerical methods is usually necessary.

#### THE SINGLE LAYER APPROXIMATION

It is common practice in one layer models (12) of the euphotic zone to approximate the effect of the settling velocity on the population by comparing  $w/L$  to the growth rate  $G$ . This approximation comes from the resulting differential equation for the euphotic zone layer:

$$\frac{dP}{dt} = (G - D - w/L)P + E' (P_1 - P) \quad (68)$$

for  $E'$  the bulk mixing coefficient and  $P_1$  the hypolimnion concentration. It is clear that in this approximation, changes in the  $w/L$  can be exactly compensated for by changes in  $G$ . To check the validity of this approximation against the continuous solution consider Fig.34, a plot of  $w/L$  vs.  $G$ , both normalized by  $D+\mu$ . The exponentially decreasing growth rate case is used. It is clear that no positive asymptotic growth rate exists if  $w/L > G$  so to this extent the approximation conveys the correct impression. In order to interpret this figure in more detail, assume that  $D+\mu$  and  $L$  are fixed, and the plot is  $w/L$  versus  $G$  for varying dispersion coefficient. For large vertical dispersion,  $L\sqrt{D+\mu}/E$  is small and the solution is independent of  $w/L$ , or, put another way,  $w/L$  can change without demanding a compensating change in  $G$  to keep  $\mu$  constant. What is occurring is that the settling biomass is being rapidly remixed into the euphotic zone so that the loss



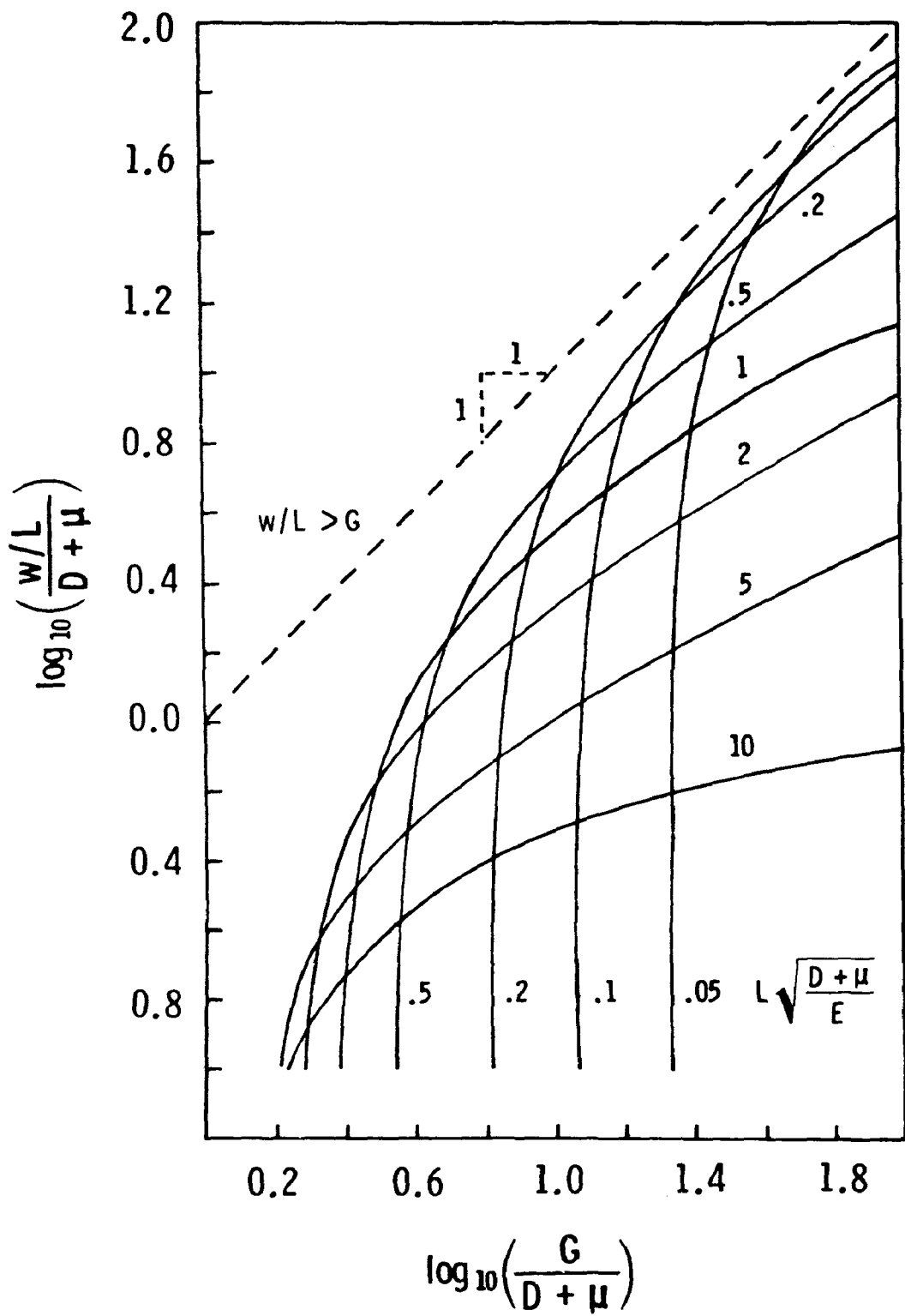


Figure 34. Settling velocity-growth rate interaction. The effect of dispersion. Exponentially decreasing growth rate case.



via this mechanism is small relative to the loss by dispersive mixing. On the other hand, for a small vertical dispersion the curves bend to such an extent that their slope is greater than 1, indicating that for this situation it requires larger than proportional increases in  $G$  to compensate for increases in  $w/L$ . The meaning of this unexpected result will become clear subsequently.

In order to investigate these interrelationships in a systematic way a series of plots is presented to indicate how each parameter affects  $\mu$  while holding others constant. The exponentially decreasing growth rate is employed for these calculations.

#### THE EFFECT OF INCREASING GROWTH RATE

For various euphotic zone depths (assuming the transport parameters  $w$  and  $E$  are constant) the effect on  $\mu$  of increasing  $G$  is shown in Fig.35. It is immediately clear that no solutions are possible for which  $\mu > G - D$ , which is obviously true since such a situation would require that mixing and settling have no effect on the population and that the fact that  $G(z)$  decreases in depth is unimportant. Perhaps a more unexpected result is that the slopes of the curves are greater than one, indicating that a change in  $G$  causes a larger than proportional change in  $D + \mu$ . As  $G$  is further increased, however, the population growth rate asymptotically approaches  $G - D$  as expected, and since there are non zero values of  $G$  for which  $D + \mu$  is zero, it is reasonable that the slopes are greater than one to enable  $D + \mu$  to, in effect, catch up with  $G$ . The condition  $G = D + \mu$  occurs at smaller  $G$  for deeper euphotic zone, as expected.



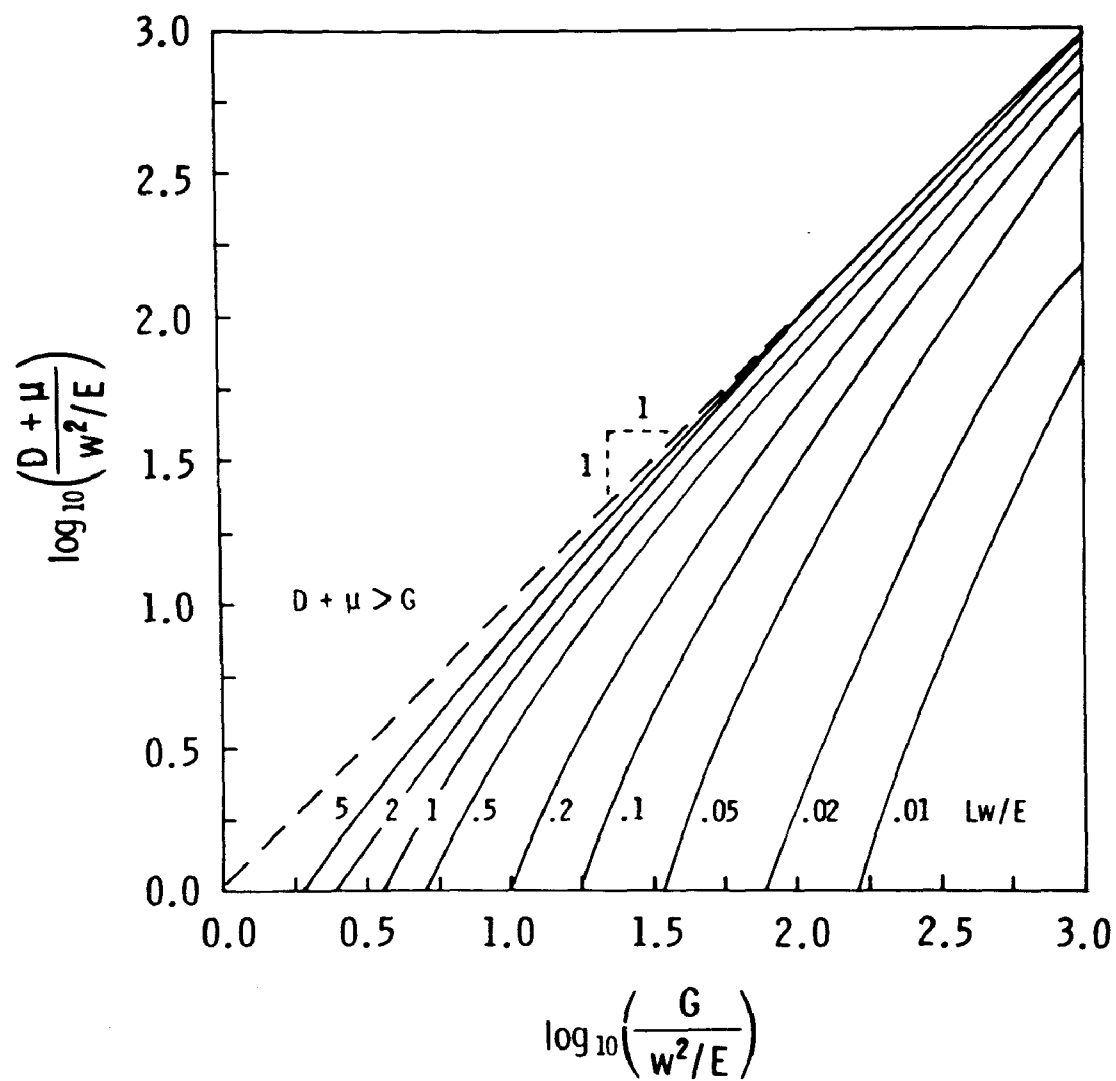


Figure 35. Population growth rate versus maximum growth rate. The effect of Euphotic zone. The exponentially decreasing growth rate case.



#### THE EFFECT OF INCREASING SETTLING VELOCITY

For various euphotic zone depths (assuming  $G$  and  $E$  are constant) the effect on  $\mu$  of increasing  $w$  is shown in Fig. 36. As  $w$  is increased the population growth rate is not affected until a critical range is reached at which time the effect begins. Further increases cause a sharp drop off in  $\mu$  until population growth is no longer possible.

#### THE EFFECT OF INCREASING DISPERSION

The effect on  $\mu$  of increasing the dispersion coefficient,  $E$ , for various euphotic zone depths (assuming  $G$  and  $w$  are constant) is shown in Fig. 37. A most surprising result is that for the range of the parameter,  $EG/w^2$  below one and  $LG/w < 10$ , increasing the dispersion increases the asymptotic growth rate. At first glance this appears to be incorrect since the mixing causes the population in the euphotic zone to be transported out of the zone, on balance, and therefore, would tend to decrease population growth. However, biomass is also being advected out of the zone via the settling velocity. With a small dispersion coefficient there is very little biomass at the surface since there is no way for the population, which grows as it sinks, to return to the surface layers. Hence, increasing the mixing actually benefits the population by allowing more biomass to accumulate in the surface layers where the growth rates are largest. It is this phenomena which causes the slopes greater than one in Fig. 34 for small dispersion coefficients.

#### THE EFFECT OF BOUYANCY

It is well known that certain species of phytoplankton exhibit negative sinking velocity and an in situ measurement has confirmed an example<sup>(13)</sup> so that instead of a liability their



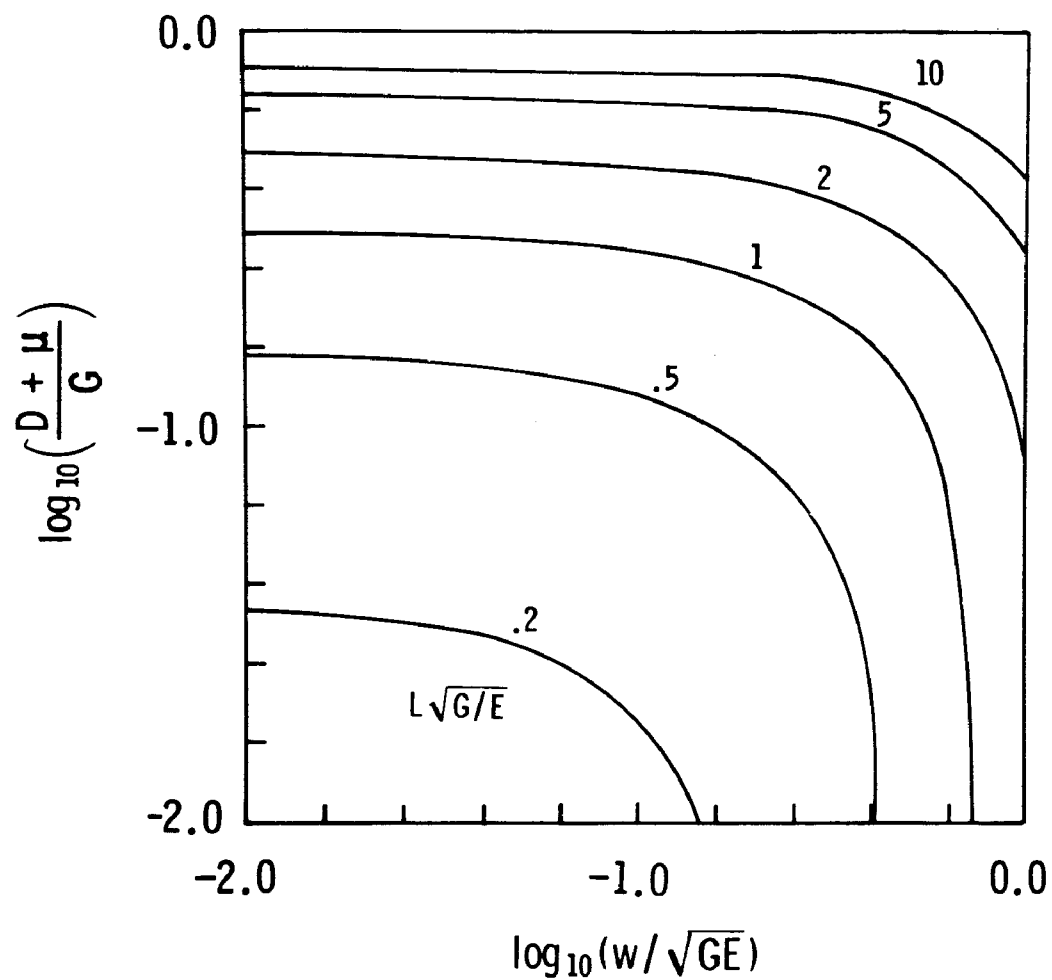


Figure 36. Population growth rate versus settling velocity--- the effect of Euphotic zone depth. The exponentially decreasing growth rate case.



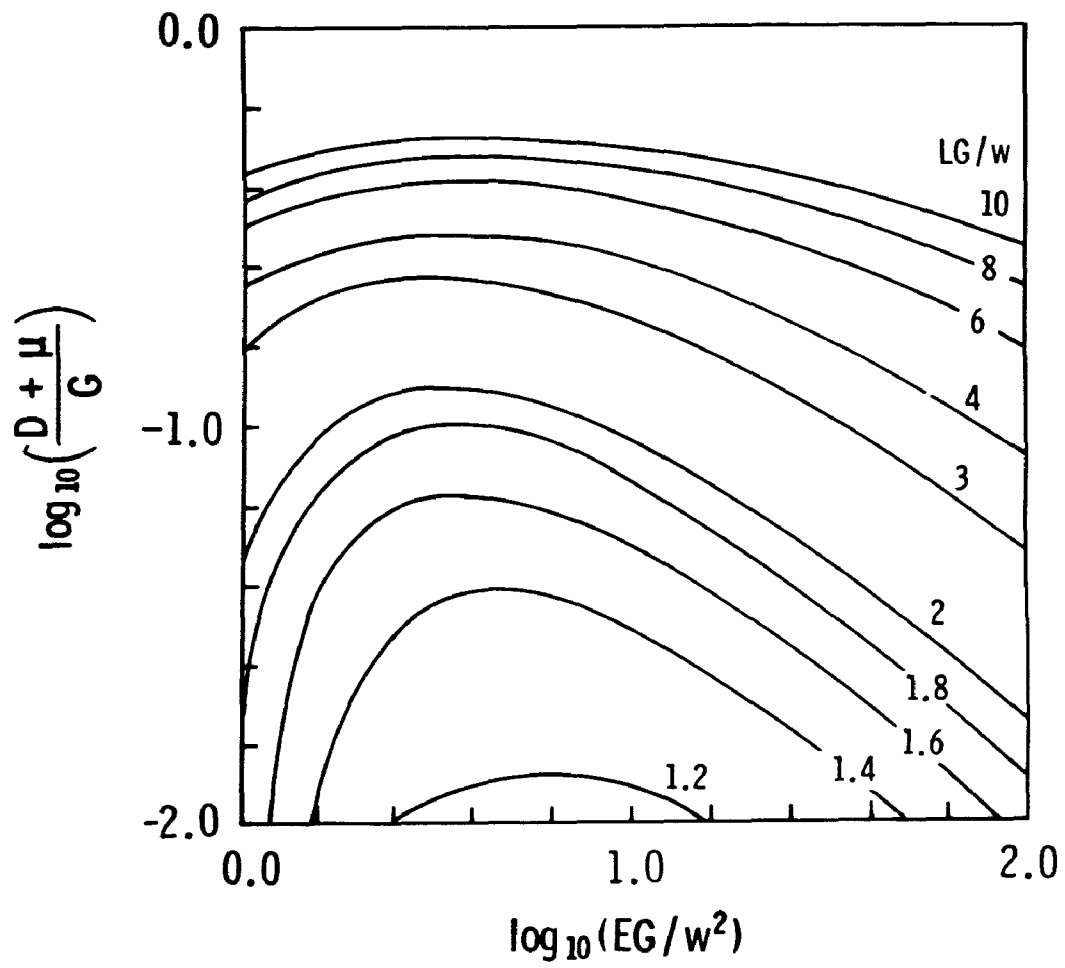


Figure 37. Population growth rate versus dispersion coefficient and the effect of Euphotic zone depth. The exponentially decreasing growth rate case.



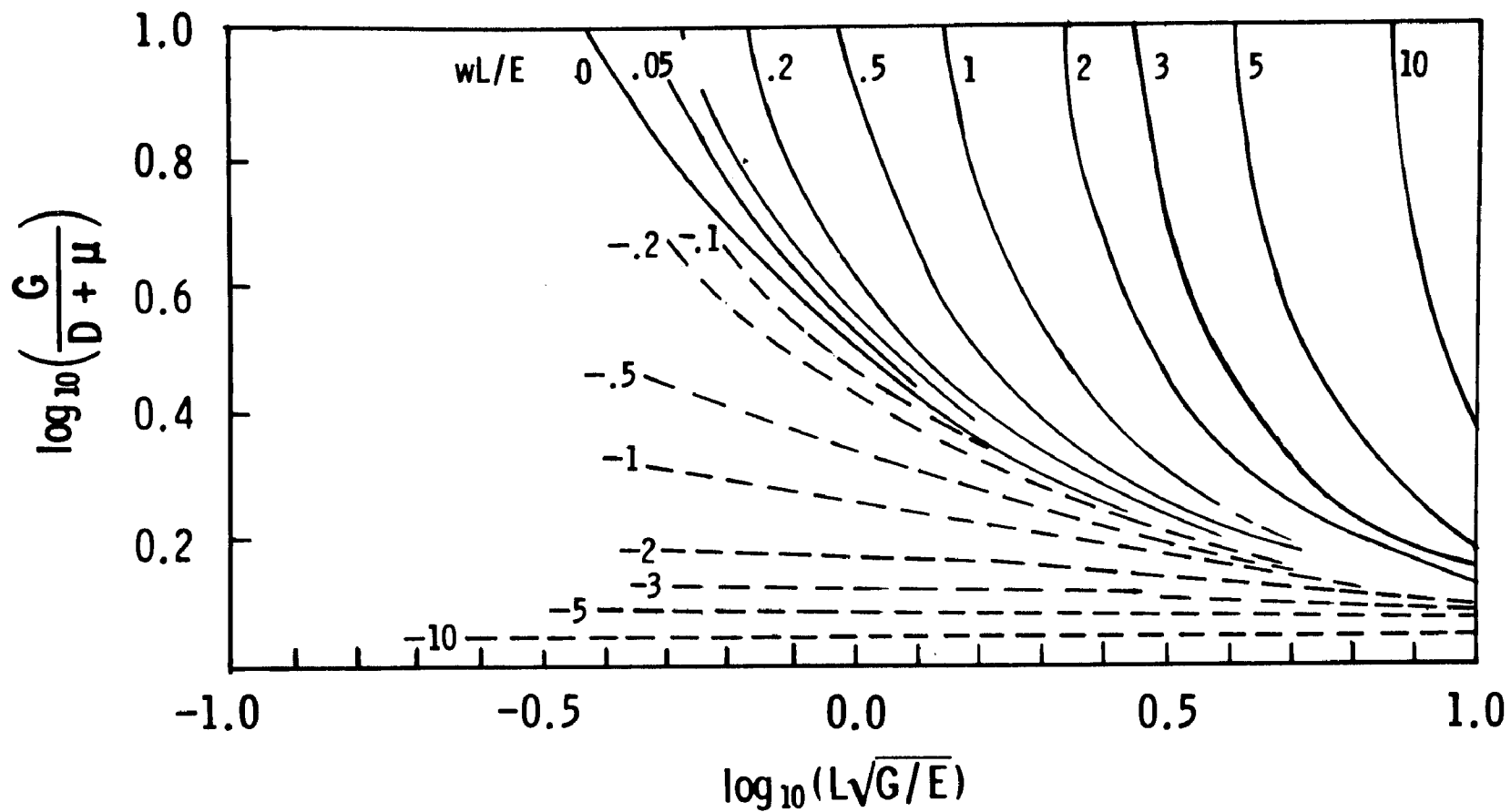


Figure 38. The effect of negative sinking velocity. The exponentially decreasing growth rate case.



bouyancy is an asset which should increase their population growth rate. Fig. 38 presents the results. For negative peclet numbers with magnitude less than 0.2, not much increase in  $\mu$  is calculated. However, as  $|w|L/E$  increases further, the population growth rate approaches the maximum possible, i.e.,  $\mu \rightarrow G-D$ , independent of  $L\sqrt{G/E}$  as indicated by the horizontal lines in the figure. The effect of the upward advection is to pile the biomass at the surface where it can grow at the kinetic rate,  $G-D$ , independent of the dispersive forces tending to mix it downward. This effect occurs for the negative peclet numbers greater than 1.0, provided  $L\sqrt{G/E}$  exceeds 0.3.

#### PRELIMINARY APPLICATIONS

As a first step in exploring the utility of the preceding analysis, a series of representative values for the dimensionless parameters are shown in Fig. 39. The majority come from the coastal ocean<sup>(1)</sup> with two lakes included. It is interesting to note that the values of  $G/D+\mu$  are comparable whereas the value of  $L\sqrt{G/E}$  span an order of magnitude. The major difficulty with increasing the number of points on this graph is in estimating the vertical dispersion coefficient and settling velocity. Values for  $G$ ,  $D$  and  $L$  for a given temperature, light intensity and extinction coefficient can be approximated;  $\mu$  is obtained from population observation, vertical dispersion can be obtained from vertical temperature models in which case the analysis, to within the accuracy of the assumption of constant parameters, can provide vertical settling velocities.

It is interesting to note that these data, when plotted on the figure which investigates the effect of dispersion, are in the range of the



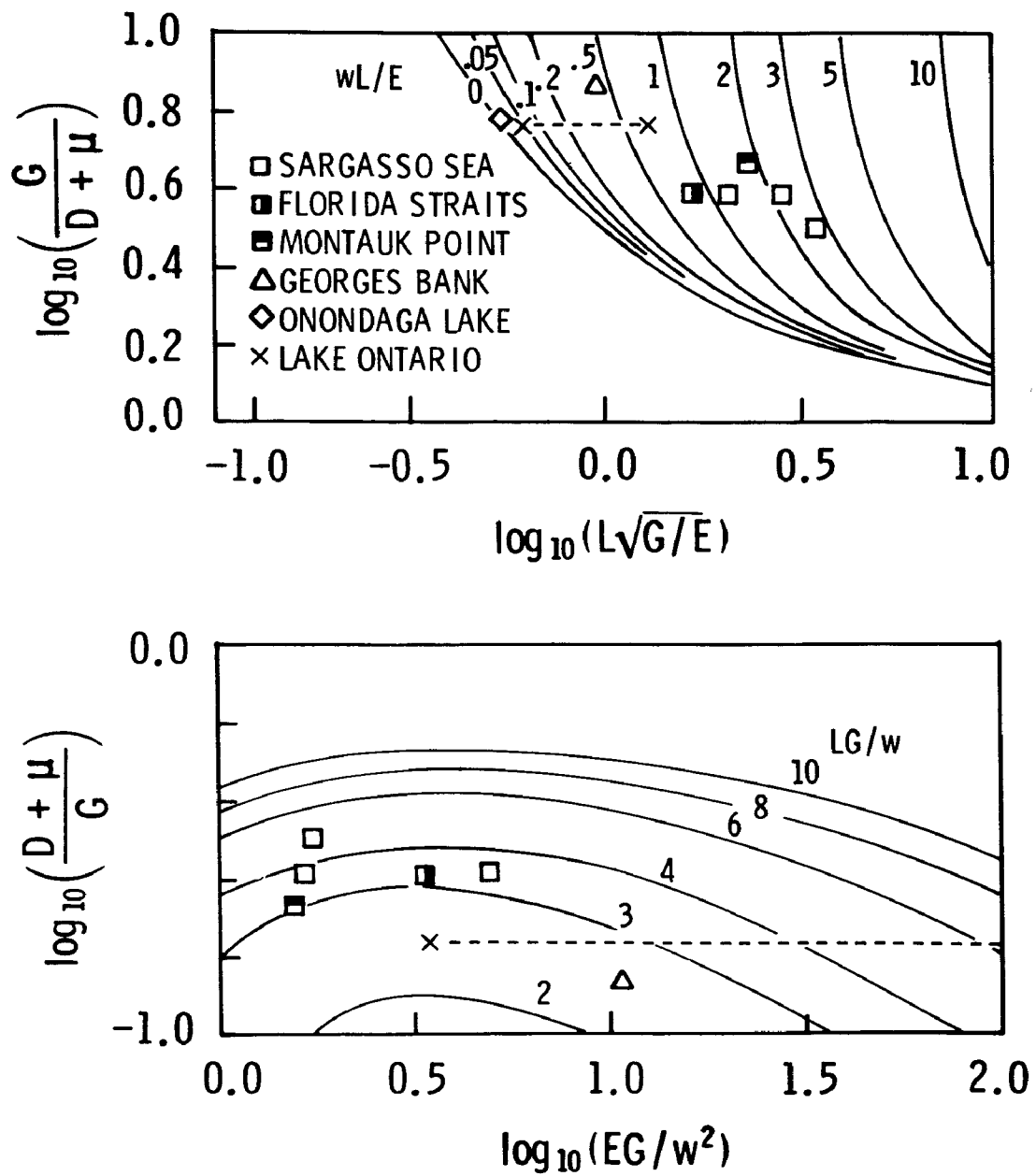


Figure 39. Application to Lakes and Oceans---the range of biologically relevant dimensionless numbers.



maxima for the oceanic situations and in the decreasing regions for the shallower situations. Whether this indicates some adaptive mechanisms for the characteristics of the marine phytoplankton is an interesting speculation but it is probably beyond the precision of the analysis to pursue this point.

#### SUMMARY OF MATHEMATICAL FACTS

The properties of eq.(56) are best illucidated by examining a spatially discretized version.

Let  $P_i(t) = P[(i + \frac{1}{2}) \Delta z, t]$  for a finite set of points starting at  $\Delta z/2$  and spaced  $\Delta z$  apart thereafter. The spatially discrete version of the differential equation follows by using the approximations:

$$\frac{\partial^2 P}{\partial z^2} \approx \frac{P_{i-1} - 2 P_i + P_{i+1}}{\Delta z^2} \quad (69)$$

$$\begin{aligned} \frac{\partial P}{\partial z} &\approx \frac{P_i - P_{i-1}}{\Delta z} && \text{for } w > 0 \\ &\approx \frac{P_{i+1} - P_i}{\Delta z} && \text{for } w < 0 \end{aligned} \quad (70)$$

There results a set of ordinary differential equations which can be written in matrix form as:

$$\frac{dP}{dt} = AP \quad (71)$$



Two properties of A are important:

(i) A is essentially nonnegative, i.e.

$$a_{ij} > 0 \quad i \neq j \quad (72)$$

(ii) A is irreducible, i.e. for any  $i, j$  there exists a finite sequence of indices  $k(0) = i, k(1), \dots, k(r) = j$  such that  $a_{k(h-1), k(h)} \neq 0$  for  $h=1, \dots, r$ .

Property (i) follows directly from the fact that the off diagonal elements of A are made up of sums of  $E/\Delta z^2$  and  $w/\Delta z$  which are positive. Property (ii) essentially requires that mass from any segment  $i$  can eventually be transported to any segment  $j$ , which is clear from the geometry of any reasonable problem.

The theorem <sup>(14)</sup> of interest is:

The matrix A satisfying (i) and (ii) has a unique (up to a multiplicative constant) strictly positive eigenvector  $\phi_1$ , with real simple eigenvalue  $\mu_1$ , i.e.

$$A\phi_1 = \mu_1\phi_1 \quad (73)$$

and  $\mu_1$  is the largest eigenvalue in the sense that

$$\mu_1 > \text{Re } [\mu_j] \quad (74)$$

for all the other eigenvalues,  $\mu_j$ , of A.

It follows directly from this fact that the asymptotic solution of the differential equations (71) has the form

$$P(t) = k e^{\mu_1 t} \phi_1 + o(e^{\mu t}) \quad (75)$$



where

$$\mu_1 > \mu > \max_{j \neq i} \operatorname{Re}[\mu_j]$$

and  $k$  is a constant.

This fact can be proven directly <sup>(14)</sup>. However, to see what is occurring assume that all eigenvalues  $\mu_j$  are distinct so that an eigenvalue expansion of the solution exists <sup>(15)</sup> of the form.

$$P(t) = \sum_j k_j e^{\mu_j t} \phi_j \quad (76)$$

where  $k_j$  are constants related to the initial condition  $P(z,0)$ . If  $\mu_1$  is positive and  $\operatorname{Re}[\mu_j]$  negative for all other  $j$ , then clearly the positive eigenvalue part of the solution dominates after a time on the order of  $1/\mu_1$ . If both  $\mu_1$  and  $\mu_2$  are positive (and  $\mu_2$  real for simplicity) the solution in segment  $i$  approaches:

$$\begin{aligned} P_i(t) &\approx k_1 e^{\mu_1 t} \phi_{1i} + k_2 e^{\mu_2 t} \phi_{2i} \\ &= k_1 e^{\mu_1 t} \phi_{1i} \left( 1 + \frac{k_2 \phi_{2i}}{k_1 \phi_{1i}} e^{(\mu_2 - \mu_1)t} \right) \end{aligned} \quad (77)$$

but  $\mu_2 < \mu_1$  so that the exponent is negative and it becomes small relative to 1 after a time on the order of  $1/(\mu_1 - \mu_2)$  and again the maximum eigenvalue solution dominates.



## SECTION VII

### REFERENCES

1. Riley, G.A., H. Stommel and D.F. Bumpus. "Quantitative ecology of the plankton of the western North Atlantic," Bull. Bingham Oceanog. Coll. 12(3):1-169. 1949.
2. DiToro, D.M., D.J. O'Connor, R.V. Thomann and J.L. Mancini. "Preliminary phytoplankton, zooplankton nutrient model of western Lake Erie," in Systems Analysis and Simulation in Ecology, Vol. 3. Academic Press, New York. 1973. In press.
3. Canale, R.P., S. Nachiappan, D.J. Hineman and H.E. Allen. "A dynamic model for phytoplakton production in Grand Traverse Bay," in Proc. 16th Conf. Great Lakes Res., pp.21-23. International Association, Great Lakes Research. 1973.
4. Thomann, R.V., D.M. DiToro, D.J. O'Connor and R.P. Winfield. "Mathematical modeling of eutrophication of large lakes," in Annual Report - Year 1. Manhattan College, Bronx, New York. 1973.
5. Kierstead, H. and L.B. Slobodkin. "The size of water masses containing plankton blooms," J. Mar. Res. 12:141-147. 1953.
6. DiToro, D.M., D.J. O'Connor and R.V. Thomann. "A dynamic model of the phytoplankton population in the Sacramento-San Joaquin Delta," Advances in Chemistry, No. 106, pp.131-180. American Chemical Society, Washington, D.C. 1971.
7. Eppley, R.W. "Temperatures and phytoplankton growth in the sea," Fishery Bull. 70(4):1063-1085. 1972.



## REFERENCES

8. Burns, N.M. and C. Ross. Project Hypo., CCIW Paper No. 6 and EPA TS-05-71-208-24. U.S. Environmental Protection Agency, Washington, D.C. February 1972.
9. O'Brien and Gere Engineers Incorporated. Onondage Lake Study. U.S. EPA Publication 11060, SAE 4/71, U.S. Government Printing Office. 1971.
10. Platt, T. and B. Irwin. Primary Productivity Measurements in St. Margaret's Bay, Tech. Report No. 203. Fish. Res. Bd. of Canada. 1973.
11. Murphy, G.M. Ordinary, Differential Equations and Their Solutions. D. Van Nostrand Co., Princeton, N.J. 1960.
12. Steele, J.H. "Plant production on fladen ground," Jour. Mar. Bio. Assoc., U.K. 35:1-33. 1956.
13. Burns, N.M. and A.E. Pashley. "In situ measurements of the settling velocity profile of particulate organic carbons in Lake Ontario," Jour. Fish. Res. Bd., Canada 31(3):291-297. 1974.
14. Birkhoff, G. and R.S. Varga. "Reactor criticability and nonnegative matrices," Jour. SIAM 6(4):354-377. 1958.
15. Bellman, R. Introduction to Matrix Analysis. McGraw-Hill, New York. 1960.



## SECTION VIII

### PRELIMINARY LAKE 3 MODEL

As shown in Fig. 40, the Lake 3 model represents a synthesis of spatial geometry and transport structure with the biological and chemical kinetic interactions of the Lake 1 and 2 models. Lake 3 is therefore a three-dimensional time variable model which does permit some analysis of phenomena in the near-shore region as compared to the open lake region. The structure of Lake 3 represents a further step beyond the simple Lake 1 model, the extent of the step incorporating such factors as computational time for a one year run and availability of survey data.

The work reported here is of a preliminary nature since considerably more effort is required to assure the veracity of the computed results both in terms of the numerical output and the degree to which the model verifies observed data. The full detailing and documentation of Lake 3 will be the subject of a future report.

The basic segmentation used for the Lake 3 model is shown in Fig. 40. As shown, 67 segments are used distributed over five vertical layers. The upper two layers, 0-4 meters and 4-17 meters are considered to represent the epilimnion during periods of vertical stratification. A "ring" of segments extending 10 km out from the coast is used to represent the near-shore environment. All cross-sectional areas for interfaces in three dimensions between the segments were planimetered and volumes were computed and summed to within 10% of total lake volume.

#### CIRCULATION AND DISPERSION

The emphasis in Lake 3 is on the biological and chemical kinetics



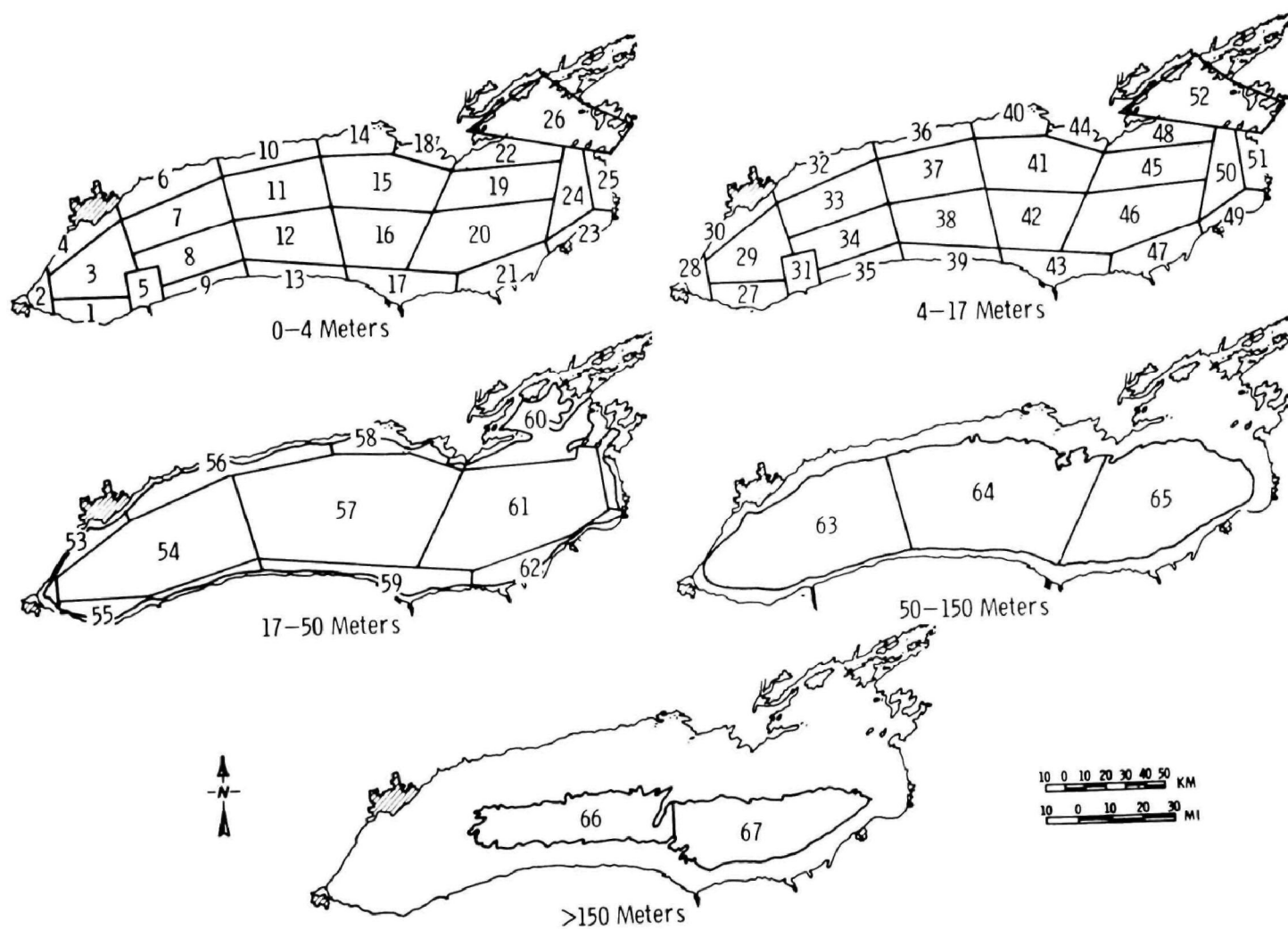


Figure 40. Lake 3 segmentation



rather than the hydrodynamic circulation although the interaction between the kinetics and transport is important. The hydrodynamic circulation is therefore considered to be externally supplied through inferences from observations and/or hydrodynamic model output. An extensive literature exists on the circulation of Lake Ontario and relatively sophisticated mathematical models have been developed<sup>1,2,3</sup>. A review of the complete development is given by Simons<sup>3</sup>. It is not intended in this report to provide a detailed review of the circulation in the Lake and the various analytical and numerical model schemes that have been used to estimate the circulation. Rather, the purpose here is to simply report on the circulation that was used in some of the preliminary Lake 3 phytoplankton runs and the approximate sensitivity of phytoplankton dynamics to changes in the assumed circulation patterns.

This discussion will therefore outline the procedure used for establishing circulation patterns and flow exchanges in the 67 segment - 5 layer, Lake 3 model. Two flow balances are presented, one corresponding to "summer circulation" and the other to "winter circulation".

It is known that Lake Ontario has two distinct net surface circulation patterns. During summer and fall the prevailing winds, the dominant factor governing water circulation, are from the west and southwest and one distinct circulation pattern is set up ("summer circulation"). During winter and spring, the prevailing winds are from the west and northwest and a different circulation pattern is established ("winter circulation"). The summer and winter circulations in Lake Ontario are associated



with the stratified and isothermal temperature states of the water, respectively.

The International Joint Commission<sup>4</sup> and the E.P.A.<sup>5</sup> have published summer circulation patterns for Lake Ontario. Mean monthly resultant velocity vectors that were observed and used by EPA for establishing their circulation patterns were obtained from them for use in assigning velocity values to the general circulation vectors. Wide variance in magnitude and direction over each sampling station was encountered however, even to the point where resultant velocity direction did not agree with the general circulation pattern. Typical stations were also chosen where values were assumed to be reflective of the average observed magnitude and direction. This procedure, however, yielded a poor flow balance and the scheme was discarded in favor of using the general values assigned to the summer circulation pattern by IJC<sup>4</sup> as a guideline.

The water budget information contained in the IJC report was used for establishing tributary inflows to the various shoreline segments. It was decided to split the major inflow to Lake Ontario from the Niagara River (195,000 cfs) over the first and second vertical layers (0-4, and 4-17 meters) while restricting all other tributary inflow (Oswego River, Genesee River, 12 mile Creek, etc.) to the first layer (0-4 meters). The Niagara inflow was split volumetrically between segments 5 and 31 each receiving 4/17 and 13/17 of the flow, respectively.

Having established tributary inflow to the segments, segment flow balances were established and intersegment velocities were back calculated to check for agreement with the general values assigned



by IJC. The final circulation pattern, as given by inter-segment velocity values can be seen in Fig.41. It should be noted that since the Niagara River inflow was split between the first two layers only, there is no inflow and hence can be no outflow from the third layer. This is a good approximation since the average depth of the northeastern most segment (26 and 52 in top two layers), the outflow segment, is only 20-25 meters while the third layers extend from 17 to 50 meters. In any event the bathymetry dictates that there would not be much outflow in the third layer. No flows were assigned to segments in the fourth layer since with only three adjoining segments any inflow to one of the segments from another would have to be countered with the same back flow for a flow balance. The same applies to the fifth layer.

For the winter, the EPA general circulation pattern corresponding to winds out of the west was used for establishing a flow balance. Bonham-Carter's wind driven numerical model outputs a fairly similar circulation for a west wind.<sup>6</sup> The model, however, indicates easterly flow along the north shore, while the EPA circulation pattern indicates upwelling along the north shore. Since both agree the general transport is to the east, there would have to be return flow or upwelling and since the EPA circulation pattern indicates areas of upwelling it was decided to use their general circulation pattern as a guideline for establishing a winter flow balance. Later discussion will indicate how Bonham-Carter's modelled circulation was set up to this segmentation scheme. The balanced velocity vectors are



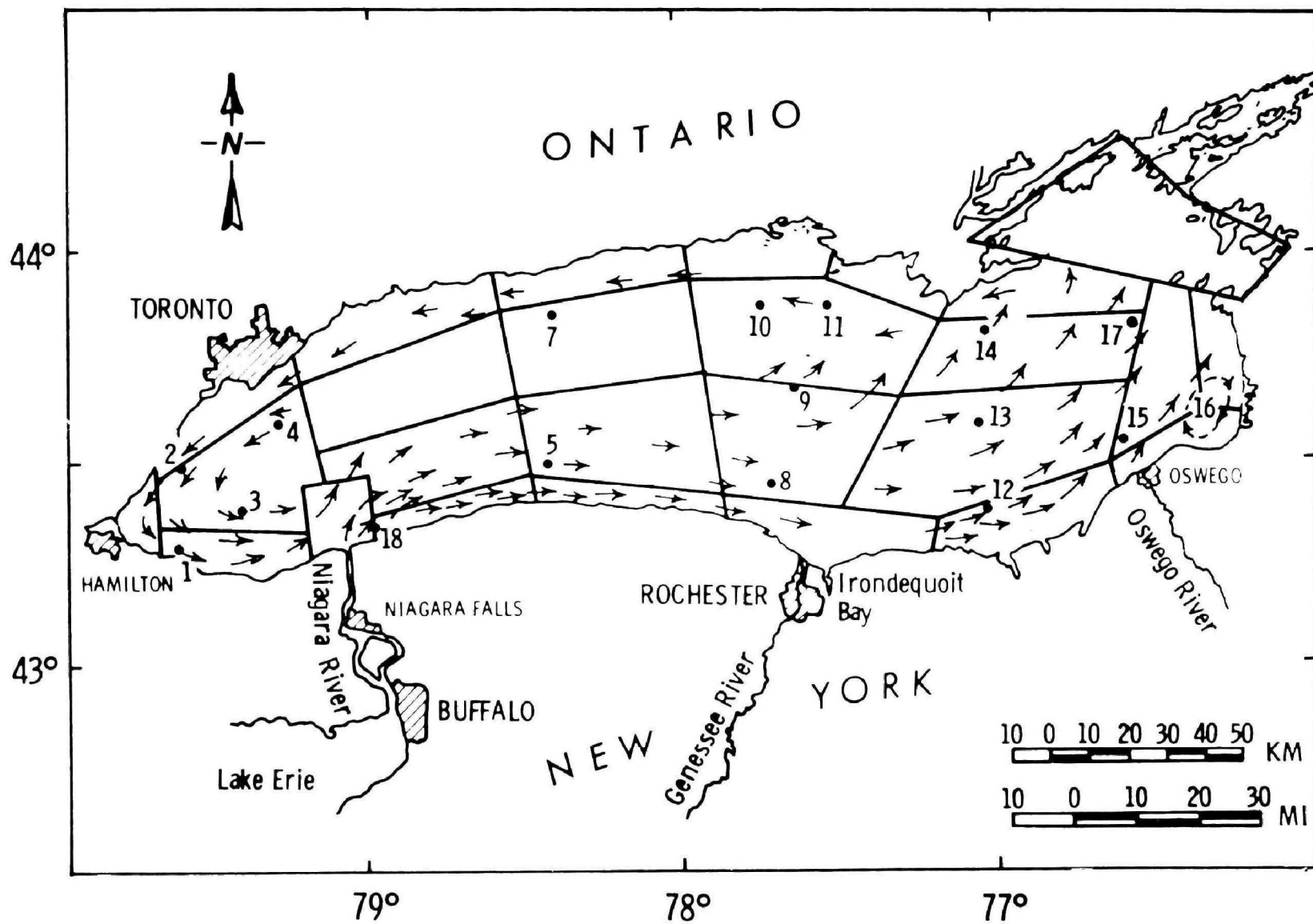


Figure 41. Assumed summer circulation for Lake 3 model.



shown in Figure 42 and represent the assumed circulation for the winter condition. It should be noted that discrepancies exist in the literature in regard to Lake Ontario circulation, and that many of the numerical circulation models are awaiting IFYGL current measurements for verification. However, the Lake Ontario circulation must be calculated from the smaller (approximately 5km) grid on to the larger grid of the phytoplankton model. As additional information becomes available, adjustments to the circulation structure can be made.

Time and space varying horizontal and vertical dispersion coefficients are incorporated to simulate some of the more predominant features such as the thermal bar and vertical stratification. Horizontal coefficients are constant for the winter and are set to zero for the stratification period to simulate the thermal bar effect resulting in restriction of the mixing of near shore waters with main lake waters. Vertical dispersion is also time varying in Lake 3 in a fashion similar to Lake 1 and is constant in the winter, lower and depth varying in the summer, and evaluated on the basis of a straight line function during the transition period.

Fig. 43 illustrates the time varying horizontal and vertical exchange coefficients to be used in this model.



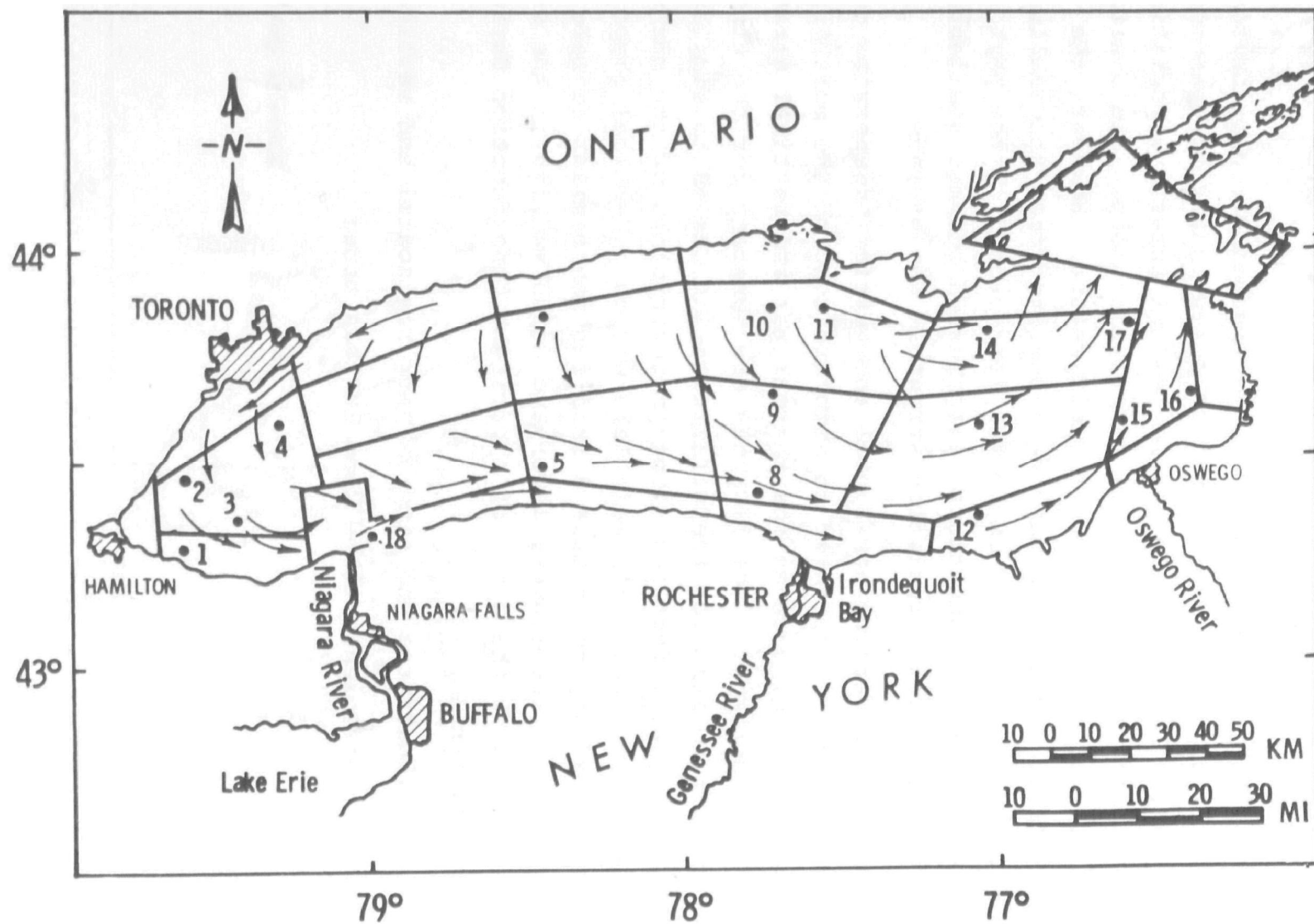


Figure 42. Assumed winter circulation for Lake 3 model



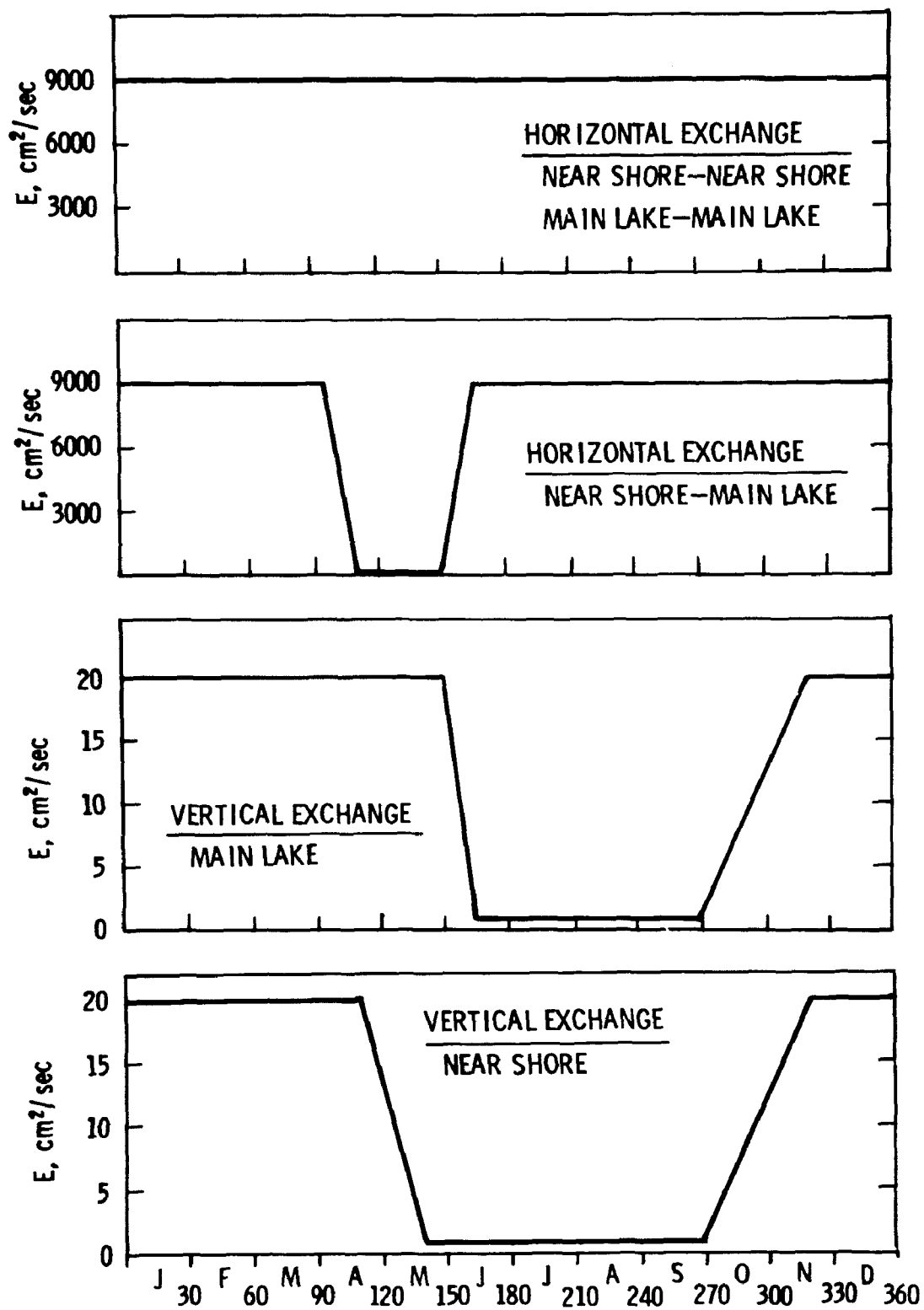


Figure 43. Assumed horizontal and vertical dispersion coefficients for Lake 3 model



## VALIDITY OF ASSUMED CIRCULATION

Since the preceding circulation represents only the crudest estimate of flow transport in Lake Ontario, analyses must be made to determine the validity (or lack thereof) of the assumed circulation structure. The strategy therefore at this stage of the Lake 3 model is to input a circulation pattern into the kinetic structure that is at least reasonable in its broadest outlines. Since the segments of the Lake 3 model are large (10-40km), much of the fine scale detail of the circulation will not be reproduced. Indeed, one of the functions of this effort at this time is to determine the degree to which a detailed circulation is required for the phytoplankton dynamics.

Initial Lake 3 model runs therefore were aimed at verification of transport regimes using water temperature as an indicator. The analysis, while crude, served the purpose of providing some estimate of the validity of the transport regime that was assumed. An annual temperature function is inputted to the top layer of the lake as a time variable forcing function, and the hypothesized flow and dispersion regimes transports this heat throughout the entire lake, computing the time variable temperature response in each of the segments. This response is then compared to observed regional thermal properties of Lake Ontario.

The temperature input used is based on the work of Rodgers and Sato<sup>7</sup> for IFYGL, who have computed values of monthly heat flux terms for 1965 thru 1968. Though discrepancies between their results and observed data are reported, the computation of a total heat storage term,  $Q_t$ , proves to be ideal for coupling to the Lake 3 model and permits inputting temperature as a lake



surface forcing function.

Using Lake Ontario meteorological data and empirical relationships, these heat storage values were computed using the formula:

$$Q_t = Q_s - Q_r - Q_b - Q_h - Q_e \quad (78)$$

$Q_t$  is the heat storage;  $Q_s$ , the incident solar radiation;  $Q_b$ , the net back radiation;  $Q_h$ , the heat transfer to atmosphere and  $Q_e$  is the evaporation energy where all units are  $\text{cal/cm}^2\text{-day}$ .

With the monthly heat flux terms, values of  $Q_t$  were calculated for the five year period studied. These values are listed in Table 11 and the five year average values were used in the Lake 3 runs.

Once  $Q_t$ , the total heat flux term or total heat storage in the lake, is known, then

$$T_s(t) = Q_t/H \quad (79)$$

where  $T_s(t)$  is the temperature forcing function for the surface layer ( $^{\circ}\text{C/day}$  or  $\text{cal/cm}^3\text{-day}$ ) and  $H$  is the depth (cm) of the first segment.

This computed temperature forcing function was inputted to the top layer segments (0 - 4 ) of the Lake 3 model, and was then advected and dispersed throughout the model by the hypothesized flow and dispersion regime. The computed time variable temperature response in each of the segments was then compared with a regional analysis of Lake Ontario thermal properties.

The degree of data manipulation involved to manipulate a transport regime in this 67 segment model, with its 187 dispersion interfaces and its 142 flow interfaces, is extensive so that a transport regime based on verification against generalized temperature



TABLE 11 -

## MONTHLY HEAT FLUX VALUES

MONTH	1965 $Q_t^*$	1966 $Q_t$	1967 $Q_t$	1968 $Q_t$	1969 $Q_t$	5 year average
JANUARY	-329.1	-392.0	-214.2	-329.2	-275.5	-308.0
FEBRUARY	-216.6	-139.5	-278.1	-244.9	-153.6	-206.54
MARCH	4.6	80.3	48.4	88.4	11.3	46.6
APRIL	275.2	207.0	318.8	361.1	313.1	295.04
MAY	533.2	413.7	420.6	353.7	448.1	380.8
JUNE	463.0	610.9	618.6	471.7	475.4	464.8
JULY	270.7	307.0	303.0	293.3	-----	293.5
AUGUST	67.0	69.5	51.2	198.5	-----	96.55
SEPTEMBER	-43.7	-55.2	-92.7	102.1	-----	-22.375
OCTOBER	-235.8	-64.4	-108.7	-46.9	-----	-113.95
NOVEMBER	-200.6	-162.4	-254.8	-206.7	-----	-206.125
DECEMBER	-226.1	-349.1	-296.8	-370.2	-----	-310.55

\*  $\frac{(\text{cal})}{(\text{cm}^2 \text{ day})}$



properties rather than one verified against one year of data with its specific meteorological conditions, was considered to be more feasible.

Based on these considerations, the verification medium chosen was the temperature characterization of Lee<sup>8</sup>. Composite temperature data for the years 1960 - 1969 were used and distinct horizontal variations of water temperature in Lake Ontario were noted. Lee distinguishes seven distinct regions of the lake where thermal properties seemed to be seasonally consistent on a year to year basis. This regional division of the lake, seen in Figure 44 is similar to the underlying basis of surface layer segmentation for Lake 3, namely a near shore ring around the lake and large main lake segments. This similarity coupled with the fact that Lee's data are based on a generalized analysis of ten years of data prompted the use of this data set for temperature verification of transport regimes in the Lake 3 model.

Several different regimes were investigated with emphasis on the vertical and horizontal dispersion characteristics. The degree of verification of the computed output as compared with Lee's data is presented in Figs. 45, 46. Table 12 lists the equivalence between Lee's regions and the Lake 3 segments, and the values which are overplotted against Lee's data are the means of the appropriate Lake 3 segments at times corresponding to the median cruise dates reported by Lee.

Figure 45 also shows the effect of several sensitivity runs. The effects of using vertical dispersions only with no horizontal dispersion or flow, and the effect of reversing the direction of



TABLE 12 -  
REGIONAL TO LAKE 3 SEGMENTATION EQUIVALENCE

Lee (region)	SEGMENT OF LAKE 3				
	1	2	3	4	5
1	26	52	60	-----	-----
2	1,2,4,6	27,28,30, 32	53,55,56	-----	-----
3	10,14,18	36,40,44	56,58	-----	-----
4	21,22,23, 25	47,48,49, 51	60,62	-----	-----
5	3,7,8,11, 12	29,33,34, 37,38	54,57	63,64	66
6	15,16,19, 20,24	41,42,45, 46,50	57,61	64,65	66,67
7	5,9,13,17	31,35,39, 43	55,59	-----	-----



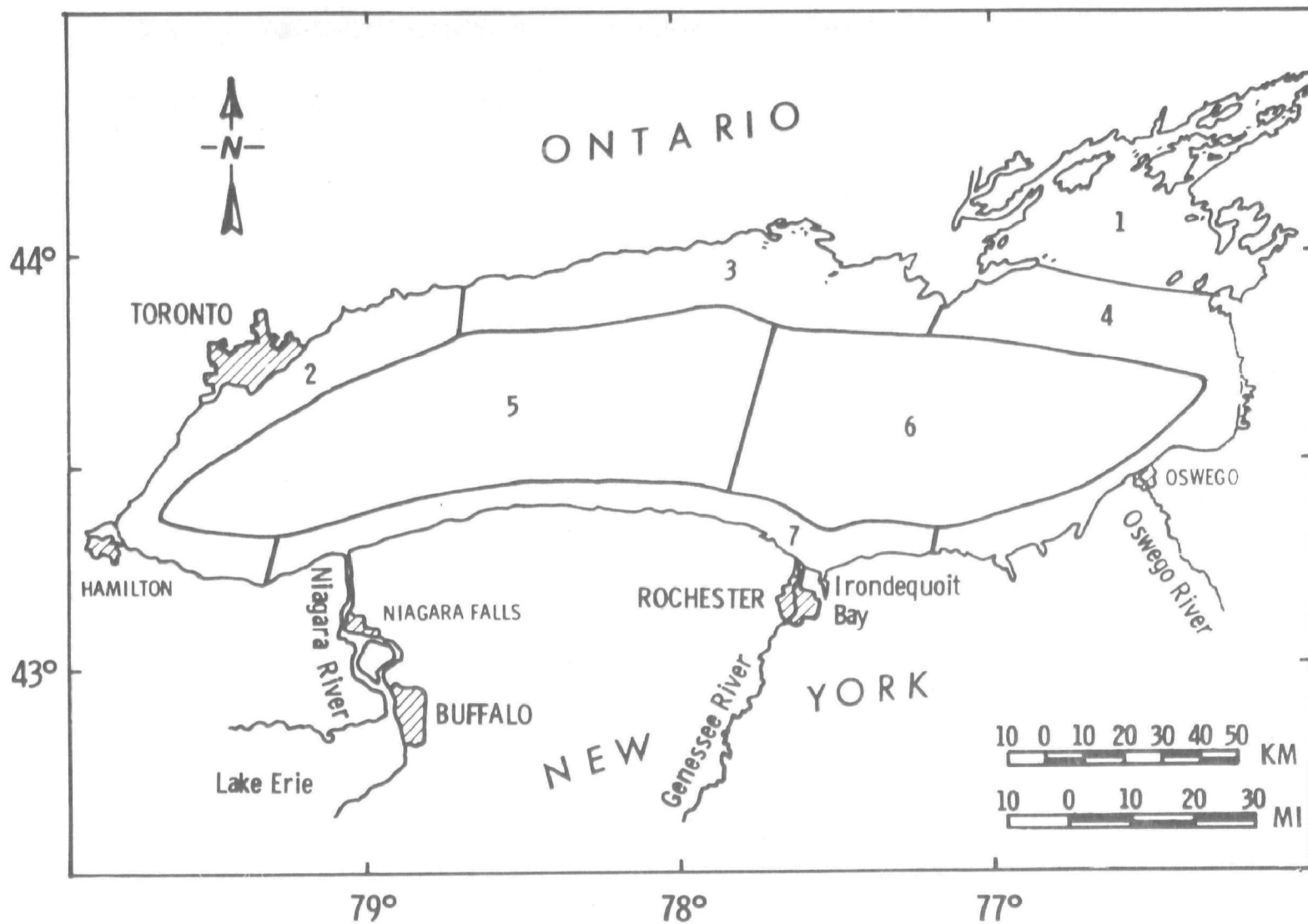


Figure 44. Regional division of Lake Ontario by Lee<sup>8</sup>.



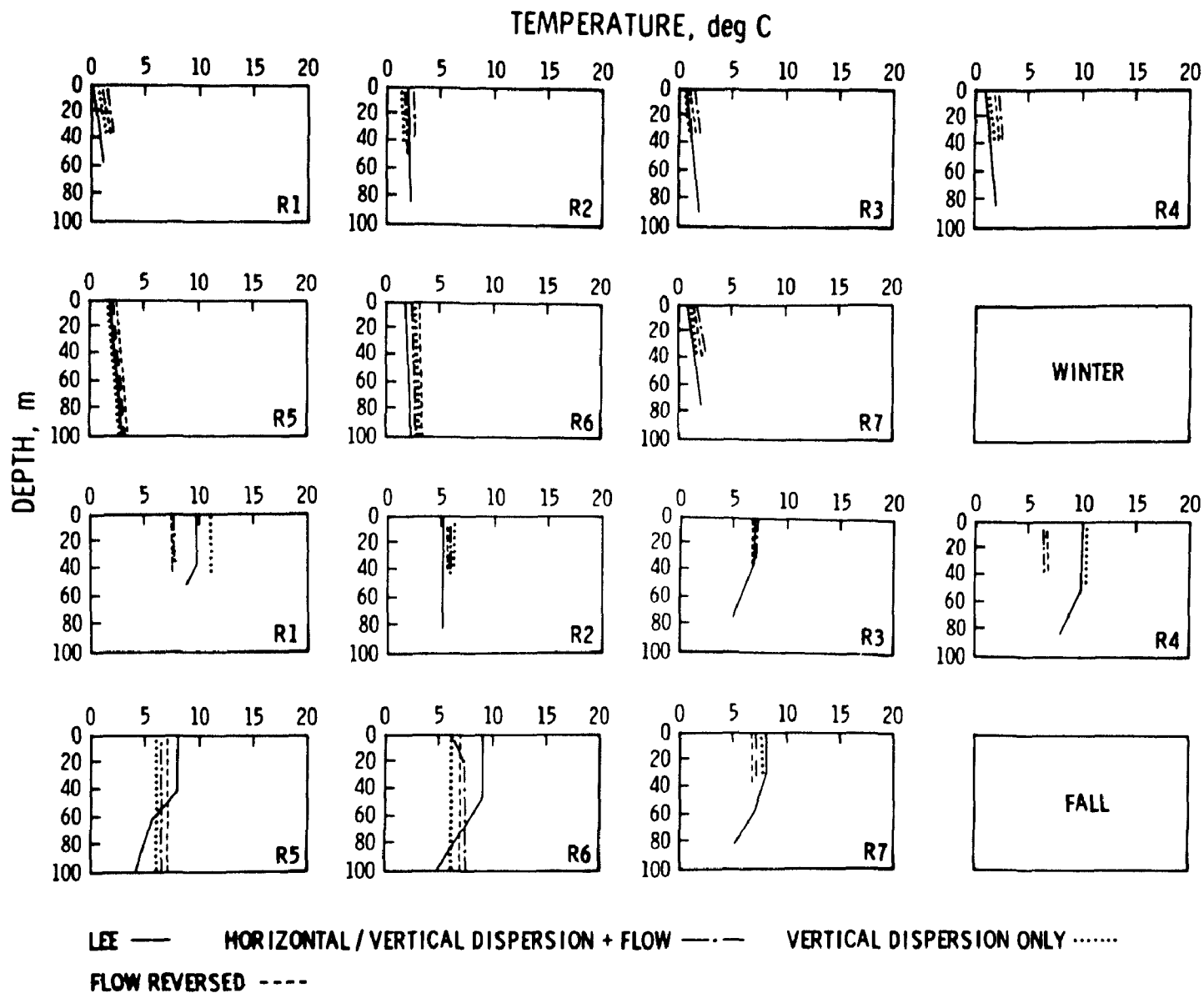


Figure 45. Comparison of computed temperatures from Lake 3 model with data from Lee<sup>8</sup>, winter, fall.



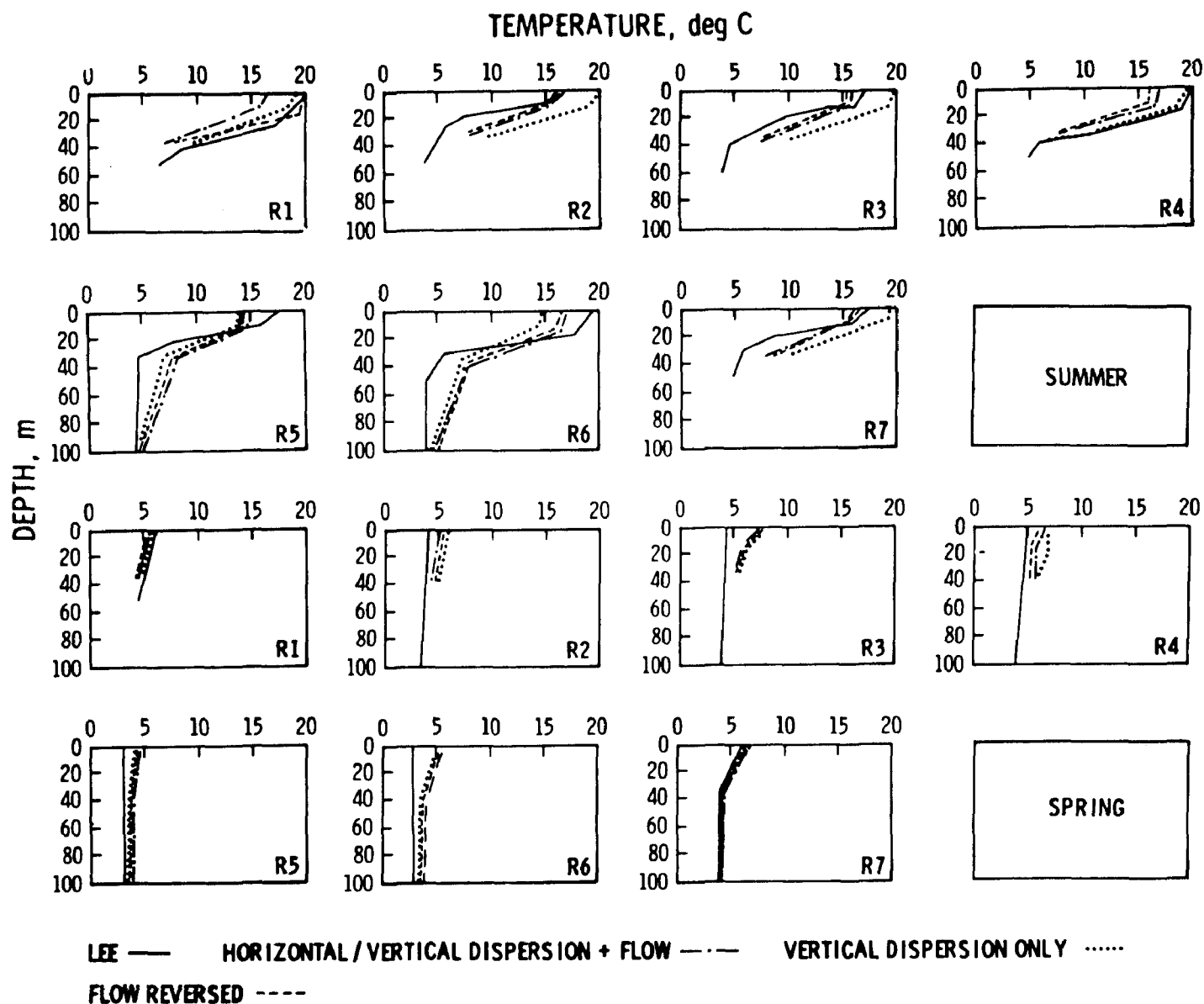


Figure 46. Comparison of computed temperatures from Lake 3 model with data from Lee<sup>8</sup>, summer, spring



the flow field were investigated.

As can be seen, no marked effect on the temperature verification results when the flow transport is turned off or when flow is reversed. Though this appears to be odd, the reason is clear when one considers the size of the segments in the Lake 3 model. Though the model is large from a computational point of view and it does, because of its spatial detail, give near shore to main lake resolution, the surface areas of the segments are so large that the interfaces for vertical transport are much greater than those for horizontal and flow transport. Hence vertical dispersion terms dominate.

The grid is not fine enough and effects such as near shore thermal bar flow restriction and changing wind pattern effect on horizontal transport cannot be investigated with any degree of accuracy. A grid fine enough such that these effects could be seen, does not appear to be computationally feasible at this time.

The dispersion regime resulting from this analysis is presented in Figure 43. Its underlying features consist of lowering vertical dispersion in the summer to simulate stratification, lowering near shore to mid-lake segments horizontal dispersion for a period in the spring to simulate the thermal bar, and simulating stratification earlier in the near shore segments than in the main lake segments. This is the dispersion regime which is used in Lake 3 for the full biological and chemical systems verification runs.

Though this analysis has many shortcomings, it did serve to give some basis in theory for coupling of flow transport and dispersion to the kinetics of the Lake 3 model and it appears that this approach of treating temperature as a conservative tracer is a reasonable method of analysis.



## PRELIMINARY PHYTOPLANKTON COMPUTATIONS

Several runs have been made of the Lake 3 model using the transport and dispersion regime discussed previously and the system kinetics given in Section V. The purpose of these early runs is to determine the general direction of the output with special reference to spatial differences in phytoplankton biomass. Considerably more work remains to be done on Lake 3 including detailed verification analyses and simulation of effects of nutrient reduction.

The primary data source at this point in the analysis is the results from the IFYGL effort. The cruise stations are mapped on to the Lake 3 grid and only those stations for which a reasonably complete set of data were available are included in the mapping. Fig.47 shows the location of the data stations and the Lake 3 grid. Some segments have only one station for comparison while other segments (primarily near-shore stations) may have three stations for comparison. Data retrievals have been completed from the Storet system and "segment-depth" averages (and other statistics) by month and record length have been completed. This data set will then form the basis for the detailed verification analysis.

Fig.48 shows early very preliminary results of phytoplankton biomass at three segments across the lake. This run did not include any vertical settling velocity. Segment #17 represents the Rochester embayment and as seen reaches peak values of almost 15  $\mu\text{g}$  chlorophyll/l at the end of May while the more open lake area (segment #16) lags by about one-half month. Peak values at the open lake segment are about half of the Rochester segment. At the end of May therefore, at day 150, a lateral gradient of chlorophyll of about



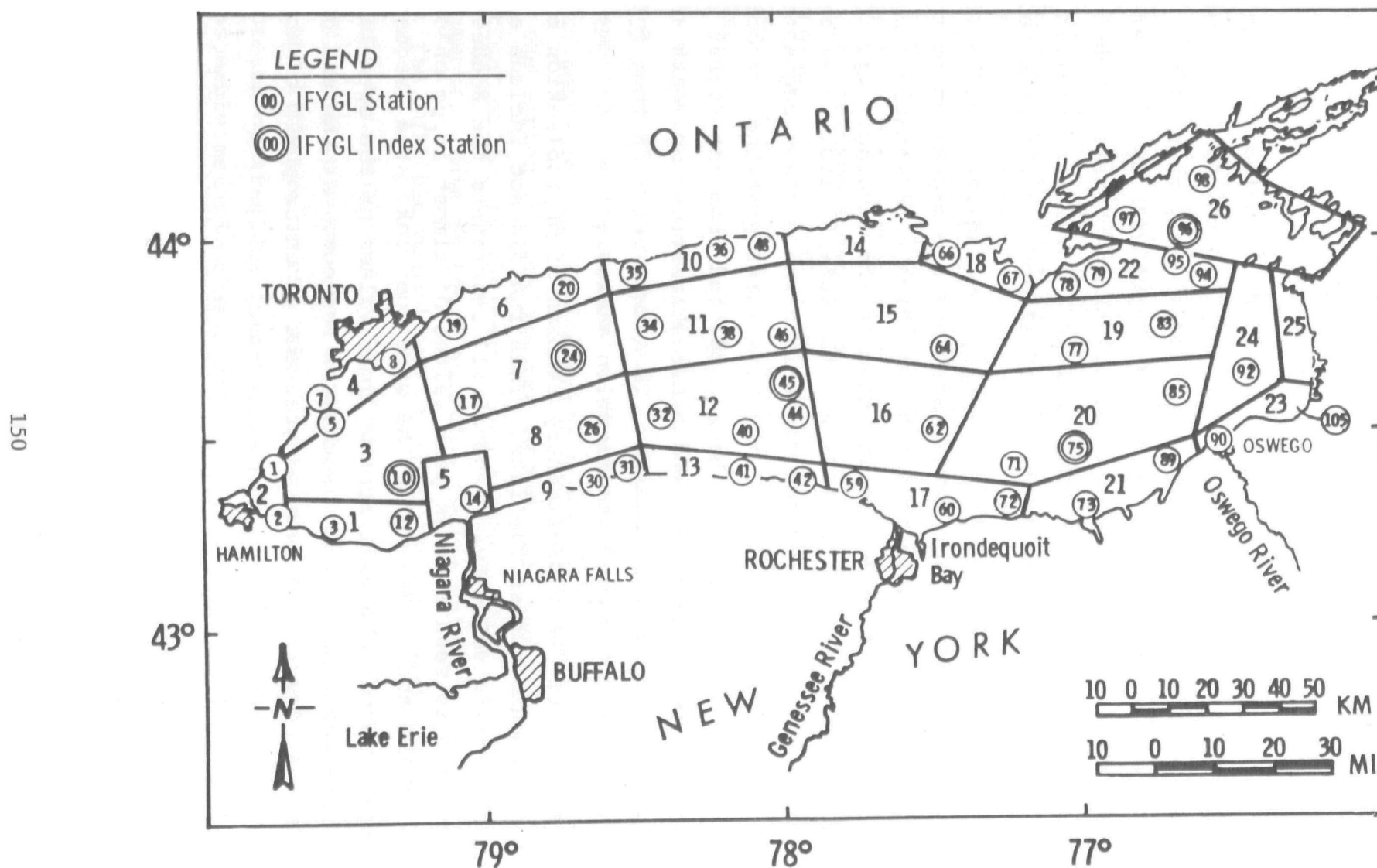


Figure 47. Principal IFYGL stations and the Lake 3 grid.



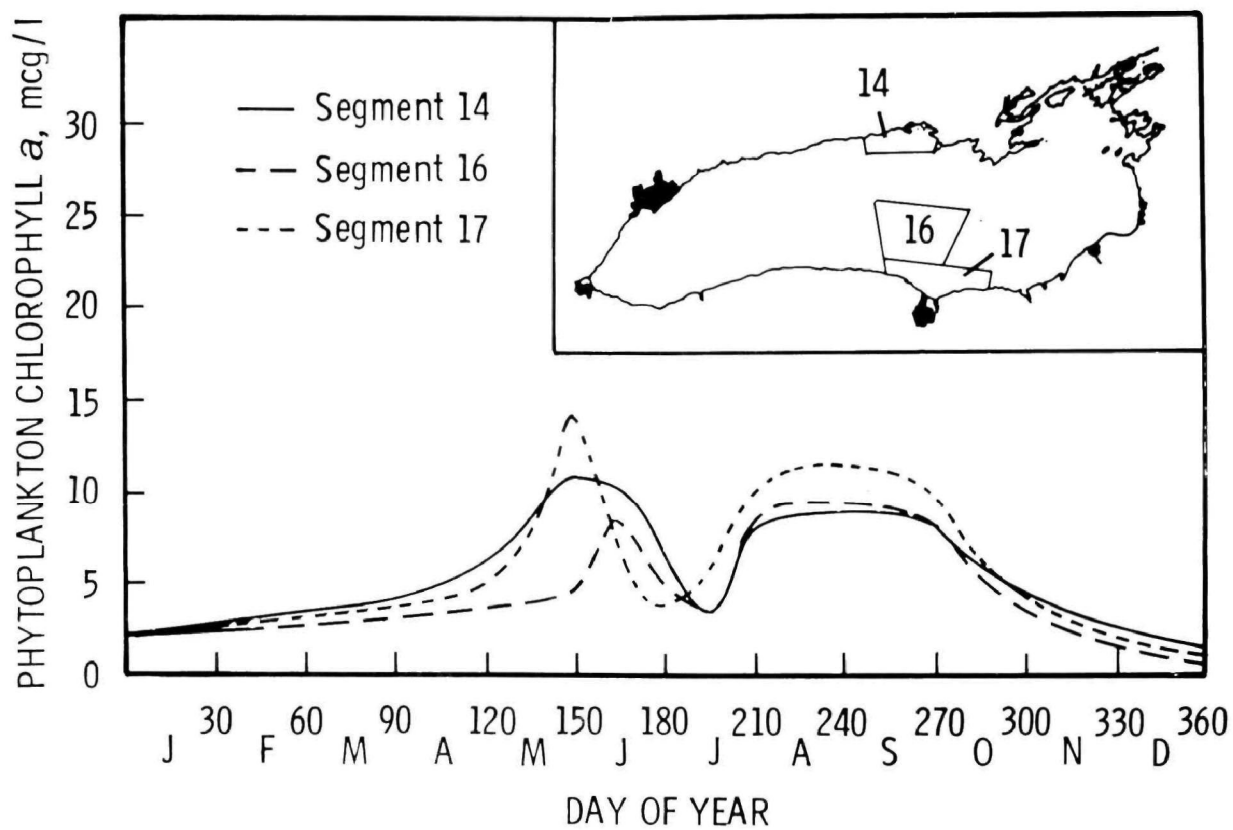


Figure 48. Preliminary results of Lake 3, 0 - 4 meters



10 $\mu$ g/l is computed. This results primarily from the thermal bar effect simulated by variations in the horizontal dispersion (see Fig.43). Gradients across the lake in the fall are not pronounced and reflect the general well-mixed character of the lake at that time.

Fig.49 explores the vertical variation for two segments during the month of June and compares the results to data collected during IFYGL. Maximum biomass occurs in the upper layer and then decreases with depth. The mean values and range of the computed values agree quite well with the observed chlorophyll data. In fact, the agreement is so surprisingly good that further investigation is warranted to determine why the agreement was obtained so rapidly. This is especially important when it is recognized that the run shown in Figs.48 and 49 is for zero phytoplankton settling velocity.

#### Output Data Display

The Lake 3 model generates a substantial output totalling thousands of numbers that represent the time variable response of each variable at each segment. In addition, output on the growth and death kinetics, nutrient recycle and nutrient fluxes are also obtained. The size of Lake 3 makes it difficult to fully comprehend the output so some effort is being devoted to further analysis and display of the output. In this way, it is hoped that further understanding and insight can be obtained on the behavior of the solutions that are generated.

Fig.50 shows the output flow diagram that is presently being utilized. Output from the model is written on tape in addition to hard copy and digital overplots. The latter plots are for general screening



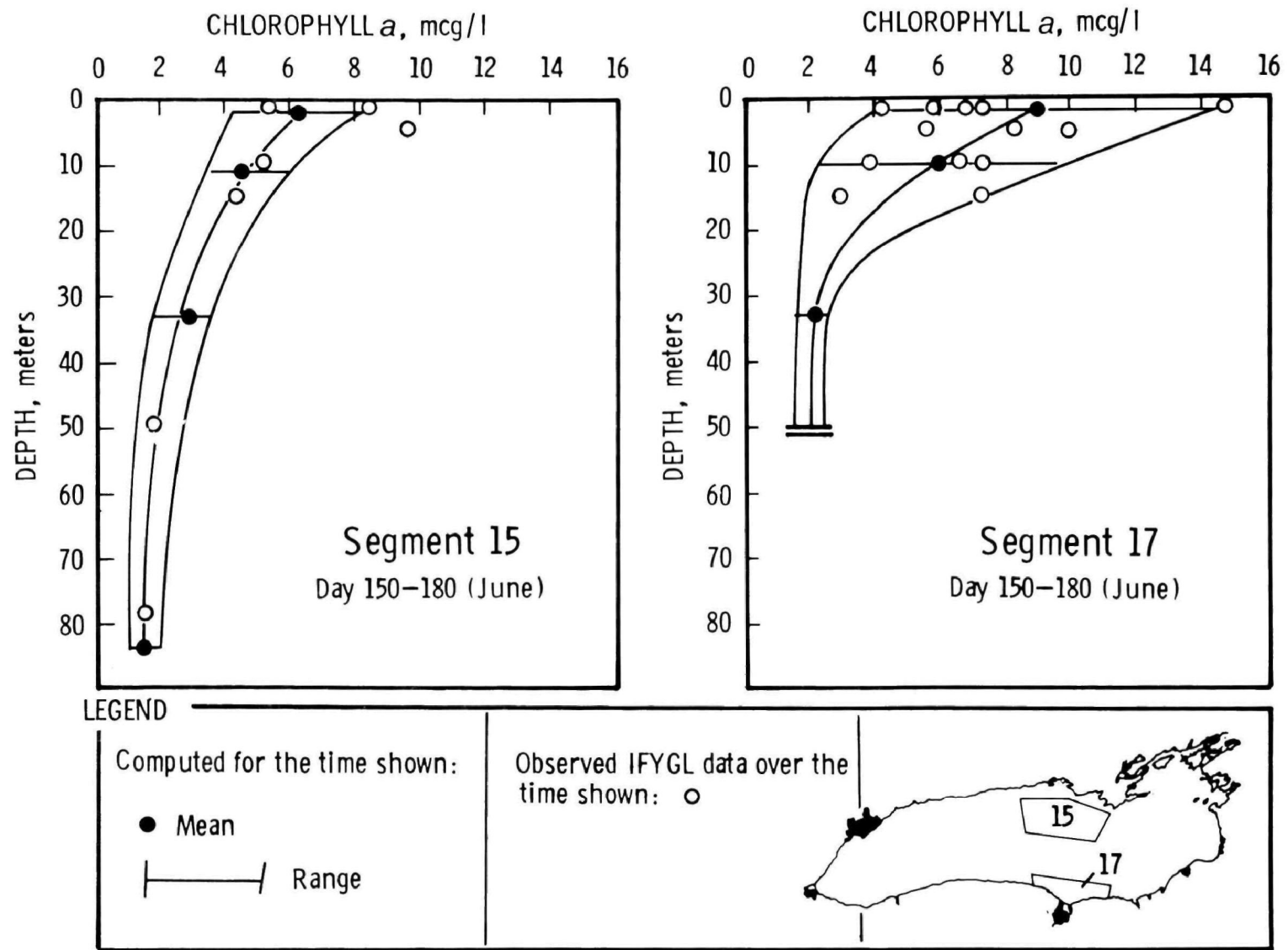


Figure 49. Preliminary comparison of Lake 3 output to observed data at two segments for June



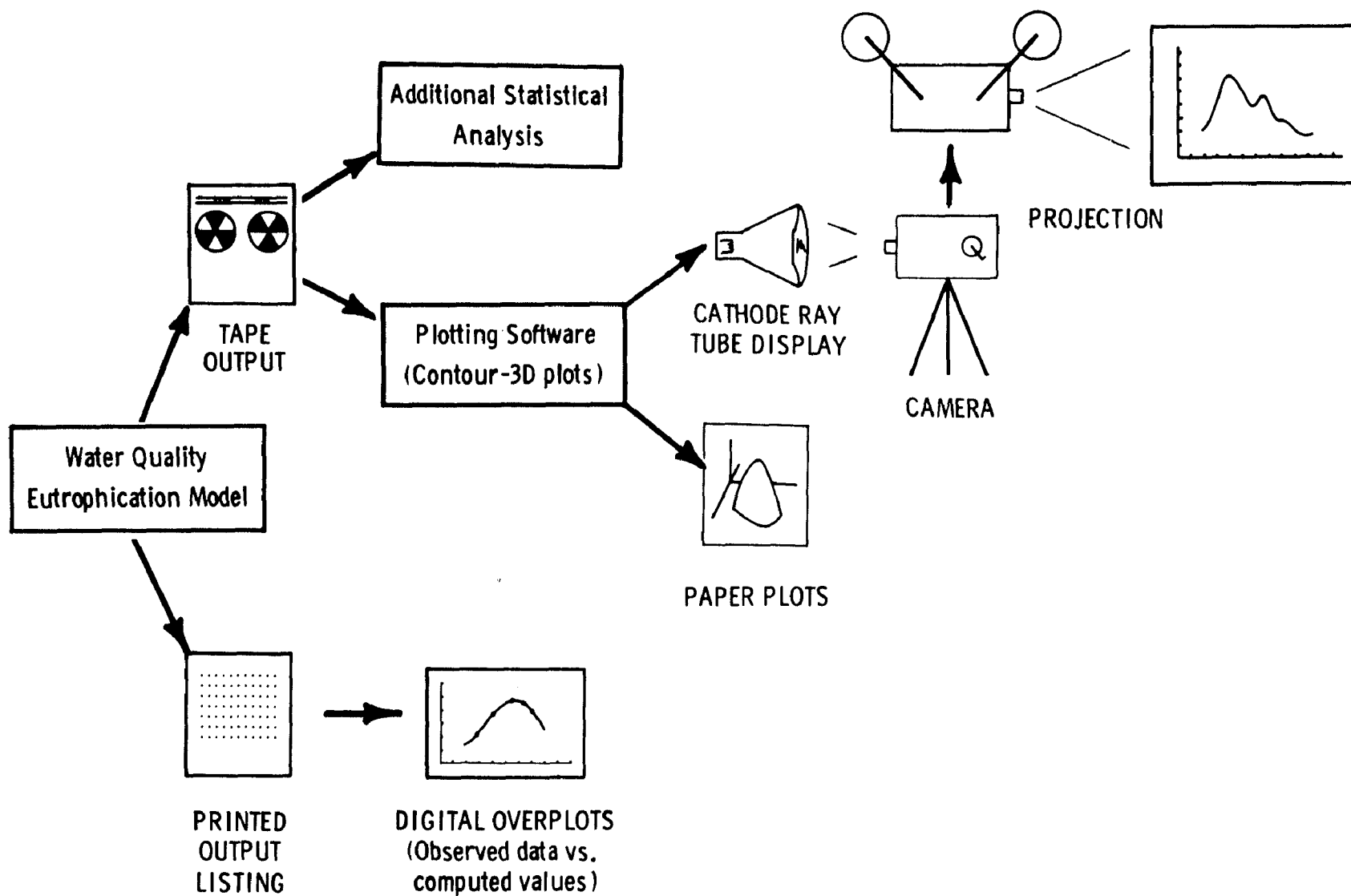


Figure 50. Data output flow diagram used for verification and display purposes



by the analyst. Plotting software is then employed on the tape output from a model run. Paper contour plots and three dimensional plotting routines are employed to provide further perspective on the output. Fig.51 shows a three dimensional plot of output of phytoplankton biomass in the 0-4 meter layer from a view looking down the lake from east to west. Plots such as these reveal the structure of the solution in a meaningful way and also permit scanning of the output to determine any strange or anomalous results that may indicate a flaw in the numerical computations.

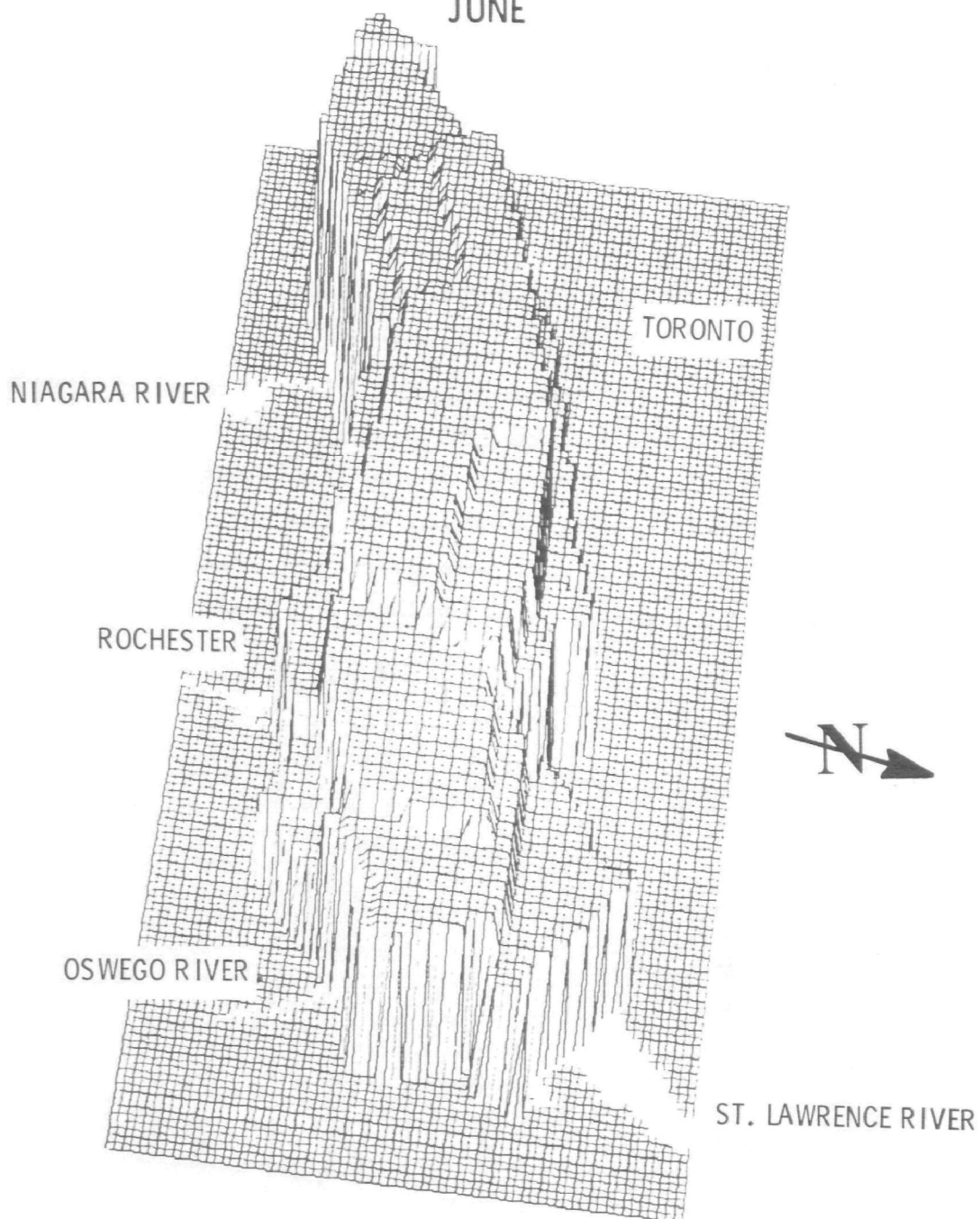
Returning to Fig. 51 the three-dimensional plots are also displayed on a cathode ray tube, microfilmed and prepared for a motion picture of the complete output over time. A screening of this film then reveals the dynamic and spatial behavior of the solution in a very unique way. At this stage, a film has been prepared of a preliminary run for a full year of the surface phytoplankton chlorophyll.



# LAKE ONTARIO-LAKE 3 MODEL

LAYER 1 (0-4 METERS)

JUNE



PHYTOPLANKTON CHLOROPHYLL  $a$  Maximum,  $8.2 \mu\text{g/l}$

Figure 51. Three dimensional plot of phytoplankton chlorophyll calculated from Lake 3 model - June, 0 - 4 meters.



## SECTION VIII

### REFERENCES

1. Simons, T.J. Development of Numerical Models of Lake Ontario. Proc. 14th Conf. Great Lakes Res. IAGLR, pp.654-669, (1971).
2. Simons, T.J. Development of Numerical Models of Lake Ontario, Part 2. Proc, 15th Conf. Great Lakes Res., IAGLR, pp.655-672, (1972).
3. Simons, T.J. Development of Three-Dimensional Numerical Models of the Great Lakes. Scientific Series No. 12, Inland Waters Dir., CCIW, Burlington, Ontario, 26 pp., (1973).
4. Report to the International Joint Commission on the Pollution of Lake Ontario and the International Section of the St. Lawrence River - Vol. 3 - International Lake Erie Water Pollution Board and the International Lake Ontario - St. Lawrence River Water Pollution Board. (1969)
5. Casey, Donald J. Lake Ontario Environmental Summary 1965. U.S. Environmental Protection Agency Region V. Lake Ontario Basin Office, Rochester, N.Y.
6. Bonham-Carter, Graeme, John H. Thomas and David Lackner  
A Numerical Model of Steady Wind-Driven Currents in Lake Ontario and the Rochester Enbayment Based on Shallow-Lake Theory. Report Number 7 International Field Year For the Great Lakes - Rochester Enbayment Project - Department of Geological Sciences, University of Rochester, (1973)



7. Rodgers, G.K. and G.K. Sato. Energy Budget Study for Lake Ontario. Canadian Meteorological Research Report, Atmospheric Environment Service, Jan. (1971)
8. Lee, A.H. Regional Characterizations of the Thermal Properties of Lake Ontario. Proc. 15th Conf. Great Lakes Research, IAGLR, 625-634, (1972)



## APPENDIX A

### LAKE 1

#### INPUT AND PROGRAM LISTING

##### INPUT INFORMATION

###### Introduction

Lake 1 is a kinetic interactive model spatially defined by three vertical, mixed layers representing the epilimnion, hypolimnion and benthos of Lake Ontario as shown in Figure 9. The purpose of this appendix is to summarize the input information needed to run the model, and to present where available, the background information from which this information was drawn. Units for the information given are consistent with those required by the computational software used, which is named Water Analysis Simulation Program (WASP). A listing of WASP and sample output are included.

###### MORPHOMETRY AND HYDRODYNAMIC REGIME

The information required to describe the morphometry of Lake Ontario, for the Lake 1 model is presented in Table A-1, with the associated hydrodynamic regime.

The bulk of the morphometric data was generated using data supplied by the Canada Centre for Inland Waters (CCIW), Descriptive Limnology Section<sup>1</sup>. The bathymetric data, supplied on punched cards, were depth averages for a square grid laid on a polyconic projection of Lake Ontario, with geographical areas of  $4\text{km}^2$ .

These surface areas were defined by sides which were actually curves on the earth's surface. These data were processed to yield the



TABLE A-1

## LAKE 1 PHYSICAL PARAMETERS

Segment	Inter-segment	Representation	Volume [10 <sup>6</sup> CF]	Depth [Feet]	Intersegment Areas [FT <sup>2</sup> ]	Inflow [cfs]	Outflow [cfs]	Dispersion Coefficient [mi <sup>2</sup> /day]
1	1 - 2  2-3	Epilimnion	1.05x10 <sup>7</sup>	55.8	1.76x10 <sup>11</sup>  0.959x10 <sup>11</sup>	43,500.	43,500.	see Fig. A-4
2		Hypolimnion	4.85x10 <sup>7</sup>	240.5		188,400.	188,500.	
3		Benthos	4.80x10 <sup>4</sup>	0.5		0.0	0.0	0.0



necessary information. The average depth of Lake Ontario is 296 feet, (90 meters). The International Joint Commission<sup>2</sup> reports the average depth of the developed thermocline is 55.8 feet (17 meters). This depth is used in the representation of the epilimnion. The remainder of the volume is placed in the hypolimnion. The benthos, which is currently used only to track accumulation of depositions, was given an arbitrary depth of 0.5 feet. Figures A-1 and A-2 which show the variation of volume and surface area with depth were generated with the CCIW supplied data.

The hydrodynamic regime is inputted into WASP, as opposed to a modelling configuration which would incorporate a hydrodynamic sub-model internally. This differentiation is most significant for more spatially defined models than Lake 1. The hydrodynamics must therefore be obtained from a data base, the literature, or an external hydrodynamic sub-model. The mean annual outflow for Lake Ontario is 232,000 cfs.<sup>2</sup> Inflow was set equal to outflow and was split proportionally to the segment depths, as shown in Table A-1.

The development of the thermocline was simulated by temporally varying the vertical dispersion coefficient as shown in Fig. A-3, The establishment of the thermocline prevents exchange between the epilimnion and hypolimnion. This phenomena was incorporated by setting the vertical dispersion between segments 1 and 2 to zero during the period of stratification. For the remainder of the year exchange takes place between segment 1 and segment 2. The vertical dispersion coefficient was set at  $0.0003 \text{ mi}^2/\text{day}$  ( $90 \text{ cm}^2/\text{sec}$ ) for periods of non-stratification, which is in the range reported in Limnological Systems Analysis<sup>3</sup>.



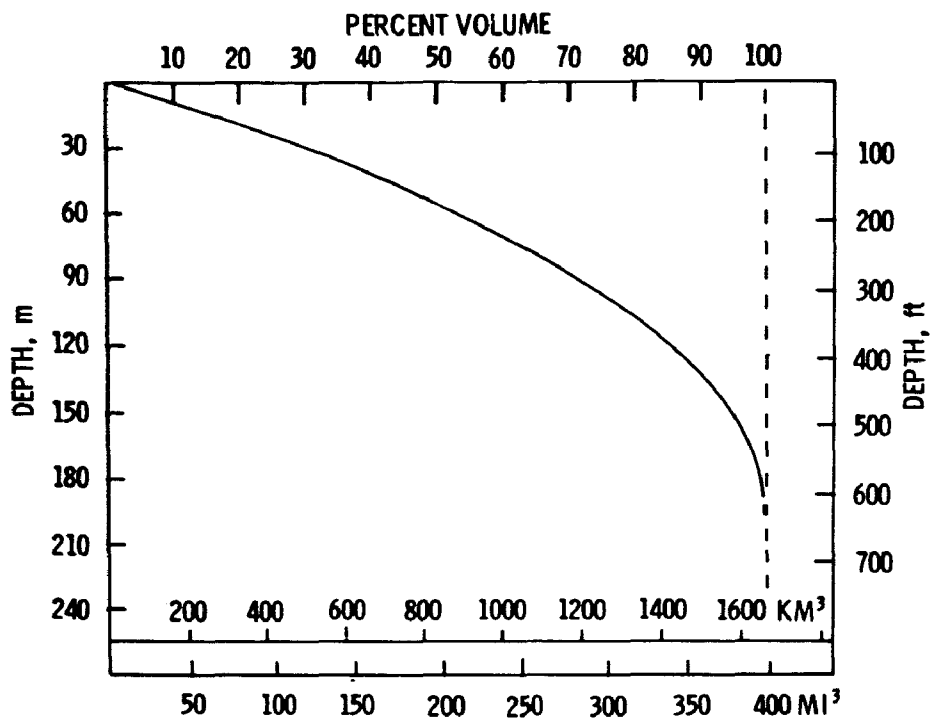


Figure A-1. Variation of volume with depth

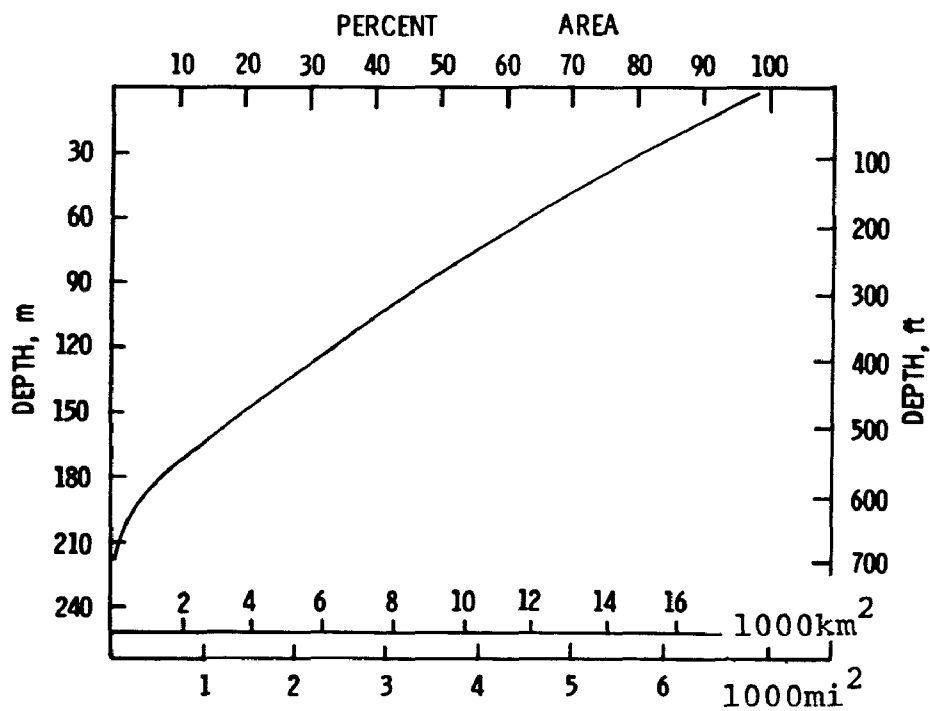


Figure A-2. Variation of area with depth.



## PHYSICAL EXOGENEOUS VARIABLES

1. Water Temperature - the temporal variation of water temperature used in Lake 1 is shown in Fig. A-4. Since the segments represent completely mixed volumes, representative temperatures were chosen. Data averaged from CCIW's Limnological Data Reports (1966,1967,1968,1969) were used as temperature input<sup>4</sup>. Only stations with depths over 50 meters were considered. These were viewed as representative of main lake conditions.
2. Solar Radiation - data recorded at Brockport, New York, and at Toronto-Scarborough, Ontario<sup>6</sup> were available. The Toronto-Scarborough data were used as this comprised the longest period of record. The Toronto-Scarborough data were adjusted using an over land radiation to over lake radiation ratio proposed by Richards and Loewen<sup>7</sup>. The over land radiation data, lake to land ratio and adjusted temporal lake radiation function used is shown in Fig. A-5.
3. Photo Period - that fraction of the day from sunrise to sunset is variable during the year, and is a function of latitudinal position. Sunset, sunrise data from the World Almanac<sup>8</sup> were used to obtain the functions shown in Fig. A-6. The Lake Ontario photo period function was obtained by interpolating to the equivalent of 43° 40' N latitude.
4. Background Water Clarity - the variation of the extinction coefficient with time is a function of the phytoplankton concentration in the water body. Given no phytoplankton, there



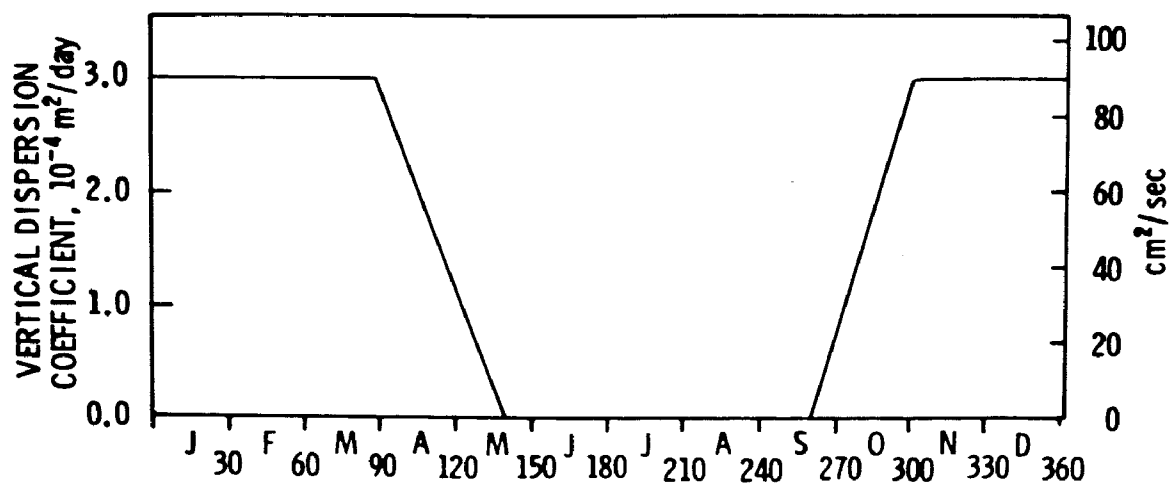


Figure A-3. Temporal variation of vertical dispersion coefficient-- interface 1-2

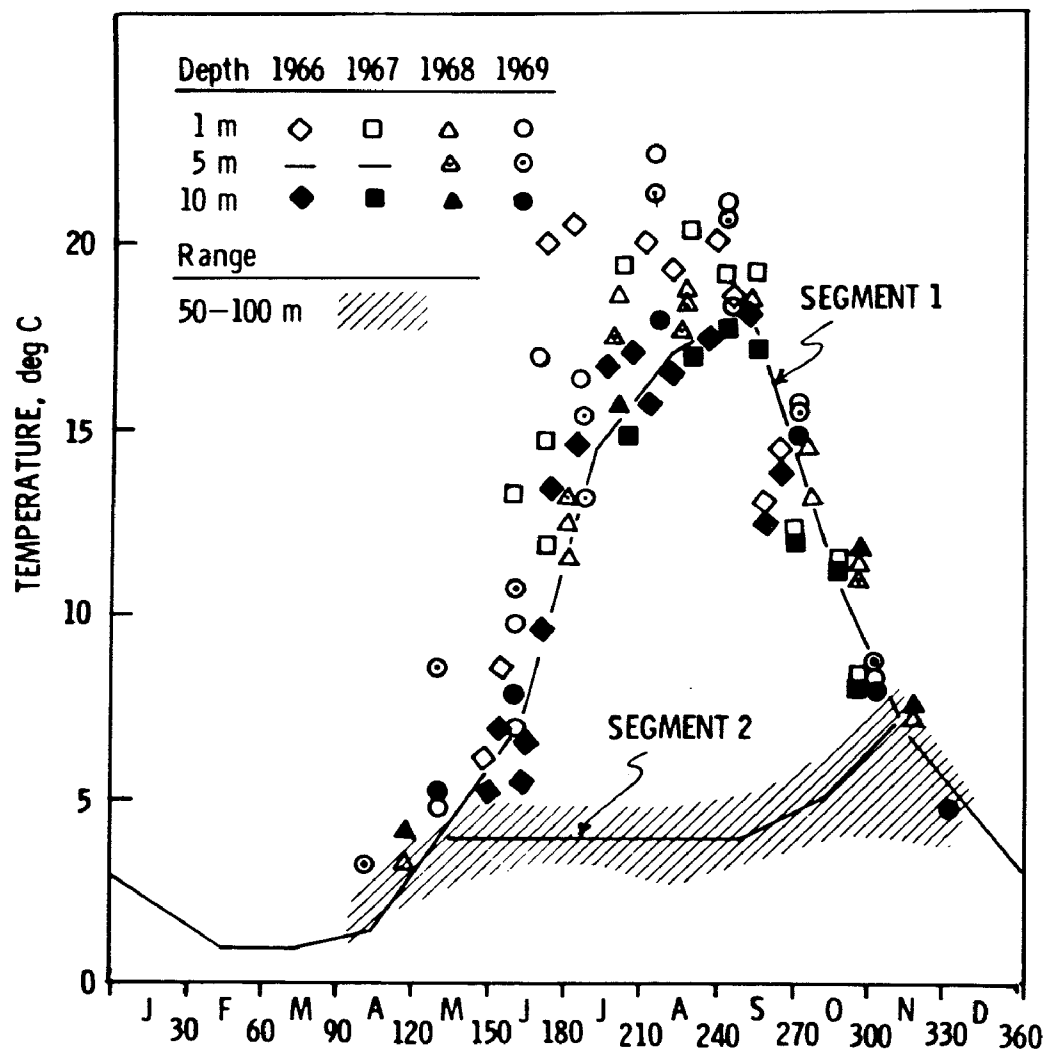


Figure A-4. Temporal variation of water temperature



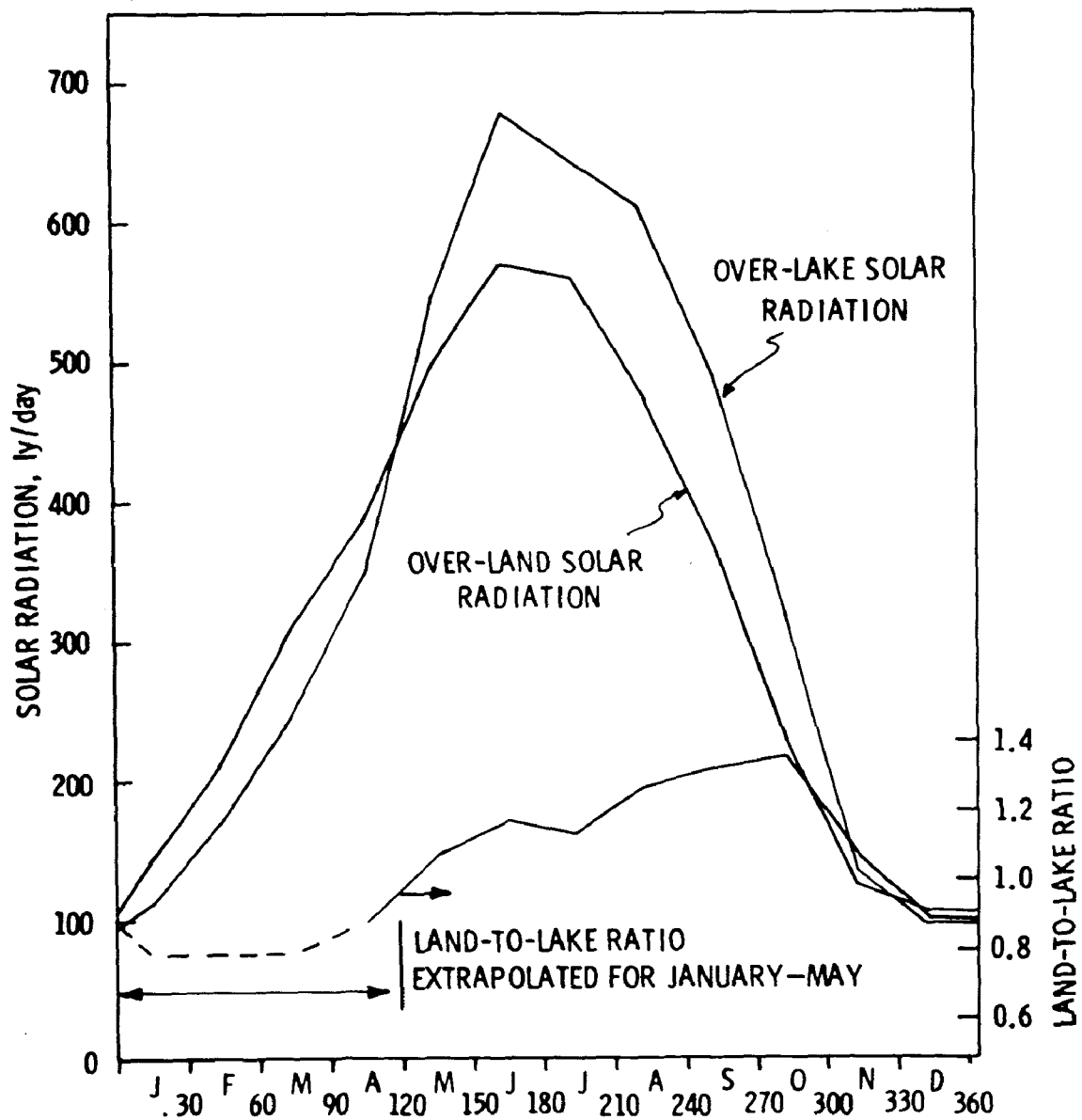


Figure A-5. Temporal variation of solar radiation



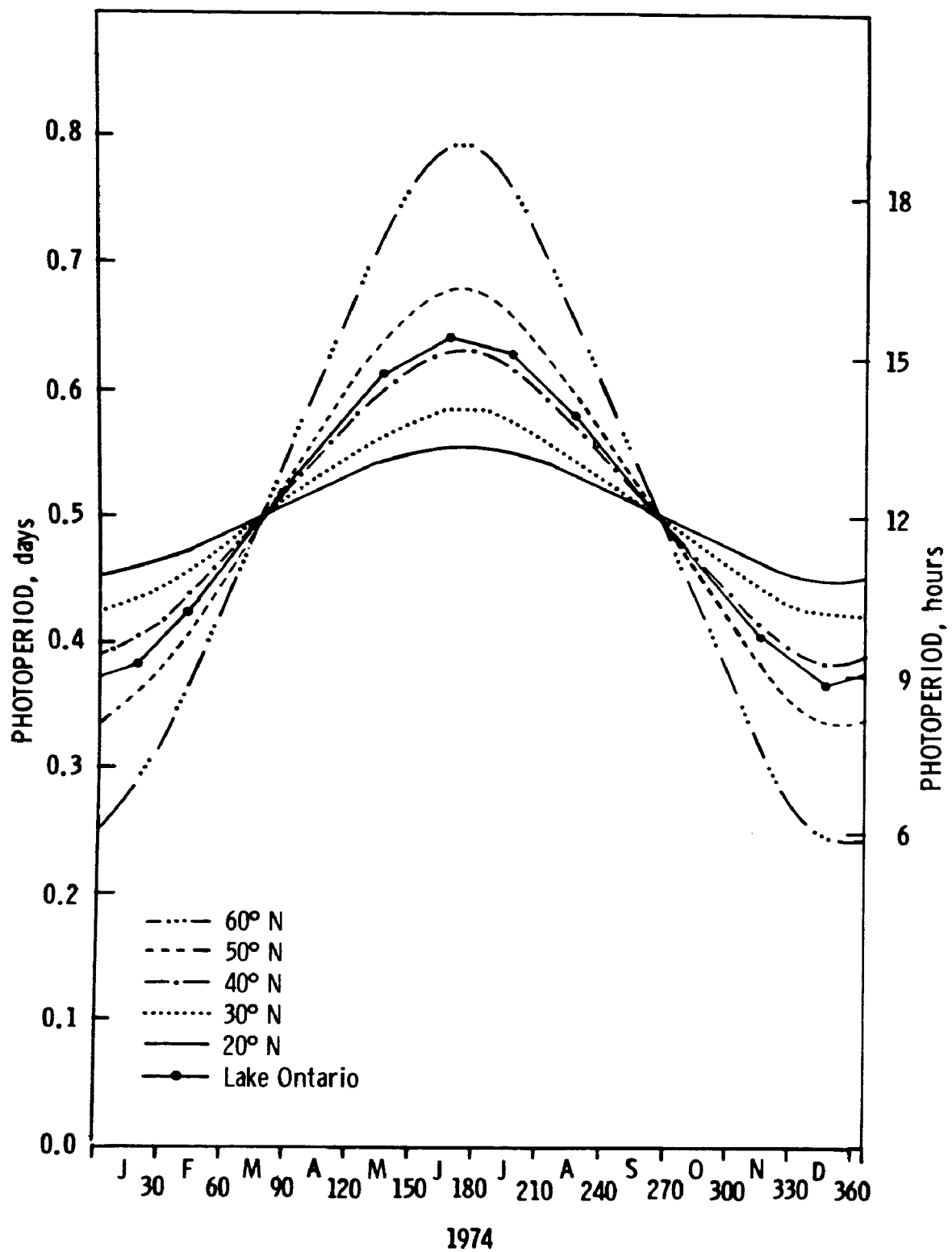


Figure A-6. Temporal variation of photoperiod



would still be extinction of light as it passes through the water column attributable to other factors. This fraction of the extinction coefficient, which is a function of background water clarity, was determined by plotting chlorophyll and extinction coefficient as shown in Fig. A-7. The extinction coefficient was taken to be:

$$K_e = \frac{1.9}{\text{secchi depth}}$$

after Beeton.<sup>9</sup>

#### BIOLOGICAL AND CHEMICAL EXOGENEOUS VARIABLES

1. Mass Loadings and Boundary Concentrations - sources of nutrient input into Lake Ontario are varied. Tributary runoff, direct municipal and industrial discharges comprise the principal sources of nutrients. Mass loadings (mass/ unit time) are normally thought of as direct inputs to a water body. Boundary concentration conditions (mass/unit volume) are usually thought to be associated with tributary inflow or in dispersive situations with the 'downstream' portion of the water body. Boundary conditions, since they are always associated with a flow regime (volume/ unit time), can also be viewed as mass loadings into the water body. WASP has capabilities to input nutrients using either mass loadings or boundary conditions, with the associated flow regime. Lake 1 in its present configuration just utilizes the boundary condition form of mass input. The loading information used for the various nitrogen and phosphorous species used in the nutrient systems (non-living organic, ammonia and nitrate,



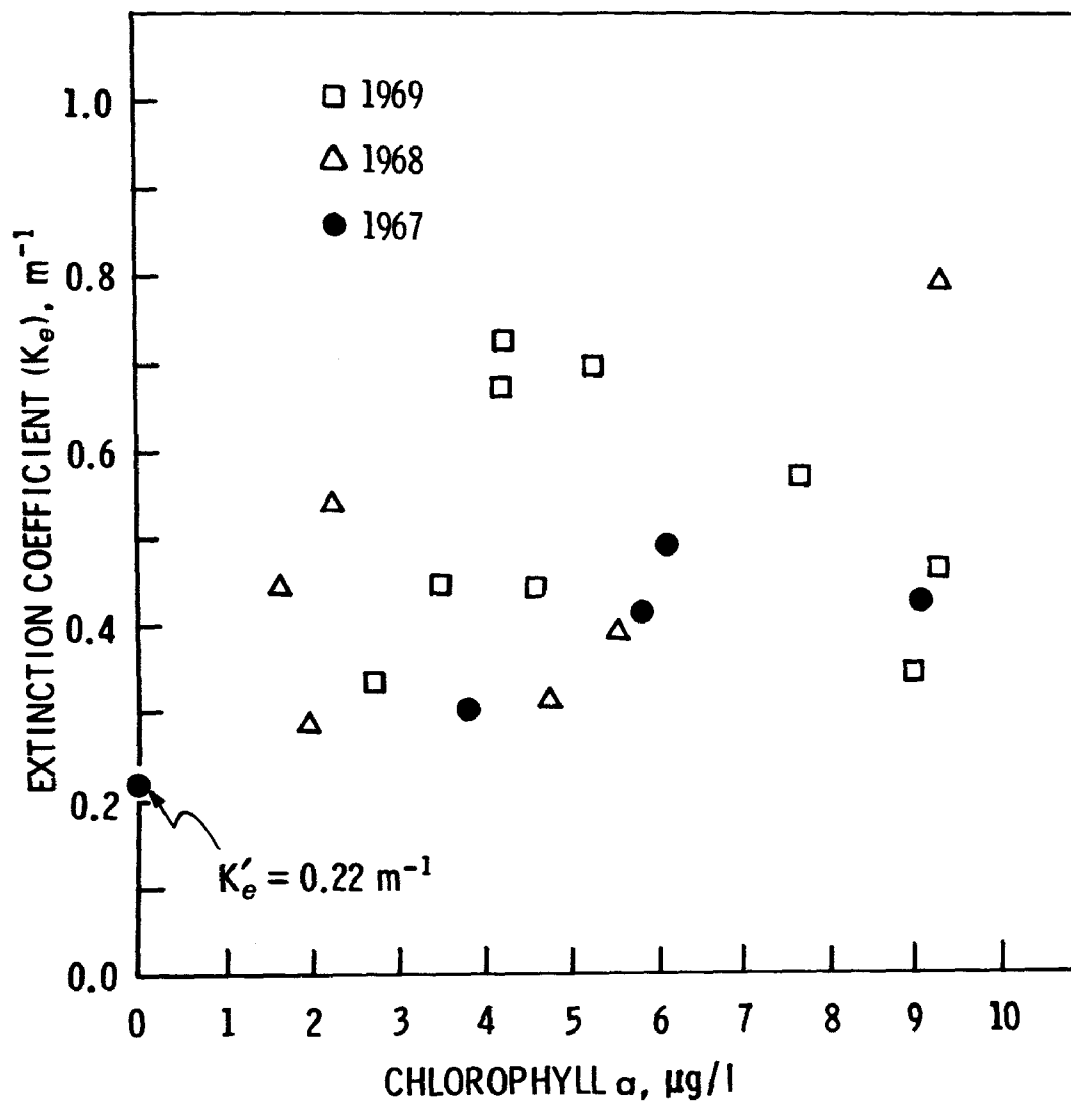


Figure A-7. Determination of background water clarity -  $K_e$



nitrogen, non-living organic and available phosphorus) was not available. Only total nutrient information was given. Species loads were set at initial conditions for the inorganic nutrients with the remainder placed in the respective non-living organic system. Loading information and breakdown is shown in Table A-2.

2. Initial Conditions - the initial conditions for Lake 1 are shown in Table A-2. The integration starts the first of January and these values reflect the measured values for this part of the year.

#### CHEMICAL AND BIOLOGICAL ENDOGENEOUS VARIABLES

1. System Parameters - the various constants and parameters which define the interaction between the various biological and chemical systems are listed in Table A-3. Units are those required by the present configuration of Lake 1.



TABLE A - 2

## LAKE 1

## MASS LOADINGS AND INITIAL CONDITIONS

System	Boundary Concentration (mg/l)	Initial Conditions (mg/l)
Phytoplankton	1.0	2.0
Zooplankton - Herbivorous	.05	.005
Nitrogen		
Non-living Organic	.443	.090
Ammonia - N	.0150	.0150
Nitrate - N	.250	.250
Phosphorus		
Non-living Organic	.0454	.005
Available - P	.0143	.0143
Zooplankton - Carnivorous	.01	.005
Zooplankton - Upper Trophic Level 1	by-passed system	
Zooplankton - Upper Trophic Level 2	by-passed system	



TABLE A - 3  
SYSTEM PARAMETERS

<u>System - Parameter</u>	<u>Symbol</u>	<u>Value</u>	<u>Units</u>
Phytoplankton Chlorophyll a			
1. Saturated Growth Rate ( $\theta_0$ )	K1T	1.066	None
	K1C	0.580	day <sup>-1</sup>
2. Saturating Light Intensity	IS	350.	ly/day
3. Michaelis Constant for Nitrogen	KMN	0.025	mg-N/l
4. Michaelis Constant for Phosphorus	KMP	0.002	mg-P/l
5. Endogenous Respiration Rate ( $\theta_{20}$ )	K2T	1.08	None
	K2C	0.10	day <sup>-1</sup>
6. Carbon to Chloro- phyll Ratio	CCHL	0.05	mg-C/ $\mu$ gChla
7. Sink Velocity	SVEL	0.10	m/ day
8. Preference Structure for Inorganic Nitrogen	PNH <sub>3</sub>	0.5	None



TABLE A - 3  
SYSTEM PARAMETERS  
(Continued)

<u>System - Parameter</u>	<u>Symbol</u>	<u>Value</u>	<u>Units</u>
Non-living organic Nitrogen			
1. Organic N - NH <sub>3</sub> Hydrolysis Rate	K34T K34C	0.00175 0	(day°C) <sup>-1</sup> day <sup>-1</sup>
2. Nitrogen to Chlorophyll <sub>a</sub> Ration	NCHL	0.010	mgN/mg Chl <sub>a</sub>
3. Sink Coefficient	K33	0.001	day <sup>-1</sup>
Ammonia Nitrogen			
1. NH <sub>3</sub> -NO <sub>3</sub> Nitrification Rate	K45T K45C	0.002 0	(day°C) <sup>-1</sup> day <sup>-1</sup>
Nitrate Nitrogen - none			
Non-living organic Phosphorus			
1. Organic P-Inorganic P conversion rate	K67T K67C	0.007 0	(day°C) <sup>-1</sup> day <sup>-1</sup>
2. Phosphorus to chorophyll a Ratio	PCHL	0.001	mgP/μg Chl <sub>a</sub>
3. Sink Coefficient	K 66	0.001	day <sup>-1</sup>
Available Phosphorus			
1. Sink Coefficient	K 77	0	day <sup>-1</sup>



TABLE A - 3  
SYSTEM PARAMETERS  
(Continued)

<u>System - Parameter</u>	<u>Symbol</u>	<u>Value</u>	<u>Units</u>
Herbivorous Zooplankton-carbon			
1. Grazing Rate	CGC	0	1/mgC/day °C
	CGT	0.06	1/mgC/day
2. Michaelis Constant for Phytoplankton	KMPL	10	µgChla/l
3. Conversion Efficiency	AZP	0.60	none
4. Endogenous Respiration Rate	K4T	0.001	(day°C) <sup>-1</sup>
	K4C	0.0	(day) <sup>-1</sup>
Carnivorous Zooplankton-carbon			
1. Grazing Rate	CGT8	0.06	1/mgC/day°C
	CGC8	0	1/mgC/day
2. Conversion Efficiency	A8Z	0.60	none
3. Endogenous Respiration Rate	K8T	0.001	(day°C) <sup>-1</sup>
	K8	0	day <sup>-1</sup>
Upper Trophic Level 1 - carbon			
1. Grazing Rate	CGT9	0.01	1/mgC/day°C
	CGC9	0	1/mgC/day
2. Conversion Efficiency	A98	0.60	none
3. Endogenous Respiration Rate	K9T	0.00	(day°C) <sup>-1</sup>
	K9	0.0	(day) <sup>-1</sup>



TABLE A - 3  
SYSTEM PARAMETERS  
(Continued)

System - Parameter	Symbol	Value	Units
Upper Trophic Level 2 - carbon			
1. Grazing Rate	CGT0	0.06	1/mg C/day °C
	CGC0	0	1/mgC/day °C
2. Conversion Efficiency	Al09	0.60	None
3. Endogenous Respiration Rate	Kl0T	0.002	(day °C) <sup>-1</sup>
	Kl0	0	day <sup>-1</sup>



NOTE:

Source listings for Lake 1 model and sample input and output are available from EPA, Grosse Ile Laboratory, Grosse Ile, Michigan.

This program is currently operational on the Control Data Corp. 6600 at Courant Institute of New York University.

A version will be available on Optimal Systems Inc., in the near future.



## REFERENCES

1. Canada Centre for Inland Waters, Descriptive Limnology Section, personal communication.
2. International Lake Erie Water Pollution Board and the International Lake Ontario - St. Lawrence River Water Pollution Board. Report to the International Joint Commission on the Pollution of Lake Ontario and the International Section of the St. Lawrence River, Volume 3, 1969.
3. Hydrosience Inc. Limnological Systems Analysis of the Great Lakes-Phase I. Hydrosience Inc., Westwood, N.J. 1973.
4. Canada Centre for Inland Waters. Limnological Data Reports, Lake Ontario. Canadian Oceanographic Data Centre, Burlington, Ontario.
5. Hubbard, John E. Department of Geology & Earth Science, State University College, Brockport, N.Y., personal communication.
6. Phillips, D.W. & J.A.W. McCulloch. The Climate of the Great Lakes Basin. Climatological Study No. 20, Environment Canada, Toronto. 1972.
7. Richards, T.L. and P. Lowen. A preliminary investigation of solar radiation over the Great Lakes as compared to adjacent land areas. Proc. Eight Conf. Great Lakes Res., Great Lakes Res. Division, Univ. of Michigan. pp. 278-282. 1965.



## REFERENCES

(Continued)

8. The World Almanac and Book of Facts. Newspaper Enterprise Association, New York. 1974.
9. Beeton, A.M. Relationship between Secchi disc readings and light penetration in Lake Huron, Am. Fish. Soc. Trans. 87:73-79. 1958.



**TECHNICAL REPORT DATA**  
(Please read instructions on the reverse before completing)

1. REPORT NO. EPA-660/3-75-005		2.		3. RECIPIENT'S ACCESSION NO.	
4. TITLE AND SUBTITLE Mathematical Modeling of Phytoplankton in Lake Ontario 1. Model Development and Verification				5. REPORT DATE October 1974	
				6. PERFORMING ORGANIZATION CODE	
7. AUTHOR(S) Robert V. Thomann                  Richard P. Winfield Dominick M. DiToro                Donald J. O'Connor				8. PERFORMING ORGANIZATION REPORT NO. EPA-660/3-75-005	
9. PERFORMING ORGANIZATION NAME AND ADDRESS Manhattan College Environmental Engineering and Science Program Bronx, N.Y. 10471				10. PROGRAM ELEMENT NO. 1BA026	
				11. CONTRACT/GRANT NO. R800610	
12. SPONSORING AGENCY NAME AND ADDRESS U.S. Environmental Protection Agency National Environmental Research Center Grosse Ile Laboratory 9311 Groh Rd., Grosse Ile, Michigan 48138				13. TYPE OF REPORT AND PERIOD COVERED Final, Part 1	
				14. SPONSORING AGENCY CODE	
15. SUPPLEMENTARY NOTES					
16. ABSTRACT The basic mathematical structure for describing the dynamics of phytoplankton in Lake Ontario is presented in this report. Data on chlorophyll and principle nutrients are reviewed and summarized and the mathematical modeling strategy is detailed. The modeling strategy begins with the construction of a horizontally completely mixed lake with vertical layers, LAKE 1. This spatially simplified model is used to develop the interactions and kinetic behavior of the various components of each subsystem. A more detailed 3-dimensional model is then used to describe open lake and near shore variations in phytoplankton biomass. Ten biological and chemical variables are used in both models and include four trophic levels above the phytoplankton, chlorophyll a as a measure of phytoplankton biomass two phosphorus components and three nitrogen components. Under reasonable sets of model parameters as reported in the literature, the Lake 1 model output compared favorably with observed data on the dependent variables. Spring growth and peak chlorophyll concentrations are related primarily to increasing light and temperature. The model indicates that growth ceases due to phosphorus limitation. The results to date indicate that the mathematical model of phytoplankton in Lake Ontario as developed herein is a reasonable first approximation to observed data. As such, the model can form a basis for preliminary estimates of the effects of nutrient reduction programs on Lake Ontario.					
17. KEY WORDS AND DOCUMENT ANALYSIS					
a. DESCRIPTORS		b. IDENTIFIERS/OPEN ENDED TERMS		c. COSATI Field/Group	
Mathematical Models, Computer Models, Eutrophication, Water Quality, Nutrients, Cycling Nutrients, Dispersion, Mass Transfer, Simulation Analysis		Great Lakes, Lake Ontario			
18. DISTRIBUTION STATEMENT		19. SECURITY CLASS (This Report)		21. NO. OF PAGES	
		20. SECURITY CLASS (This page)		22. PRICE	